Effective Data Association Algorithms for Multitarget Tracking

EFFECTIVE DATA ASSOCIATION ALGORITHMS FOR MULTITARGET TRACKING

BY

BIRUK K. HABTEMARIAM, B.Sc., M.A.Sc.

A THESIS

SUBMITTED TO THE DEPARTMENT OF ELECTRICAL & COMPUTER ENGINEERING

AND THE SCHOOL OF GRADUATE STUDIES

OF MCMASTER UNIVERSITY

IN PARTIAL FULFILMENT OF THE REQUIREMENTS

FOR THE DEGREE OF

DOCTOR OF PHILOSOPHY

Doctor of Philosophy (2014) McMaster University

(Electrical & Computer Engineering) Hamilton, Ontario, Canada

TITLE:	Effective Data Association Algorithms for Multitarget Tracking
AUTHOR:	Biruk K. Habtemariam B.Sc., (Electrical Engineering) Mekelle University, Mekelle, Ethiopia M.A.Sc., (Electrical and Computer Engineering) McMaster University, Hamilton, ON, Canada
SUPERVISOR:	Prof. T. Kirubarajan
NUMBER OF PAGES:	xvii, 144

To my parents

Abstract

In multitarget tracking scenarios with high false alarm rate and low target detection probability, data association plays a key role in resolving measurement origin uncertainty. The measurement origin uncertainty becomes worse when there are multiple detection per scan from the same target. This thesis proposes efficient data association algorithms for multitarget tracking under these conditions.

For a multiple detection scenario, this thesis presents a novel Multiple-Detection Probabilistic Data Association Filter (MD-PDAF) and its multitarget version, Multiple-Detection Joint Probabilistic Data Association Filter (MD-JPDAF). The algorithms are capable of handling multiple detection per scan from target in the presence of clutter and missed detection. The algorithms utilize the multiple-detection pattern, which accounts for many-to-one measurement set-to-track association rather than one-to-one measurement-to-track association, in order to generate multiple detection association events. In addition, a Multiple Detection Posterior Cramer-Rao Lower Bound (MD-PCRLB) is derived in order to evaluate the performance of the proposed filters with theoretical bound.

With respect to instantaneous track update, a continuous 2-D assignment for multitarget tracking with rotating radars is proposed. In this approach, the full scan is divided into sectors, which could be as small as a single detection, depending on

the scanning rate, sparsity of targets and required track state update speed. The measurement-to-track association followed by filtering and track state update is done dynamically while sweeping from one region to another. As a result, a continuous track update, limited only by the inter-measurement interval, becomes possible.

Finally, a new measurement-level fusion algorithm is proposed for a heterogeneous sensors network. In the proposed method, a maritime scenario, where radar measurements and Automatic Identification System (AIS) messages are available, is considered. The fusion algorithms improve the estimation accuracy by assigning multiple AIS IDs to a track in order to resolve the AIS ID-to-track association ambiguity. In all cases, the performance of the proposed algorithms is evaluated with a Monte Carlo simulation experiment.

.

Acknowledgements

Foremost, I would like to thank my supervisor Prof. T. Kirubarajan for his expert advice and guidance during my graduate studies. It has been a great privilege and invaluable learning experience to work with Prof. Kiruba and I would like to express my deep appreciation to his support and encouragement.

My gratitude extends to my committee members Prof. I. Bruce and Prof. S. Sirouspour for their guidance and feedback to this thesis work. I am very grateful to Dr. R. Tharmarasa for the discussions and insights on various research problems. I would also like to thank Dr. M. Pelletier from FLIR radars and Dr. M. McDonald from Defence Research and Development Canada for their feedback at different stages of my research. During my graduate studies I have been associated with many people in the Electrical and Computer Engineering Department and I would like to extend my appreciation to the professors, my fellow graduate students and members of estimation, tracking and fusion laboratory. My sincere thanks goes to the graduate administrative assistant Cheryl Gies. I am also very thankful for the funding from ECE department and the International Excellence Award from the Graduate School of studies. Special thanks to Williams Coffee staff for their excellent customer service.

Many thanks to my family for their continuous support, love and encouragement. Cheers to all my friends for the fun and good times we have together. Above all,

glory to the almighty God for his blessings as none of this would have been possible without his will.

Notation and abbreviations

Abbreviations

AEW	Airborne Early Warning
AIS	Automatic Identification System
CRLB	Cramer-Rao Lower Bound
DBT	Detect Before Track
EKF	Extended Kalman Filter
GPS	Global Positioning System
GM	Gaussian Mixture
FIM	Fisher Information Matrix
FISST	Finite Set Statistics
IID	Independent Identically Distributed
IMM	Interacting Multiple Model
JPDAF	Joint Probabilistic Data Association Filter
KF	Kalman Filter
MD-JPDAF	Multiple Detection Joint Probabilistic Data Association Filter
MD-PCRLB	Multiple Detection Posterior Cramer Rao Lower Bound

MD-PDAF	Multiple Detection Probabilistic Data Association Filter
MFA	Multiple Frame Assignment
ML	Maximum Likelihood
MHT	Multiple Hypothesis Tracker
MTT	Multiple Target Tracking
PCRLB	Posterior Cramer Rao Lower Bound
PDAF	Joint Probabilistic Data Association Filter
PF	Particle Filter
PHD	Probabilistic Hypothesis Density
RMSE	Root Mean Square Error
SMC	Sequential Monte Carlo
SNR	Signal-to-Noise Ratio
TBD	Track Before Detect
UKF	Unscented Kalman Filter

Contents

Abstract **iv**

Acknowledgements **vi**

Notation and abbreviations **viii**

1 Introduction **1**

1.1 Motivation 2

1.2 Contributions 4

1.3 Organization of the Thesis 6

1.4 Publications Derived from the Thesis 7

1.4.1 Journal Articles 7

1.4.2 Conference Proceedings 8

1.5 Other Publications 9

1.5.1 Journal Articles 9

2 Background **10**

2.1 System Model 11

2.1.1 Target Dynamics 11

2.1.2 Observation Model 13
2.2 TBD vs DBT 15
2.3 Data Association 16
2.3.1 Probabilistic Data Association 19
2.3.2 Multiple Hypothesis Testing 20
2.3.3 Frame Based Assignment 21
2.4 Filtering 24
2.4.1 Kalman Filter 24
2.4.2 Extended Kalman Filter 26
2.4.3 Unscented Kalaman Filter 26
2.4.4 Interactive Multiple Model 27
2.4.5 Particle Filter 27
2.5 Random Finite Set Methods 28

3 Multiple Detection Target Tracking **30**
3.1 Multiple-Detection Pattern 35
3.2 MD-PDAF and MD-JPDAF 40
3.2.1 MD-PDAF for Single Target Tracking 40
3.2.2 MD-JPDAF for Multitarget Tracking 47
3.3 MD-PCRLB 50
3.3.1 Background 50
3.3.2 Effect of Multiple Detection 52
3.4 Simulations 53
3.4.1 2D Sensor Single Target Scenario 54
3.4.2 2D Sensor Multiple Target Scenario 56

3.4.3 Over-the-Horizon Radar Scenario 57

4 Continuous association **64**

4.1 Problem Statement 67

4.2 Dynamic Sector Update 69

4.2.1 Cluster Processing 71

4.2.2 Assignment Cost 73

4.3 Continuous 2-D Assignment 75

4.3.1 Minimum Cost Bi-partite Matching 76

4.3.2 Incremental 2D Assignment 79

4.4 Simulations and Results 82

4.4.1 Simulation Setup 82

4.4.2 Simulation Results 86

5 Multi source fusion **92**

5.1 System Model 96

5.1.1 Target Dynamics 97

5.1.2 Radar Measurements 97

5.1.3 AIS measurements 97

5.2 AIS/Radar Tracking 99

5.2.1 Radar-Only Tracking 99

5.2.2 AIS-Only Tracking 101

5.3 Fused AIS-Radar Tracking 103

5.3.1 Track-to-Track Fusion 103

5.3.2 Measurement-Level Fusion 104

5.3.3 PCRLB for AIS/Radar Network 111
5.4 Simulations and Results 113
5.4.1 Simulation Setup 113
5.4.2 Simulation Results 114

6 Conclusions **122**

A MDPDA **124**
A.0.1 Probabilistic Inference 124
A.0.2 Special Case 127

B OTHR **128**
B.0.3 OTHR Model 128

List of Tables

3.1 Number of Multiple-Detection Association Events 43
4.1 Sector Numbers for Tracks State Update 73
4.2 Initial States of Simulated targets 82
5.1 Initial Conditions 113
5.2 Computational Load Comparison 121

List of Figures

2.1 Target trajectories ('·' denotes the initial point of a target and '*' denotes the end point of a target). 13

2.2 Measurement validation gate. 18

2.3 2D measurement-to-track assignment 21

2.4 Multiframe measurement-to-track assignment 23

3.1 Representative OTHR propagation modes. 32

3.2 Measurement validation gate for a single observation model/propagation path. 36

3.3 Measurement validation gate for multiple observation models/propagation paths. 37

3.4 Flow of MD-PDAF. 41

3.5 Range measurements in a single run. 54

3.6 Bearing measurements in a single run. 55

3.7 Position RMSE evaluation for MD-PDAF vs. PDAF and PCRLB ($P_{D1} = 0.05, P_{D2} = 0.90$). 56

3.8 Position RMSE evaluation for MD-PDAF vs. PDAF ($P_{D1} = 0.90, P_{D2} = 0.05$). 57

3.9 Position RMSE evaluation for MD-JPDAF vs. JPDAF (T-1 denotes the first target and T-2 denotes the second target). 58
3.10 Over-the-horizon radar planar model (Tx - transmitter, Rx - receiver, X - target). 59
3.11 Position RMSE evaluation for PDAF, MPDAF and MD-PDAF with OTHR data. 62
3.12 Position RMSE evaluation MD-JPDAF with OTHR data. 63
4.1 Measurement space of a rotating radar with eight 45^o sectors $(\mathcal{S}_1, \cdots, \mathcal{S}_8)$. The measurement validation region for each target $(X_1, \cdots, X_8)$ is shown by the corresponding ellipse. 68
4.2 Measurement-to-track association as a bi-partite matching graph . . . 77
4.3 Incremental measurement-to-track assignment 79
4.4 Measurement-to-track assignment in current sector. 81
4.5 Measurement-to-track assignment in next sector. 82
4.6 Target trajectories ('·' - start point of target and '*' - end point of target). 83
4.7 Range and bearing measurements of a rotating radar. 84
4.8 Tracks with incremental 2-D association ('·' - start point of track and '*' - end point of track). 85
4.9 Tracks with increasing latency. 87
4.10 Track with constant latency. 88
4.11 Tracks with decreasing latency. 89
4.12 Average track latency 90
4.13 Average track latency with scan time 12 s 90

4.14 Computation time 91
4.15 RMSE of position estimates 91
5.1 Measurement-level AIS/radar fusion. 106
5.2 RMSE for Target 1. 115
5.3 RMSE for Target 2. 116
5.4 AIS ID probabilities. 117
5.5 Time-averaged position RMSE of target 1 for various AIS revisit rates (σ_r =5 m, $\sigma_\theta = 0.1$ rad). 117
5.6 Time-averaged position RMSE of target 2 for various AIS revisit rates (σ_r =5 m, $\sigma_\theta = 0.1$ rad). 118
5.7 Time-averaged position RMSE of target 1 for various AIS revisit rates (σ_r =10 m, $\sigma_\theta = 0.5$ rad). 119
5.8 Time-averaged position RMSE of target 2 for various AIS revisit rates (σ_r =10 m, $\sigma_\theta = 0.5$ rad). 120
B.1 Over-the-horizon radar planar model (Tx - transmitter, Rx - receiver, X - target). 129

Chapter 1

Introduction

Due to the advances in sensor technology, a wide range of sensors are available for simultaneous deployment to monitor a specific region [14]. These sensors include radars, sonars, imaging sensors as well as Global Positioning System (GPS) devices mounted on the target (e.g., the Automatic Identification System (AIS) in maritime surveillance). However, the observations, also referred to as measurements or detection, from these sensors are corrupted by noise and clutter, which pose many challenges in target state estimation [18]. On the other hand, prior knowledge of a target's dynamics and features can be incorporated to these observations to improve the estimation accuracy [93]. With the use of prior knowledge, data association plays a key role in resolving the measurement origin uncertainty and hence acquiring optimal information about the current state of targets based on the observations and the priori data.

In a hypothetical scenario with unity probability of target detection and zero false alarm rate, there is no need for data association and the task of tracking reduces to

estimating the target states via filtering. However, whenever the probability of detecting a target is less than one and the false alarm probability not zero, measurement origin uncertainty arises. With measurement origin uncertainty, data association is needed to determine which set of measurements most likely belong to the target before filtering and state update can be carried out. The level of measurement origin uncertainty becomes worse with closely spaced targets because measurements originated from one target may fall in the validation region of another.

The data association problem in target tracking has been approached by various algorithms as one-to-one matching, probabilistic association, hypothesis testing and as constrained optimization [14][18]. Each approach has its own performance advantages depending on the surveillance scenario such as the false alarm rate and sensor conditions such as probability of target detection as well as the available computational resources.

1.1 Motivation

The motivation for this thesis comes from the limitations of current data association algorithms used in the Multitarget Tracking (MTT) domain. With the ever-increasing data processing speed, communication bandwidth and the versatile information from a network of heterogenous sensors, there is a need to develop new data association techniques that make optimal use of available resources.

One of the limitations in the current detection-based target tracking algorithms is the ubiquitous one-to-one measurement-to-track association assumption. According to this assumption, given a set of measurements for a single target scenario, at most one of them originates from the target and the rest are false alarms. For example, in

the Probabilistic Data Association (PDA) filter [15][44] and its multitarget version, the Joint Probabilistic Data Association (JPDA) filter [57][71], weights are assigned to measurements based on a Bayesian assumption that only one of the measurements is from the target and the rest are false alarms. However, a target can generate multiple detection in a scan due to multipath propagation or extended nature of the target with a high resolution radar sensor. When multiple detection from the same target fall within the association gate, the PDA filter as well as its multitarget version, the JPDA, tends to apportion the association probabilities, but still with the fundamental assumption that only one of them is correct. This led to the development of multiple detection pattern based tracking algorithms that can effectively handle multiple detection/mulipath scenarios.

Another limitation in MTT algorithms is relying on receiving all the measurements in a scan or frame to perform measurement-to-track association in order to satisfy the common one measurement per track assumption [14][19][76]. However, rotating radars are capable of returning the measurements continuously, at the instant of detection, while sweeping from one region to another. Waiting for the full set of measurements in a scan to perform data association and filtering results in delayed tracking system. This problem becomes more apparent while tracking maneuvering and high speed targets with low scan rate sensors. Furthermore, multitarget tracking algorithms like the hypothesis based MHT and the Montecarlo methods based PHD filter introduce further delay due to their high computation resource requirement. This leads to the development of continuous 2D assignment algorithm that enable within scan track update speed.

Furthermore, currently a wide range of sensors can be deployed simultaneously to

monitor a specific region. Each sensor could process the observation and report its track estimates in a distributed framework or forward the observations to a fusion center in a centralized framework. With the centralized fusion architecture consisting of a heterogenous sensor network, diverse information from multiple sources can be effectively fused to yield a single combined estimate [18]. In general, the fused estimates from multiple sources can improve overall tracking performance with respect to estimation accuracy, number of false tracks and missed detection over the corresponding values with a single source [36]. Track-to-track fusion [12][42] is one way of fusing information from multiple sensors, where separate tracks are initiated and maintained at each senor and combined later at the fusion node. Although track-to-track fusion is a computationally efficient approach, estimation error resulting from tracking at the local level and from the fusion at the global level accumulate over time and, as a result, the overall estimation errors may becomes large. Furthermore, there may be a processing delay in estimating tracks from each source before fusing and reporting the final confirmed track. This leads to the development of a measurement level fusion algorithm that offers improved tracking performance, over distributed tracking but with the requirements for more computational resources as well as sufficient bandwidth between the senors and the fusion center.

1.2 Contributions

The following are the contributions of this thesis:

- Multiple Detection Probability Data Association Filter (MD-PDAF): an algorithm that explicitly considers multiple detection is proposed for single target

tracking problem. The proposed algorithm solves the problem of multiple detection using a multiple detection pattern that considers all feasible measurement set-to-track association. The enhanced performance of MD-PDAF is compared with PDAF with multiple detection simulation experiment.

- Multiple Detection Joint Probability Data Association Filter (MD-JPDAF): the multiple detection algorithm is extended to handle closely spaced targets. The proposed tracking algorithm is applied to multitarget tracking problem with Over-the-Horizon (OTH) radars.

- Multiple Detection Posterior Cramér-Rao Bound (MD-PCRLB): in order to have a theoretical benchmark for the proposed multiple detection tracking algorithm MD-PCRLB is derived.

- Continuous 2D Assignment with Rotating Radars: a new dynamic sector processing algorithm using incremental 2D assignment is proposed for scanning radars that updates target states within the duration of a scan. With the proposed method, the full scan is dynamically and adaptively divided into sectors, which could be as small as a single detection, depending on the scanning rate, sparsity of targets and required target state update speed. Measurement-to-track association followed by filtering and target state update is done dynamically while sweeping from one region to another. Hence, a fast track update, limited only by the inter-measurement interval, becomes possible.

- Measurement-level AIS/Radar Fusion: a new measurement-level fusion of AIS messages and radar measurements is proposed based on the Joint Probabilistic

Data Association (JPDA) framework. The proposed method uses a probabilistic AIS IDs-to-tracks assignment technique to resolve the assignment ambiguity. The effectiveness of the proposed measurement level fusion algorithm is demonstrated by comparing with track-to-track fusion, radar-only and AIS-only track estimates.

1.3 Organization of the Thesis

In Chapter 2 a background on target tracking is provided. Although the focus of this thesis is on measurement-to-track data association techniques, the actual target tracking involves signal processing, detection and filtering. Hence, in Section 2.1 the basics on target dynamics and radar models for the case of linear or nonlinear observation models are discussed. Furthermore, target tracking methods and current data association techniques are discussed in Section 2.3.

In Chapter 3 multiple-detection based probabilistic data association algorithms for single target tracking, MD-PDAF, and for multitarget tracking, MD-JPDAF, are presented. The multiple-detection pattern that generates the possible measurement set-to-track association events is discussed in Section 3.1. In addition, in Section 3.3, the multiple-detection PCRLB is derived, which provides a theoretical benchmark to compare the estimation accuracy of the proposed MD-PDAF and MD-JPDAF. Section 3.4 concludes the chapter with the simulation experiment of target tracking with multiple-detection 2D radar and multipath OTH radar as well as with the performance evaluation the proposed techniques.

In Chapter 4 the dynamic sector based multitarget tracking algorithm with continuous 2-D assignment is presented. Section 4.2 focuses on the formulation of the

dyanmic sector update and Section 4.3 presents the continues tracking algorithm with incremental assignment techniques and application of the method to target tracking with rotating radars. A simulation experiment that demonstrate the continuous update capability of the proposed algorithm as well as efficient utilization of computational resources is presented in Section 4.4.

Chapter 5 deals with the measurement level fusion of AIS and radar measurements. Section 5.1 sets up a maritime environment where both the radar and AIS data are available to the fusion center. The measurement level fusion algorithm is presented in Section 5.3. The proposed fusion algorithm is compared with radar only and AIS only estimates using a simulation experiment in Section 5.4 and significant improvement in estimation accuracy is achieved.

Finally, Chapter 6 presents the conclusions to this thesis work.

1.4 Publications Derived from the Thesis

The following publication are derived from this thesis.

1.4.1 Journal Articles

- B. Habtemariam, R. Tharmarasa, T. Thayaparan, M. Mallick and T. Kirubarajan, "A Multiple-Detection Joint Probabilistic Data Association Filter." *IEEE Journal of Selected Topics in Signal Processing*, vol. 7, no. 3, June 2013.[9].

- B. Habtemariam, R. Tharmarasa, M. McDonald and T. Kirubarajan, "Continuous 2-D Assignment for Multitarget Tracking with Rotating Radars" 2013. Under second review *IEEE Transactions on Aerospace and Electronic Systems.*

- B. Habtemariam, R. Tharmarasa, M. McDonald and T. Kirubarajan, "Measurement level AIS/Radar Fusion for Multitarget Tracking" 2013. Submitted to *Signal Processing*.

1.4.2 Conference Proceedings

- B. Habtemariam, R. Tharmarasa, M. Mallick and T. Kirubarajan, "Performance Comparison of a Multiple-Detection Probabilistic Data Association Filter with PCRLB," *Proceedings of the International Conference on Control, Automation and Information Sciences*, pp. 18-23, Ho Chi Minh City, Vietnam, November 26-28 2012.[4]

- B. Habtemariam, R. Tharmarasa, Eric Meger and T. Kirubarajan, "Measurement level AIS/Radar Fusion for Multitarget Tracking", *Proc. SPIE Conference on Signal and Data Processing of Small Targets*, Baltimore, MD, USA, April 2012.[3]

- B. Habtemariam, R. Tharmarasa, N. Nandakumaran, M. McDonald and T. Kirubarajan, "Improved Multiframe Association for Tracking Maneuvering Targets", *Proc. SPIE Conference on Signal and Data Processing of Small Targets*, San Diego, CA, USA, August 2011.[6]

- B. Habtemariam, R. Tharmarasa, M. Pelletier, and T. Kirubarajan, "Dynamic Sector Processing Using 2D Assignment for Rotating Radars", *Proc. SPIE Conference on Signal and Data Processing of Small Targets*, San Diego, CA, USA, August 2011.[5]

- B. Habtemariam, R. Tharmarasa, T. Kirubarajan, D. Grimmett and C. Wakayama,

"Multiple Detection Probabilistic Data Association Filter for Multistatic Target Tracking," *Proceedings of the 14th International Conference on Information Fusion*, pp. 1-6., Chicago, IL, USA, July 2011.[8]

1.5 Other Publications

1.5.1 Journal Articles

- K. Li, B. Habtemariam, R. Tharmarasa, M. Pelletier and T. Kirubarajan, "Multitarget Tracking with Doppler Ambiguity." *IEEE Transactions on Aerospace and Electronic Systems*, vol. 49, no. 4, pp. 2640-2656, October 2013.

- B. Habtemariam, A. Aravinthan, R. Tharmarasa, K. Punithakumar, T. Kirubarajan and T. Lang, "Distributed Tracking with a PHD Filter Using EfficientMeasurement Encoding." *Journal of Advances in Information Fusion*, vol. 7, no. 2, pp. 114–130, December 2012.

- B. Habtemariam, R. Tharmarasa and T. Kirubarajan, "PHD Filter Based Track-Before-Detect for MIMO Radars." *Signal Processing*, vol. 92, no. 3, pp. 667–678, March 2012.

Chapter 2

Background

In this chapter a review of basic methods and terminologies used in target tracking is presented. The chapter starts with a discussion on state-space based mathematical models for target dynamics and radar measurements. General cases of both linear and nonlinear dynamics and measurement equations, which builds up a system model for multitarget tracking problem, are considered.

Later, a literature review of target tracking approaches such as detect-before-track and track-before-detect is discussed. With the detect-before-track framework, thresholding and measurement gating techniques are discussed. Multitarget tracking algorithms that are based on hard association, probabilistic association, hypothesis testing, optimization and random finite set methods are revisited and their pros and cons are presented. Furthermore, linear, nonlinear and Monte Carlo based filters and estimators are also discussed in this chapter.

2.1 System Model

2.1.1 Target Dynamics

The dynamics of physical systems such as airplanes, vessels, ballistic targets, etc., can be modeled using a state-space model [14][18][93]. With state-space modeling, a moving target can be represented as the transition in the state of a target driven by a process noise.

Hence, the state of the t^{th} target driven by process noise is given by [93]

$$x_t(k+1) = f(x_t(k), v_t(k)) \tag{2.1}$$

where $x_t(k) = [x, y, \dot{x}, \dot{y}]$, without loss of generality, represents the target state composed of position and velocity, $f(\cdot)$ is a general nonlinear model for system transition and $v_t(k)$ is white and independent process noise. Furthermore, for a linear time invariant system, (2.1) will reduce to

$$x_t(k+1) = F_t(k)x_t(k) + v_t(k) \tag{2.2}$$

where $F_t(k)$ is the system transition matrix.

For example, a target moving with a nearly constant velocity (NCV) can be modeled with a system transition matrix as [93]

$$F_t = \begin{bmatrix} 1 & T & 0 & 0 \\ 0 & 1 & 0 & 0 \\ 0 & 0 & 1 & T \\ 0 & 0 & 0 & 1 \end{bmatrix} \tag{2.3}$$

and the process noise covariance matrix as

$$Q_t = q \begin{bmatrix} \frac{T^3}{3} & \frac{T^2}{2} & 0 & 0 \\ \frac{T^2}{2} & T & 0 & 0 \\ 0 & 0 & \frac{T^3}{3} & \frac{T^2}{2} \\ 0 & 0 & \frac{T^2}{2} & T \end{bmatrix} \tag{2.4}$$

where q is the power spectral density [93] of the process noise, T is the scan time. Alternatively, a target with a constant turn can be modeled using the a system transition matrix as

$$F_t = \begin{bmatrix} 1 & \frac{\sin(\omega T)}{\omega} & 0 & \frac{-(1-\cos(\omega T))}{\omega} \\ 0 & \cos(\omega T) & 0 & -\sin(\omega T) \\ 0 & \frac{(1-\cos(\omega T))}{\omega} & 1 & \frac{\sin(\omega T)}{\omega} \\ 0 & \sin(\omega T) & 0 & \cos(\omega T) \end{bmatrix} \tag{2.5}$$

where ω is the turn rate. Figure 2.1 shows representative targets with a constant velocity and a constant turn trajectories.

Furthermore, maneuvering targets can be modeled using either one or combination

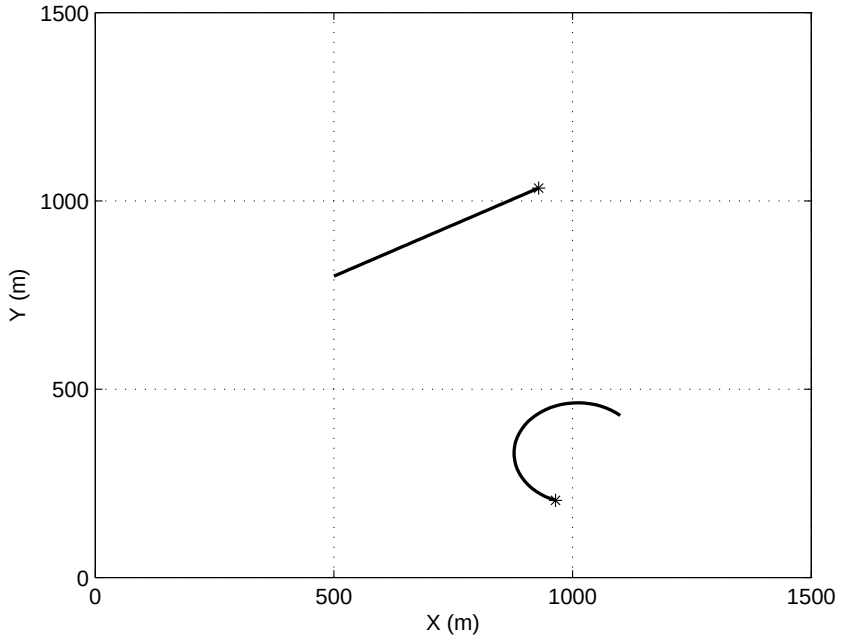

Figure 2.1: Target trajectories ('·' denotes the initial point of a target and '*' denotes the end point of a target).

of the maneuvering target motion models. These motion models include constant acceleration, white noise jerk, winer sequence acceleration models [73] and ballistic motion models [74].

2.1.2 Observation Model

Radars and sonar transmit and receive signals reflected from a target and map into a measurement space in most cases with a non linear measurement model [18]. Apart from signals reflected from a target there are signals from a clutter or a background noise. After signal processing, these sensors report measurements about kinematic parameters of the targets at regular intervals, which are generally referred as scans or frames.

At a given scan, the target-originated measurements are given by

$$z(k) = h(x_t(k)) + w(k) \tag{2.6}$$

where $h(\cdot)$ is in general a nonlinear function of target state. For example, for a 2D rotating radar with range and bearing measurements $h(x_t(k))$ is given as

$$h(x_t(k)) = \begin{bmatrix} r(x_t(k)) \\ \theta(x_t(k)) \end{bmatrix} \tag{2.7}$$

with range

$$r(x_t(k)) = \sqrt{(x_s - x)^2 + (y_s - y)^2} \tag{2.8}$$

and bearing

$$\theta(x_t(k)) = \arctan\left(\frac{y_s - y}{x_s - x}\right) \tag{2.9}$$

where $x_s(k) = [x_s, y_s]$ is the radar's coordinates at time step k. Also in (2.6), $w(k)$ is the measurement noise with a covariance R given as:

$$R = \begin{bmatrix} \sigma_r^2 & 0 \\ 0 & \sigma_\theta^2 \end{bmatrix} \tag{2.10}$$

where σ_r and σ_θ are the standard deviations in the range and bearing measurements respectively. The linear version of (2.6) is given by computing the the Jacobian of

the measurement function $h(\cdot)$ as

$$H(k) = \begin{bmatrix} \partial r(x_t(k))/\partial x & 0 & \partial r(x_t(k))/\partial y & 0 \\ \partial \theta(x_t(k))/\partial x & 0 & \partial \theta(x_t(k))/\partial y & 0 \end{bmatrix} \tag{2.11}$$

False alarms or measurements that do not originate from targets are assumed to be uniformly distributed within the senor's field of view. That is,

$$z(k) = \mathcal{U}(\mathbb{M}_{\min}, \mathbb{M}_{\max}) \tag{2.12}$$

where $\mathbb{M}_{\min}$ and $\mathbb{M}_{\max}$ represent the minimum and maximum regions of the surveillance area in the radar's measurement space $\mathbb{M}$. Furthermore, the number of false measurements is modeled by a Poisson process with known distribution function $\mu(m(k))$

$$\mu(m(k)) = e^{-\lambda \mathcal{G}} \frac{(\lambda \mathcal{G})^{m(k)}}{m(k)!} \tag{2.13}$$

where $m(k)$ is the number of measurements at time step k, $\mathcal{G}$ is the measurement gate volume and λ is the expected number of false measurements [14].

2.2 TBD vs DBT

One method to estimate the target state from the observation data is to directly process the raw signal and search for track patterns. This method is generally referred as Track-Before-Detect (TBD). This approach is effective for low Signal-to-Noise-Ratio (SNR) scenario where signal from a target is weak and indistinguishable from

the background noise [94]. TBD methods use the entire measurement set of a sensor's resolution cells and integrate tentative targets over multiple frames [95]. As a result, TBD methods are computationally demanding in most cases.

Another approach is to apply a threshold to the raw signal from the radar and extract the measurements (also referred as detection, contacts and radar plots in the literature) [14]. Based on the extracted measurements, new tracks can be initialized or already initialized tracks can be associated to measurements and their states be updated using the associated measurements [18]. As detection precedes the tracking process, this methods are collectively referred as Detect-Before-Track.

2.3 Data Association

As discussed in the previous section, the initial step in Detect-Before-Track methods is to apply a threshold to the raw signal received from the radar. The common thresholding technique is the Constant False Alarm Rate (CFAR) method [31]. The CFAR is an adaptive thresholding approach, in which a constant false alarm rate can be achieved by applying a threshold level determined by sliding window neighbourhood resolution cells averaging technique [72]. As a result, the threshold level can go up and down from one resolution cell to another depending on the local clutter situation.

Applying thresholds results in a discrete measurement set either from target or clutter distributed in the entire measurement space. Hence, a measurement-to-track data association is required to determine if a measurement is from a target or clutter [14]. Most data association techniques involve gating techniques in order to reduce the number of feasible measurement-to-track association. If a track's previous state and covariance is known, a measurement validation gate can be constructed around

the predicted track position. The simplest method is to specify a regular region that will satisfy the gate requirement [18]. A more effective approach is to define an n-dimensional ellipse around the predicted track position and choose measurements that satisfy the condition

$$\mathcal{G}(k) = \{z(k) : [z(k) - \hat{z}(k|k-1)]' S(k)^{-1} \\ [z(z) - \hat{z}(k|k-1)] \leqslant g^2\} \tag{2.14}$$

where g^2 is the gate threshold, which can be selected in order to give a specified gating probability P_G, and $S(k)$ is the innovation covariance corresponding to the measurement given by

$$S(k) = H(k)P(k|k-1)H(k)' + R(k) \tag{2.15}$$

The volume is thus given by

$$\mathcal{G}(k) = c_{n_z}|g^2(S(k)|^{1/2} \tag{2.16}$$

$$= c_{n_z} g^{n_z}|(S(k)|^{1/2} \tag{2.17}$$

where n_z is the dimension of the measurement and the coefficient c_{n_z} is the volume of the n_z-dimensional unit hypersphere ($c_1 = 2, c_2 = \pi, c_3 = 4\pi/3$, etc.) [14] [58]. Figure 2.2 shows a representative measurement validation gate for a 2D radar with range and bearing measurements, i.e., $n_z = 2$.

For implementation purpose, here it can be noted that the left hand side of (2.14) has the chi-square distribution with n degrees of freedom if the measurement error is

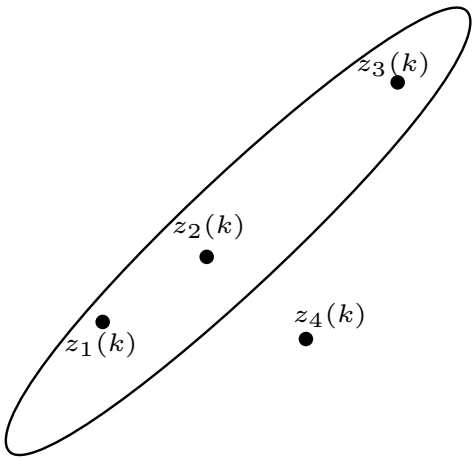

Figure 2.2: Measurement validation gate.

assumed to be n-variable Gaussian distributed. In this case, n refers to the number of independent measurements. Therefore, according to this approach the value of g^2 can be determined using a χ^2 table and the relationship [18][46]

$$p(\chi^2 > g^2) = 1 - P_G \tag{2.18}$$

Thresholding and gating yield the potential measurement candidates to be associated with a track. Referring back to Figure 2.2, there are four measurements in the vicinity of predicted track positions and three of them are in the validation region. The simplest data association techniques based on one-to-one measurement-to-track matching are the Nearest Neighbor Filter (NNF) and Strongest Neighbor Filter (SNF) [18]. The NNF associates a track with the measurement closest to the predicted measurement among the validated measurements while the SNF associates

the measurement with the strongest intensity (assuming amplitude information is available). Accordingly, with NNF method $z_2(k)$ will be associated to track and with SNF method the measurement with strongest amplitude among $\{z_1(k), z_2(k), z_3(k)\}$ will be associated to the track.

These data association techniques are computationally efficient and perform reasonably in a scenario where the target return is very strong and the false alarm rate is low. However, with degraded target observability, dense clutter and closely-spaced targets, such approaches begin to fall short [8] to resolve the measurement origin uncertainty. Under such conditions, a more practical approach to deal with measurement origin uncertainty to applying Bayesian association techniques.

2.3.1 Probabilistic Data Association

The Probabilistic Data Association Filter (PDAF) [15] [14], also referred as the all-neighbors data association filter [19], implements a Bayesian approach for data association. In PDAF, weights are assigned to the measurements based on probabilistic inference made on the number of measurements and location of the measurements relative to the predicted track state [14]. For example, for the scenario in Figure 2.2 each validated measurement, i.e., $\{z_1(k), z_2(k), z_3(k)\}$, is assigned a weight in contrast to choosing a single measurement as in NNF and SNF methods. Track state is updated with the innovations from each measurements are combined according to the assigned weights.

Whenever there are multiple targets close to each other, joint association events can be considered in order to resolve from which target a measurement is originated uncertainty as in Joint Probabilistic Data Association Filter (JPDA) [23][20]. The

PDAF as well as its multitarget variant, JPDAF, assume that track/tracks are already uninitialized. Tracks can be initialized, for example, with two-point track initialization method [14]. Furthermore, in a more robust approach, target existence models can be incorporated into the PDA framework as in Integrated Probabilistic Data Association Filter (JIPDA) [28] and similarly to the JIPDA framework as in Joint Integrated Probabilistic Data Association Filter (JIPDA) [57]. With target existence model, the JIPDA handles time varying number of targets and track management tasks such as track initiation, confirmation and deletion.

2.3.2 Multiple Hypothesis Testing

In the Multiple Hypothesis Testing (MHT) [19][78] approach a hypothesis will be generated and tested with the received measurements in the current scan or frame. For a given measurement the hypotheses could be the measurement is originated from one of initialized tracks, or is originated from a new target or is a false alarm [18]. A Bayesian approach will be used to compute the probabilities of each hypothesis. The valid hypotheses derived from sequences of measurements are evaluated and propagated over time, each of them generating a set of new hypotheses at every sample time k.

The major drawback in implementing the MHT algorithm for practical applications is the exponential growth in the number of the assignment hypotheses as time of a scan and number of measurement increases. This leads to the development of several hypothesis pruning, hypothesis merging and gating techniques [18][29].

2.3.3 Frame Based Assignment

Frame based assignment algorithms formulate the measurement-to-track assignment as a global cost minimization problem. At a given time step, only the current frame (e.g. 2D assignment) or the current frame and previous frames (e.g. multiframe assignment) can be considered for the association.

2D Assignment

In 2D assignment, at a time a single frame is used to associate the detection with tracks. Let $z_1, \cdots, z_n$ that z denotes the measurements from the sensors at a given fame and n the total number of measurements, to be associated with $x_1, \cdots, x_m$, where x denotes the tracks and m denotes the number of targets as shown in Figure 2.3

	z_1	z_2	$\cdots$	z_n
x_1	$c_{1,1}$	$c_{1,2}$	$\cdots$	$c_{1,n}$
x_2	$c_{2,1}$	$c_{2,2}$	$\cdots$	$c_{2,n}$
$\vdots$	$\vdots$	$\vdots$	$\ddots$	$\vdots$
x_m	$c_{m,1}$	$c_{m,2}$	$\cdots$	$c_{m,n}$

Figure 2.3: 2D measurement-to-track assignment

The cost of measurement-to-track association is determined by the negative log-likelihood ratio of target-originated measurement likelihood to false alarm density [14]. Formulated as a discrete optimization problem, the 2D assignment looks for the best

assignment by minimizing the total cost given by

$$\begin{aligned} \min \quad & \sum_{i=1}^{n}\sum_{j=1}^{m} c_{ij}\phi_{ij} \\ \text{subject to} \quad & \sum_{i=1}^{n} \phi_{ij} = 1 \qquad \forall j = 1, 2, \cdots, m \\ & \sum_{j=1}^{m} \phi_{ij} = 1 \qquad \forall i = 1, 2, \cdots, n \end{aligned} \tag{2.19}$$

where ϕ is the assignment operator, $\phi \in \{0, 1\}$ that ensures a one-to-one measurement-to-track association.

In the literature, several algorithms have been proposed to solve the combinatorial optimization problem with polynomial computation complexity [16][17][21][55][80]. For example, the Hungarian algorithm [48] and Jonker-Volgenant-Castanon (JVC) [40] algorithm solve the measurement-to-track association problem in polynomial time, $O(n^3)$, where n is the maximum number of measurements or tracks to be associated.

Multiframe Assignment

Multiframe assignment, also called multidimensional assignment, extends the 2D problem into optimization of assignment from sequence of frames [76][91] as shown in Figure 2.4.

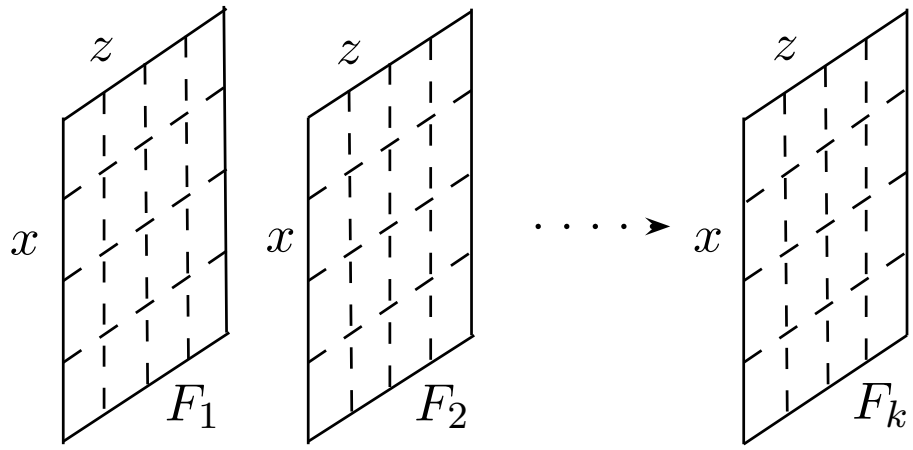

Figure 2.4: Multiframe measurement-to-track assignment

The optimization problem is given as

$$\begin{aligned}
&\min \sum_{i_1=1}^{n_{F_1}} \sum_{i_2=1}^{n_{F_2}} \cdots \sum_{i_f=1}^{n_{F_k}} c_{i_1,i_2,\cdots,i_f} \phi_{i_1,i_2,\cdots,i_f} \\
&\text{subject to} \sum_{i_2=1}^{n_{F_2}} \sum_{i_3=1}^{n_{F_3}} \cdots \sum_{i_f=1}^{n_{F_k}} \phi_{i_1,i_2,\cdots,i_f} = 1 \qquad i_1 = 1,2,\cdots,n_{F_1} \\
&\qquad \sum_{i_1=1}^{n_{F_1}} \sum_{i_3=1}^{n_{F_3}} \cdots \sum_{i_f=1}^{n_{F_k}} \phi_{i_1,i_2,\cdots,i_f} = 1 \qquad i_2 = 1,2,\cdots,n_{F_2} \\
&\qquad\qquad \vdots \qquad\qquad\qquad\qquad \vdots \\
&\qquad \sum_{i_1=1}^{n_{F_1}} \sum_{i_2=1}^{n_{F_2}} \cdots \sum_{i_{f-1}=1}^{n_{F_{k-1}}} \phi_{i_1,i_2,\cdots,i_f} = 1 \qquad i_f = 1,2,\cdots,n_{F_k}
\end{aligned} \tag{2.20}$$

The multiframe assignment algorithm determins the most likely set of frames such that each measurements is assigned to one and only one track, or declared as false alarm, and each track receives at most one detection from each frame used for association. The multiframe assignment improves the association accuracy compared to the 2D assignment at the cost of increased computation and latency corresponding

to the number of frames used in the association.

The main challenge in associating data from three or more sequence of frames is that the resulting optimization problem is NP-hard. This issue is addressed by using a Lagrangian relaxation-based methods are used to successively solve the association problem as a series of 2-D assignments [62][63][64][67]. Accordingly, the constraints in (2.20) are relaxed one set at a time there by solving the resulting subproblem iteratively and then reconstructing a feasible solution for the original multidimensional discrete optimization problem.

2.4 Filtering

Once a track is associated to a measurement, filtering methods can be used in order to estimate the current state of target. If no measurement is associated with a track, the track will be updated with the predicted state [18]. There are various filtering methods to estimate the current state of the target based on the associated measurement. One of the early filtering techniques is $\alpha-\beta$ filters [43] that use a fixed tracking coefficients.

2.4.1 Kalman Filter

For target dynamics that is Markov and Gaussian, the Kalman filter is the optimal estimator. Note that in a Gaussian process the distribution of target state $x(k)$ at any time k is Gaussian, and the multivariate distribution on target states at any finite set of times is also a multivariate Gaussian. Furthermore, it is assumed that the measurement equation is a linear function of target state with additive Gaussian noise.

Formulated as the maximum a posteriori estimate, the Kalman filter minimizes the expected square error between the estimate and true target state. The recursive Kalman filter involves a prediction and update steps as follows:

- Prediction:

  Using the target dynamics equation (2.2) predict the state and the covariance as

$$x(k+1) = F(k)x(k) \tag{2.21}$$

$$P(k+1) = F(k)P(k)F(k)' + Q(k) \tag{2.22}$$

  and using the measurement equation (2.11) predict the measurement and innovation covariance as

$$\hat{z}(k) = H(k)x(k) \tag{2.23}$$

$$S(k) = H(k)P(k)H(k)' + R(k) \tag{2.24}$$

- Update:

  Compute the innovation and filter gain as

$$v(k) = z(k) - \hat{z}(k) \tag{2.25}$$

$$W(k) = P(k)H(k)'S(k)^{-1} \tag{2.26}$$

and update the state and the covariance as

$$\hat{x}(k) = x(k+1) + W(k)v(k) \tag{2.27}$$

$$\hat{P}(k) = P(k) - W(k)H(k)P(k) \tag{2.28}$$

Note that if multiple measurements are assigned to a track, as in the case of PDAF, the state and the covariance are updated using a combined weighted innovation from the measurements.

2.4.2 Extended Kalman Filter

Although the Kalman filter provides an optimal solution for sensors with a linear observation model, practical sensors such as 2D radars and over-the-horizon radars report measurements as a nonlinear functions of target state. In this case, the observation equations can be substituted with their linear approximations and then the Kalman filter can be used for approximate solution. In the literature, this approach is commonly referred as the Extended Kalman Filtering (EKF) [93].

The linear approximation process of the state transition and observation model involves computing the partial derivatives of $f(\cdot)$ and $h(\cdot)$, respectively.

2.4.3 Unscented Kalaman Filter

If the system transition and observation models are highly nonlinear, the EKF approximation would not be efficient. In the worst case the partial derivatives might not exist or are hard to compute. In such cases, the sampling based Unscented Kalaman Filter (UKF) [41][90] can be used for estimation.

The UKF, also classified as the Sigma-Point Kalman Filters, linearizes a non-linear system transition and observation functions of a random variable through a linear regression between n points drawn from the prior distribution of the random variable [90]. The sigma points are chosen so that their mean and covariance to be exactly the previous target state and covariance. Each sigma point is then propagated through the nonlinear functions to yield the cloud of transformed pointed. Finally, the new estimated mean and covariance are then estimated based on the propagated sigma points statistics [41].

2.4.4 Interactive Multiple Model

Maneuvering targets exhibit different motion modes during their life time. The aforementioned KF family requires knowledge of the underlying state transition model. If incorrect model is used in the KF family filters, the estimation result would be inaccurate. In this case, multiple filters can be run in parallel, and in each filter the target motion is assumed to be in one of the n possible modes. This method is referred as the Interactive Multiple Model (IMM) filter [30]. The IMM is able to estimate the state of a dynamic system with several system transition modes, which can switch from one to another [30].

2.4.5 Particle Filter

For nonlinear, non-Gaussian problems, Particle Filters, which are based on Sequential Monte Carlo (SMC), can provide approximate solution [54]. Particle filters use large number of weighted samples $\left\{x_p^i(k)|i=1,\cdots,N_p\right\}$, also called particles, to approximate the posterior density.

- Prediction:

  Using the target dynamics equation (2.1) predict the state for each particle $\left\{x_p^i(k)|i=1,\cdots,N_p\right\}$

$$x_p^i(k+1) = f(x_p^i(k), v(k)) \tag{2.29}$$

- Update:

  Compute the posterior probabilities of the particles using the measurement likelihood function as:

$$w^i(k+1) = \frac{w^i(k)p(z(k+1)|x_p^i(k+1))}{\sum_{j=1}^{N_p} w^j(k)p(z(k+1)|x_p^j(k+1))} \tag{2.30}$$

- Resample:

  Resample N_p particles of equal weight $\left\{x_p^i(k)|i=1,\cdots,N_p\right\}$ from the weighted $\left\{(x_p^i(k), w^i(k))|i=1,\cdots,N_p\right\}$.

At the end of each cycle, the estimate $\hat{x}(k)$ can be computed from the posterior distribution's mean as

$$\hat{x}(k) = \frac{1}{N_p}\sum_{i=1}^{N_p} x_p^i(k) \tag{2.31}$$

2.5 Random Finite Set Methods

The Probability Hypothesis Density (PHD) filter [10][11][89] is a Bayesian multitarget tracking estimator initially proposed in [56]. The PHD filter is developed based on the Random Finite Set (RFS) theory, point processes, and Finite Set Statistics (FISST). It estimates all the targets states at once, as a multitarget state, projected on the

single-target space.

The PHD filter has been shown an effective way of tracking a time-varying multiple number of targets that avoids model-data association problems [56]. A Gaussian mixture implementation of PHD filter (GM-PHD) is presented in [89]. For nonlinear measurements, the Sequential Monte Carlo (SMC) implementation of the PHD filter is presented in [10].

Chapter 3

Multiple Detection Target Tracking

Most detection-based target tracking algorithms assume that a target generates at most one detection per scan with probability of detection less than unity. In this case, the data association uncertainty is only the measurement origin uncertainty [14] [92]. Thus, given a set of measurements in a scan, at most one of them can originate from the target and the rest have to be false alarms. This basic assumption results in the formulation of one-to-one measurement-to-track association as an optimization or enumeration problem. For example, in the Probabilistic Data Association (PDA) filter[1][15][44][92] and its multitarget version, the Joint Probabilistic Data Association (JPDA) filter [2][20][57][71], presented in Chapter 2, weights are assigned to measurements based on a Bayesian assumption that only one of the measurements is from the target and the rest are false alarms. Similarly, in the Multiple Hypothesis Tracker (MHT) [19][45][49][69] hypotheses are generated based on one-to-one measurement-to-track association. This assumption extends to the Multiframe Assignment (MFA) algorithm [76][91] since the measurement-to-track association is evaluated as one-to-one combinatorial optimization in the best global hypothesis. In all these cases, the

one-to-one assumption is fundamental for the correct measurement-to-track associations and accurate target state estimation.

However, a target can generate multiple detection in a scan due to, for example, multipath propagation or extended nature of the target with a high resolution radar. When multiple detection from the same target fall within the association gate, the PDAF and its multitarget version, the JPDAF, tend to apportion the association probabilities, but still with the fundamental assumption that only one of them is correct. When the measurements are not close to one other, as in the case of multipath detection, the PDAF and JPDAF initialize multiple tracks for the same target. The MHT algorithm tends to generate multiple tracks to handle the additional measurements from the same target due to the basic assumption that at most one measurement originated from each target. Thus, an algorithm that explicitly considers multiple detection from the same target in a scan needs to be developed so that all useful information in the received measurements about the target is processed with the correct assumption. The presence of multiple detection per target per scan increases the complexity of a tracking algorithm due to uncertainty in the number of target-originated measurements, which can vary from time to time, in addition to the measurement origin uncertainty. However, estimation accuracy can be improved and the number of false tracks can be reduced using the correct assumption with multiple-detection.

Multiple-detection is a common phenomenon in target tracking with over-the-horizon radars (OTHRs) [34][37], which provides the motivation for this research work. This is due to the OTHR's reliance on the ionospheric layers for signal transmission and reception. The signal transmitted from an OTHR will be scattered by

one of the ionospheric layers, then scattered from the target, and finally scattered by another or the same ionospheric layer before it is collected by a receiver as shown in Figure 3.1. Hence, there will be multiple propagation paths due to multiple ionospheric layers that grow with the number of ionospheric layers. Among the various possible signal propagation paths, a target might be either detected or missed in one or more propagation paths. A tracker has to determine from which propagation path(s) a target is detected while processing multiple target-originated measurements.

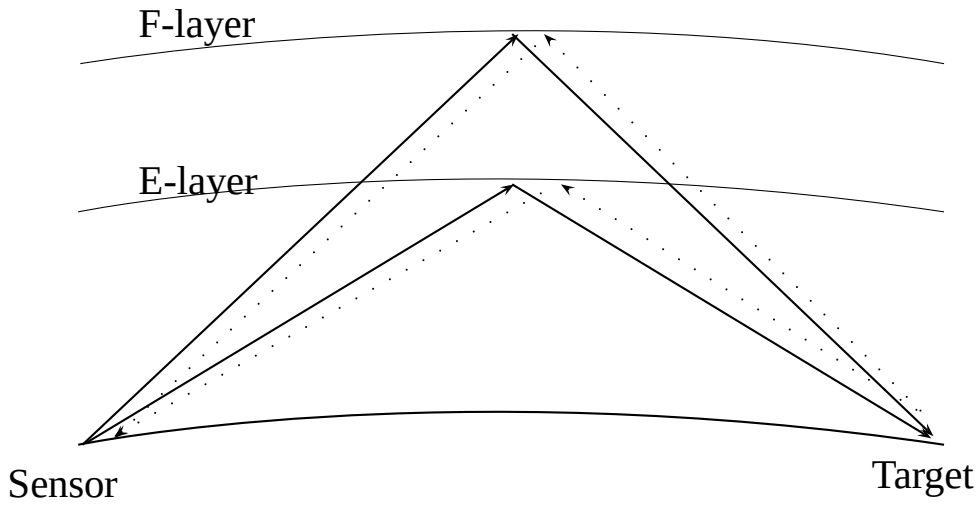

Figure 3.1: Representative OTHR propagation modes.

In the literature, different techniques have been proposed to solve the multipath problem with OTHRs. With respect to target localization, the maximum likelihood coordinate registration for the OTHR is developed in [47]. Furthermore, using the OTHR, target localization based on a Markov model is presented in [1] and maneuvering target detection using adaptive clutter rejection is presented in [32]. A multiple hypothesis tracking-based multipath fusion algorithm is presented in [81], MHT for

multiple simultaneous measurements in [85], a multipath track association with Langragian relaxation is presented in [50], a track fusion in [61] and MCMC data association in [26]. PDAF versus PMHT Performance on OTHR Data is presented in [75] and a multipath PDAF (MPDAF) is proposed in [65][66].

However, in this MPDAF approach, identical probabilities of target detection for all propagation modes are assumed, which might not be always the case. Furthermore, the MPDAF is limited to a single target tracking problem and its formulation assumes that the target exists or is observable in all propagation modes although it may not be detected by one or more modes in practice. A related work is also done to jointly associate measurement from multiple sensors [38][77] and multiple scans [39] using probabilistic data association. A random finite set (RFS) based approach to solve the problem of multiple detection per target per scan is proposed in [10] using 2D position-only measurements.

A new Multiple-Detection Joint Probabilistic Data Association Filter (MD-JPDAF) is proposed for multitarget tracking. While the algorithm is motivated by the OTHR problem, it is applicable to any multitarget tracking problem with multiple detection per target. The filtering algorithm is derived with the explicit assumption of multiple detection so that a multiple-detection pattern would account for all possible many-to-one measurement set-to-track association rather than a one-to-one measurement-to-track association. In the proposed MD-JPDAF, combinatorial association events are formed to handle the possibility of multiple measurements from the same target in a scan. Multiple association events are formed by creating φ out of m combinations of multiple measurements to track assignment, where φ is the number of target-originated measurements and m is the total number of measurements in the

validation gate. Priori information on the number of target-originated measurements can also be used, if available, to determine the probability of detection conditioned on the number of target-originated measurements and to reduce the total number of association events. For each association event, the event probabilities are calculated based on probabilistic inference made on no measurement, one measurement or a set of measurements originating from the target. With this explicit multiple-detection, many-to-one measurement set-to-track formulation, the proposed algorithm can handle the uncertainty in the number of target-originated measurements in addition to measurement origin uncertainty.

If the target is detected only once per scan, the MD-JPDAF will reduce to the conventional JPDAF. In simulations, the performance of different tracking algorithms are analyzed by generating multiple-detection measurements from a target observed in clutter. In addition, the proposed algorithm is applied to tracking in multipath with OTHRs. Performance of the proposed MD-JPDAF is compared with that of the conventional JPDAF. Results of performance evaluation show the effectiveness of the new algorithm with respect to estimation accuracy. However, the computational complexity of the proposed algorithm is higher due to increased number of association events.

The rest of the chapter is organized as follows. In Chapter 3 multiple-detection based probabilistic data association algorithms for single target tracking, MD-PDAF, and for multitarget tracking, MD-JPDAF, are presented. Multiple-detection pattern that generates the possible measurement set-to-track association events is discussed in Section 3.1. In addition, in Section 3.3, the multiple-detection PCRLB is derived, which provides a theoretical benchmark to compare the estimation accuracy of the

proposed MD-PDAF and MD-JPDAF. Section 3.4 concludes the chapter with the simulation experiment of target tracking with multiple-detection 2D radar and multi-path OTH radar as well as with the performance evaluation the proposed techniques.

3.1 Multiple-Detection Pattern

If multiple detection from the same target fall within the association gate, a measurement or a set of measurements will be associated with a track. Data association uncertainty corresponding to a number of target-originated measurements as well as measurement source can be resolved by generating a multiple-detection pattern. The multiple-detection pattern will consider all possible events for many-to-one measurement set-to-track association.

Here, it is assumed that the target state $x(k)$ evolves according to the nearly constant velocity model equation 2.2. The nonlinear measurement model for the measurement z of dimension n_z is described by

$$z(k) = h_{\varphi}(x(k)) + v_{\varphi}(k) \tag{3.1}$$

where h_{φ} and $v_{\varphi}(k)$ are the nonlinear measurement function and measurement noise, respectively, corresponding to the φ-th measurement mode. The measurement noise is assumed to be zero-mean white Gaussian with covariance $R_{\varphi}(k)$. The process and measurement noises are assumed to be independent.

After signal processing, thresholding and extracting the detection, gating has to be applied to reduce the number of measurements as shown in Figure 3.2 for a single observation model and in Figure 3.3 for a multiple observation models (propagation

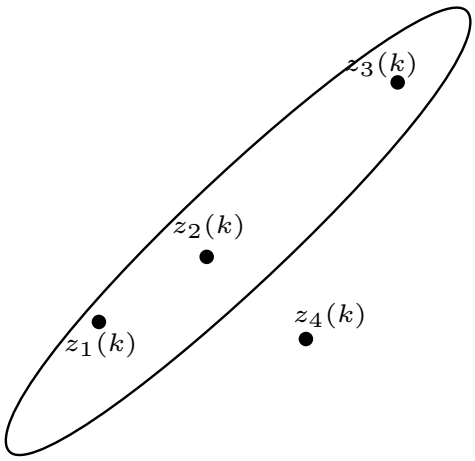

Figure 3.2: Measurement validation gate for a single observation model/propagation path.

paths). As a result, the number of feasible events that are generated based on the measurements will be reduced. The multiple mode validation gate is the union of n_z-dimensional ellipses given by

$$\begin{aligned} \mathcal{G}(k) &= \bigcup_{\varphi=1}^{\varphi_{max}} \mathcal{G}_\varphi(k) \\ \mathcal{G}_\varphi(k) &= \{z(k) : [z(k) - \hat{z}_\varphi(k|k-1)]' S_\varphi(k)^{-1} \\ &\qquad [z(k) - \hat{z}_\varphi(k|k-1)] \leqslant g^2\} \end{aligned} \tag{3.2}$$

Here, g^2 is the gate threshold, $\hat{z}_\varphi(k|k-1)$ is the predicted measurement, and $S_\varphi(k)$ is the innovation covariance that corresponds to the φ-th measurement, which

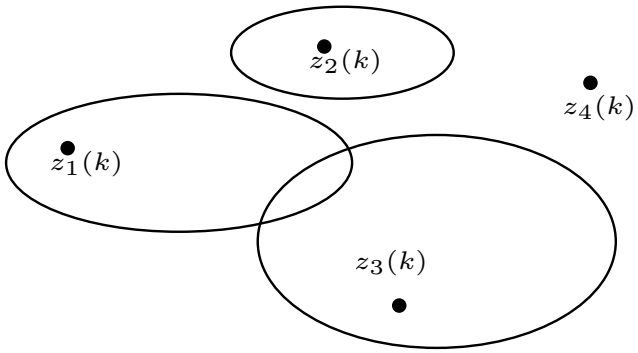

Figure 3.3: Measurement validation gate for multiple observation models/propagation paths.

is given by

$$S_{\varphi}(k) = H_{\varphi}(k)P(k|k-1)H_{\varphi}(k)' + R_{\varphi}(k) \tag{3.3}$$

where $P(k|k-1)$ is the predicted covariance and $H_{\varphi}(k)$ is the Jacobian matrix of the nonlinear measurement function h_{φ}.

For $m(k)$ measurements inside the validation gate, φ out of $m(k)$ association events are evaluated. Here, φ runs from 1 to the maximum number of target-originated measurements. Then,

$$N_a = \sum_{i=0}^{\varphi_{max}} C_i^{m(k)} \tag{3.4}$$

where N_a is the total number of measurement set-to-track association events and C_x^y

is the number of combinations of x out of y objects defined by

$$C_x^y = \begin{cases} \frac{y!}{x!(y-x)!}, & 1 \leq x \leq y \\ 1, & x = 0 \end{cases} \tag{3.5}$$

The total association event count, N_a, represents all possible events from zero target-originated measurement to all of the measurements being target-originated. For example, as depicted in Figure 3.2 and Figure 3.3, there are four measurements, $(z_1(k), z_2(k), z_3(k), z_4(k))$, in the scan. Out of the four measurements, three of them, $(z_1(k), z_2(k), z_3(k))$, are inside the validation gate. Combinatorial association events are created only for those measurements that fall inside the validation gate. The maximum number of target-originated measurement is assumed to be $\varphi_{max} = 3$. Thus the possible events are:

- none of the measurements is target-originated
  - $\varphi = 0$, $n_\varphi = 1$.
- one of the measurements is target-originated
  - $\varphi = 1$, $n_\varphi = C_1^3 = 3$,
  - 3 measurement set-to-track association events,
  - $z_1(k)$ or $z_2(k)$ or $z_3(k)$ originated from a target,

$$z_{1,1}(k) = z_1(k) \tag{3.6}$$

$$z_{1,2}(k) = z_2(k) \tag{3.7}$$

$$z_{1,3}(k) = z_3(k) \tag{3.8}$$

- two of the measurements are target-originated
  - $\varphi = 2$, $n_\varphi = C_2^3 = 3$,
  - 3 measurement set-to-track association events,
  - $z_1(k), z_2(k)$ or $z_1(k), z_3(k)$ or $z_2(k), z_3(k)$ originated form a target

$$z_{2,1}(k) = \begin{bmatrix} z_1(k) \\ z_2(k) \end{bmatrix} \tag{3.9}$$

$$z_{2,2}(k) = \begin{bmatrix} z_1(k) \\ z_3(k) \end{bmatrix} \tag{3.10}$$

$$z_{2,3}(k) = \begin{bmatrix} z_2(k) \\ z_3(k) \end{bmatrix} \tag{3.11}$$

- all of the measurements are target-originated
  - $\varphi = 3$, $n_\varphi = C_3^3 = 1$,
  - 1 measurement set-to-track association event,
  - $z_1(k), z_2(k), z_3(k)$ originated from a target,

$$z_{3,1}(k) = \begin{bmatrix} z_1(k) \\ z_2(k) \\ z_3(k) \end{bmatrix} \tag{3.12}$$

Accordingly, the measurement equation for the (φ, n_φ) event becomes

$$z_{\varphi,n_\varphi}(k) = \begin{bmatrix} h_1(x(k)) \\ \vdots \\ h_\varphi(x(k)) \end{bmatrix} + \begin{bmatrix} v_1(k) \\ \vdots \\ v_\varphi(k) \end{bmatrix} \tag{3.13}$$

3.2 MD-PDAF and MD-JPDAF

The approach of the standard PDAF is to calculate the association probabilities for each measurement that falls in the validation region around the predicted measurement [14]. If two of the measurements are target-originated, the algorithm apportions the total weight among the validated measurements with more weight to target-originated measurements, with the assumption that only one of them is target-originated. It is not the correct approach especially when there are false alarms in the validation gate. This is because the weight assigned to false alarms becomes significant compared to the divided weight assigned to target-originated measurements.

The proposed multiple-detection based algorithms evaluate the association probabilities of the events generated by multiple-detection pattern. These event probabilities are calculated based on probabilistic inference made on the number of validated measurements, the number of target-originated measurements and the measurements locations.

3.2.1 MD-PDAF for Single Target Tracking

The MD-PDAF is formulated under the following assumptions:

- Among the validated measurements, a measurement or a set of measurements

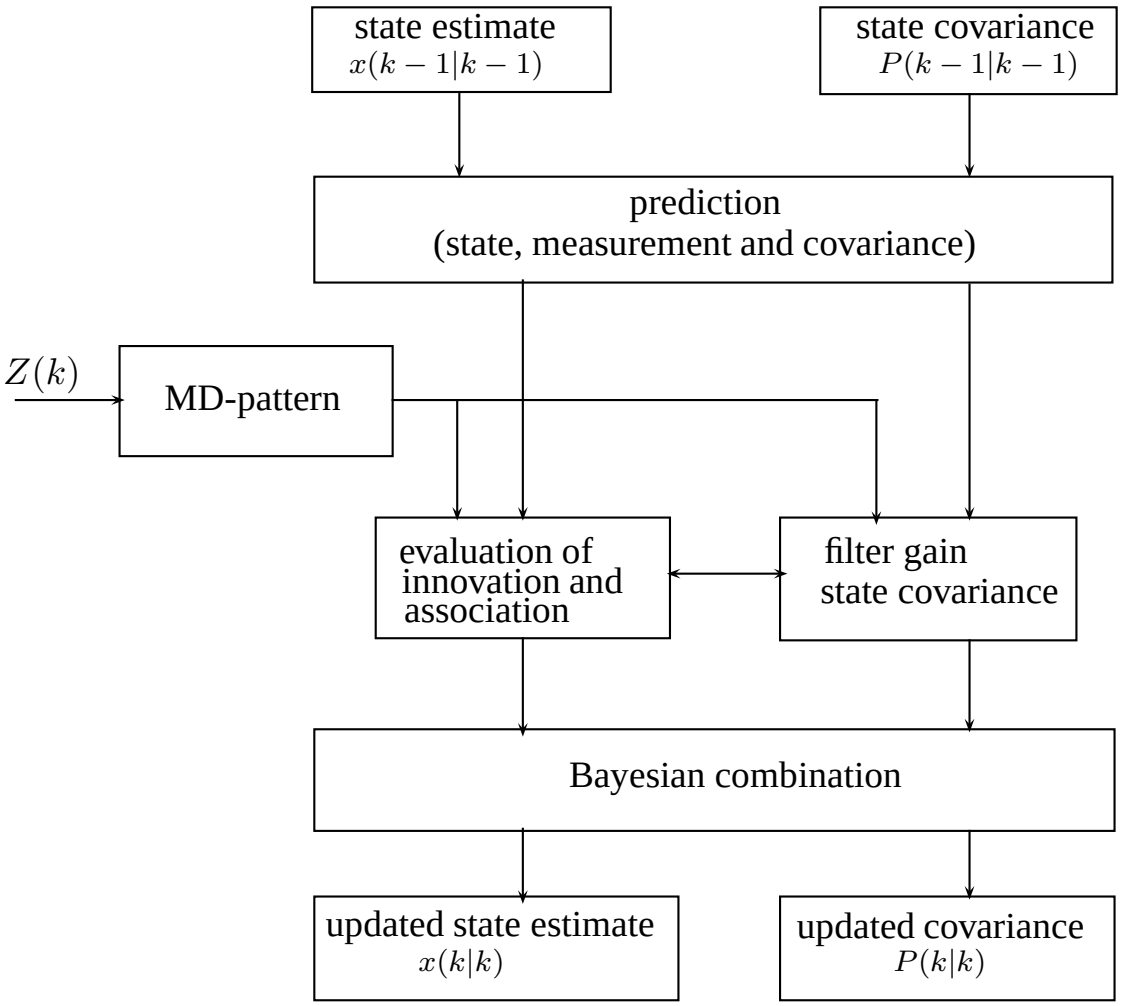

Figure 3.4: Flow of MD-PDAF.

can originate from a target.

- The target detection occur independently with known target detection probabilities.
- Clutter is assumed to be uniformly/Poisson distributed within the measurement validation gate [14].
- There is only one target of interest whose state evolves according to a dynamic equation driven by process noise as stated in (2.2). Closely spaced multiple targets are considered in Section 3.2.2.
- The track has been initiated. Note that here a one- or two-point initialization technique can be used for track initialization [93].

The MD-PDAF calculates the probability that each set of measurements, rather than a single measurement, is attributable to the target of interest. The sets of measurement candidates for association are generated from the multiple-detection pattern discussed in Section 3.1. This probabilistic (Bayesian) information based on the candidate set of measurements is used in a tracking filter that updates the target states.

Accordingly, based on the multiple-detection pattern presented in Section II, the measurement set-to-target association events are given as

$$\theta_{\varphi,n_\varphi}(k) = \begin{cases} \text{chosen } \varphi \text{ measurements are target-originated} \\ n_\varphi = 1, ..., c_{\varphi m}(k) \\ \text{none of the other measurements are target-originated} \\ n_\varphi = 0 \end{cases} \tag{3.14}$$

where n_φ is a variable that enumerates the events under the chosen φ target-originated measurements, and $c_{\varphi m}(k)$ is φ combinations out of $m(k)$ measurements given by

$$c_{\varphi m}(k) = \frac{m(k)!}{\varphi!(m(k)-\varphi)!} \tag{3.15}$$

Table 3.1: Number of Multiple-Detection Association Events

Number of Measurements $m(k)$	Number of Association Events, N_a		
	$\varphi_{max}=2$	$\varphi_{max}=3$	$\varphi_{max}=m(k)$
2	4	4	4
3	7	8	8
4	11	15	16
5	16	26	32
6	22	42	64
7	29	64	128
8	37	93	256

The number of association events grows rapidly for $\varphi > 2$ as shown in Table 3.1. However, for a practical system, the expected number of target-originated measurements can be used as a priori to reduce the number of association events. For example, for over-the-horizon radars with four possible propagation paths (e.g., only E and F layers [37]) the maximum number of target-originated measurements will be four and the association variable φ runs from zero to four.

Thus the conditional mean is given by

$$\begin{aligned}\hat{x}(k|k) &= E(x(k)|Z^k) \\ &= \sum_{\varphi=0}^{m(k)} \sum_{n_\varphi=1}^{c_{\varphi m}(k)} E(x(k)|\theta_{\varphi,n_\varphi}(k), Z^k) p(\theta_{\varphi,n_\varphi}(k)|Z^k) \qquad (3.16) \\ &= \sum_{\varphi=0}^{m(k)} \sum_{n_\varphi=1}^{c_{\varphi m}(k)} \hat{x}_{\varphi,n_\varphi}(k|k)\beta_{\varphi,n_\varphi}(k) \qquad (3.17)\end{aligned}$$

The estimate conditioned on n_φ^{th} combination of φ measurements being correct is

$$\hat{x}_{\varphi,n_\varphi}(k|k) = \hat{x}(k|k-1) + W_{\varphi,n_\varphi}(k)\nu_{\varphi,n_\varphi}(k) \qquad (3.18)$$

where the corresponding innovation is

$$\nu_{\varphi,n_\varphi}(k) = \begin{bmatrix} (z(k) - \hat{z}_1(k|k-1))' \\ \vdots \\ (z(k) - \hat{z}_\varphi(k|k-1))' \end{bmatrix} \qquad (3.19)$$

The Kalman gain $W_{\varphi,n_\varphi}(k)$ is given as

$$W_{\varphi,n_\varphi}(k) = P(k|k-1)H_{\varphi,n_\varphi}(k)'S_{\varphi,n_\varphi}(k)^{-1} \qquad (3.20)$$

where

$$S_{\varphi,n_\varphi}(k) = H_{\varphi,n}(k)P(k|k-1)H_{\varphi,n_\varphi}(k)' + R_{\varphi,n_\varphi}(k) \tag{3.21}$$

$$H_{\varphi,n_\varphi}(k) = [H_1(k), \cdots, H_\varphi(k)]' \tag{3.22}$$

$$R_{\varphi,n_\varphi}(k) = \begin{bmatrix} R_1(k) & 0 & \dots & 0 \\ 0 & R_2(k) & \dots & 0 \\ \vdots & \vdots & \ddots & \vdots \\ 0 & 0 & \dots & R_\varphi(k) \end{bmatrix} \tag{3.23}$$

Here $\beta_{\varphi,n_\varphi}(k) \propto p(\theta_{\varphi,n_\varphi}(k)|Z^k)$ is the conditional probability of the event where the probabilistic inference is made on the number of validated measurements ($m(k)$), number of target-originated measurements (φ) and measurements locations (see Appendix A.0.1). Then,

$$\begin{aligned}\beta_{\varphi,n_\varphi}(k) = \frac{1}{c}p(Z^k|\theta_{\varphi,n_\varphi}(k), m(k), \varphi, Z^{k-1}) \\ \times p(\theta_{\varphi,n_\varphi}(k)|m(k), \varphi)\end{aligned} \tag{3.24}$$

The first term in (3.24) refers to the joint density of the pdf of the correct measurement is given in (3.25) where P_G is the factor that accounts for restricting the normal density

to the validation gate. Thus,

$$p(Z^k|\theta_{\varphi,n_\varphi}(k), m(k), \varphi, Z^{k-1}) = \begin{cases} P_G^{-1}\{\bigcup_{i=1}^{\varphi}\mathcal{G}_i(k)\}^{-m(k)+\varphi}\mathcal{N}(\nu_{\varphi,n_\varphi}(k); 0, S_{\varphi,n_\varphi}(k)) \\ \qquad\qquad\qquad\qquad n_\varphi = 1, ..., c_{\varphi m}(k) \\ \{\bigcup_{i=1}^{\varphi}\mathcal{G}_i(k)\}^{-m(k)} \\ \qquad\qquad\qquad\qquad n_\varphi = 0 \end{cases} \tag{3.25}$$

The second term in (3.24) is the probability of the association events conditioned only on $m(k)$ and φ. Here,

$$p(\theta_{\varphi,n_\varphi}(k)|m(k), \varphi) = \begin{cases} \frac{1}{m(k)}\frac{P_{D\varphi}P_G\mu(m(k)-\varphi)}{\sum_{\varphi=1}^{m(k)}P_{D\varphi}P_G\mu(m(k)-\varphi)+(1-P_DP_G)\mu(m(k))} \\ \qquad\qquad\qquad\qquad n_\varphi = 1, ..., c_{\varphi m}(k) \\ \frac{(1-P_DP_G)\mu(m(k))}{\sum_{\varphi=1}^{m(k)}P_{D\varphi}P_G\mu(m(k)-\varphi)+(1-P_DP_G)\mu(m(k))} \\ \qquad\qquad\qquad\qquad n_\varphi = 0 \end{cases} \tag{3.26}$$

where $\mu(\cdot)$ is the probability mass function of the number of false alarms, $P_{D\varphi}$ is the probability of detecting a target φ times per scan and $P_D = \sum_{\varphi=1}^{\varphi_{max}} P_{D\varphi}$ is the total probability of target detection.

The state update equation is given by

$$\hat{x}(k|k) = \hat{x}(k|k-1) + \sum_{\varphi=0}^{m(k)}\sum_{n_\varphi=1}^{c_{\varphi m}(k)} W_{\varphi,n_\varphi}(k)\beta_{\varphi,n_\varphi}(k)\nu_{\varphi,n_\varphi}(k) \tag{3.27}$$

and the covariance associated with the updated state is

$$\begin{aligned} P(k|k) &= E\{[x(k)-\hat{x}(k|k)][x(k)-\hat{x}(k|k)]'|Z^k\} \\ &= \sum_{\varphi=0}^{m(k)} \sum_{n_\varphi=1}^{c_{\varphi m}(k)} \beta_{\varphi,n_\varphi}(k) E\left\{[x(k)-\hat{x}(k|k)][x(k)-\hat{x}(k|k)]'|\theta_{\varphi,n_\varphi}(k), Z^k\right\} \end{aligned} \tag{3.28}$$

Parametric or nor-parametric [14] MD-PDAF can be developed based on the assumed Poisson or diffuse a priori model used for the probability mass function of the number of false measurements.

Hence,

- Poisson model (parametric MD-PDAF):

$$\mu(m(k)) = e^{-\lambda\{\bigcup_{i=1}^{\varphi}\mathcal{G}_i(k)\}} \frac{(\lambda\{\bigcup_{i=1}^{\varphi}\mathcal{G}_i(k)\})^{m(k)}}{m(k)!} \tag{3.29}$$

  where λ is the spatial density.

- Diffuse a prior model (non-parametric MD-PDAF):

$$\mu(m(k)) = \mu(m(k)-\varphi) = K \tag{3.30}$$

  where K is a constant.

3.2.2 MD-JPDAF for Multitarget Tracking

If the targets are close to one another with overlapping validation regions, a measurement or set of measurements could be generated from more than one target. This will result in further measurement source uncertainty in addition to measurement

uncertainties associated with single target or widely separated targets.

This additional uncertainty can be resolved by considering joint measurement set-to-track association events [14]. With multiple detection the conditional probabilities based on joint association events are given as:

$$\Theta_J(k) = \bigcap_{\varphi_t=0}^{m(k)} \bigcap_{n_{\varphi_t}=1}^{c_{\varphi_t m}(k)} \theta_{\varphi_t,n_{\varphi_t}}(k) \tag{3.31}$$

where $\theta_{\varphi,n_{\varphi_t}}(k)$ is the event that measurement set $z_{\varphi_t,n_{\varphi_t}}$ originated from target t, $t = 0, 1, \cdots, \tilde{T}$, for $\tilde{T}$ number of targets. The event matrix for the joint measurement set-to-track association event $\Theta_J(k)$ is given by

$$\hat{\Omega}_J(\Theta_J(k)) = [\hat{\omega}_{\varphi_t,n_{\varphi_t}}(\Theta_J(k))] \tag{3.32}$$

where $\hat{\omega}_{\varphi_t,n_{\varphi_t}}(\Theta_J(k)) = 1$ if $\theta_{\varphi_t,n_{\varphi_t}}(k) \in \Theta_J(k)$, and is zero otherwise. A given measurement set can also originate from a target so that

$$\delta_t(\Theta_J(k)) := \sum_{\varphi=0}^{m(k)} \sum_{n_\varphi=1}^{c_{\varphi m}(k)} \hat{\omega}_{\varphi_t,n_{\varphi_t}} \leq 1 \tag{3.33}$$

Here, define a binary measurement set association indicator

$$\tau_{\varphi,n_\varphi}(\Theta_J(k)) = \sum_{t=1}^{\tilde{T}} \hat{\omega}_{\varphi_t,n_{\varphi_t}}(\Theta_J(k)) \tag{3.34}$$

in order to indicate if the measurement set $z_{\varphi_t,n_{\varphi_t}}$ is associated to a target in the event $\Theta_J(k)$. In addition, the number of unassociated measurement sets in the event

$\Theta_J(k)$ is given by

$$\phi(\Theta_J(k)) = \sum_{\varphi=0}^{m(k)} \sum_{n_\varphi=1}^{c_{\varphi m}(k)} [1 - \tau_{\varphi,n_\varphi}(\Theta_J(k))] \tag{3.35}$$

In an approach similar to (3.24), the joint measurement set-to-track association probability $p(\Theta_J(k)|Z^k)$ is equivalent to the product of the measurement likelihood function, $p(Z(k)|\Theta_J(k), m(k), \varphi_t, Z^{k-1})$, and prior probability, $p(\Theta_J(k)|m(k), \varphi_t, Z^{k-1})$. Therefore, the measurement set likelihood function is evaluated as

$$\begin{aligned} &p(Z(k)|\Theta_{Jt}(k), m(k), \varphi_t, Z^{k-1}) = \\ &\qquad \prod_{\varphi_t=0}^{m(k)} \prod_{n_{\varphi_t=1}}^{c_{\varphi_t m}(k)} p(z_{\varphi_t,n_{\varphi_t}}(k)|\theta_{\varphi_t,n_{\varphi_t}}(k), m(k), \varphi_t, Z^{k-1}) \end{aligned} \tag{3.36}$$

where the conditional pdf of a measurement given its origin is

$$\begin{aligned} &p(z_{\varphi_t,n_{\varphi_t}}(k)|\theta_{\varphi_t,n_{\varphi_t}}(k), m(k), \varphi_t, Z^{k-1}) = \\ &\qquad \begin{cases} P_G^{-1} N(z_{\varphi_t,n_{\varphi_t}}(k); \hat{z}_{\varphi_t,n_{\varphi_t}}(k|k-1), S_{\varphi_t,n_{\varphi_t}}(k)) \\ \qquad\qquad \text{if } \tau_{\varphi,n_\varphi}(\Theta_J(k)) = 1 \\ \{\bigcup_{i=1}^{\varphi} \mathcal{G}_i(k)\}^{-1} \\ \qquad\qquad \text{if } \tau_{\varphi,n_\varphi}(\Theta_J(k)) = 0 \end{cases} \end{aligned} \tag{3.37}$$

and the prior joint association probability is given as

$$\begin{aligned} p(\Theta_{Jt}(k)|m(k), \varphi_t, Z^{k-1}) = &\left(\frac{\phi(\Theta_J(k))!}{c_{\varphi_t m}(k)!} \mu(\phi) \right) \times \\ &\prod_{t=1}^{\tilde{T}} (P_{D_{\varphi_t}} P_G)^{\delta_t(\Theta_J(k))} (1 - P_{D_t} P_G)^{1-\delta_t(\Theta_J(k))} \end{aligned} \tag{3.38}$$

where $P_{D_{\varphi_t}}$ is the probability of detecting the t-th, φ times per scan and $P_{D_t} =$

$\sum_{\varphi=1}^{\varphi_{max}} P_{D_{\varphi_t}}$ is the total probability of target detection.

Furthermore, target birth and target existence modes can be incorporated into the MD-JPDAF to handle varying number of targets [28][57]. The main focus of this research is integrating the multiple detection pattern into the probabilistic data association filter for a single and multiple targets problem. However, with a similar approach, a Multiple-Detection Joint Integrated Probabilistic Data Association filter (MD-JIPDAF) can be developed.

3.3 MD-PCRLB

In this section, the Multiple Detection Posterior Cramér-Rao Lower Bound (MD-PCRLB), which is explicitly derived for the multiple-detection purpose, is presented. The PCRLB [59] provides a theoretical lower bound that can be used as a benchmark for estimation performance evaluation.

The standard PCRLB also makes the one-to-one assumption, which necessitates the new derivation of the modified MD-PCRLB that accounts for multiple detection. First, a review on PCRLB is provided and the derivation considering the effect of multiple-detection is presented next.

3.3.1 Background

Let $\hat{x}(k|k)$ be an unbiased estimate of the state vector $x(k)$ based on measurements $Z(k)$ and prior initial density $p(x_0)$. Let $P(k|k)$ be the covariance of $\hat{x}(k|k)$. Then $P(k|k)$ has a lower bound known as the PCRLB, i.e.,

$$P(k|k) = E\left[(\hat{x}(k) - x(k))(\hat{x}(k) - x(k))'|Z(k)\right] \geq J(k)^{-1} \tag{3.39}$$

where $J(k)$ is the Fisher information matrix (FIM). A recursive formula for the evaluation of the posterior FIM [59][52] is given by

$$J(k) = J_x(k) + J_z(k) \tag{3.40}$$

The first term in (3.40), i.e., the prior information regarding the target states, is given by

$$J_x(k+1) = D_{22}(k) - D_{21}(k)(J(k) + D_{11}(k))^{-1} D_{12}(k) \tag{3.41}$$

$$\tag{3.42}$$

where

$$\begin{aligned} D_{11}(k) &= E\left[-\Delta_{x_k}^{x_k} \log\, p(x(k+1)|x(k))\right] && (3.43)\\ D_{12}(k) &= (D_{21}(k))' \\ &= E\left[-\Delta_{x_k}^{x_{k+1}} \log\, p(x(k+1)|x(k))\right] && (3.44)\\ D_{22}(k) &= E\left[-\Delta_{x_{k+1}}^{x_{k+1}} \log\, p(x(k+1)|x(k))\right] \end{aligned}$$

$$\tag{3.45}$$

Δ is a second-order partial derivative operator whose (i,j)-th term is given by

$$\left[\Delta_{\alpha}^{\beta}\right]_{ij} = \frac{\partial^2}{\partial \alpha_i \partial \beta_j} \tag{3.46}$$

Here, for a linear and Gaussian system transition model, it can be shown that [59]

$$J_x(k+1) = \left[Q + F(J(k)^{-1})F'\right]^{-1} \tag{3.47}$$

The second term in (3.40), i.e., the measurement contribution factor, is given by

$$J_z(k+1) = E\left[-\Delta_{x_{k+1}}^{x_{k+1}} \log\, p(Z(k+1)|x(k))\right] \tag{3.48}$$

3.3.2 Effect of Multiple Detection

Let $m(k)$ be the total number of measurements from sensor at time k. Thus,

$$z(k) = \{z_i(k)\}_{i=1}^{m(k)} \tag{3.49}$$

Under the assumption that false alarms are uniformly distributed in the measurement space and the number of false alarms is Poisson distributed, the probability of getting $m(k)$ number of measurements out of which φ are target-originated is

$$\begin{aligned} p(m(k),\varphi) = (1-P_{D\varphi})\frac{(\lambda\{\bigcup_{i=1}^{\varphi}\mathcal{G}_i(k)\})^{m(k)}e^{-\lambda\{\bigcup_{i=1}^{\varphi}\mathcal{G}_i(k)\}}}{m(k)!} \\ +P_{D\varphi}\frac{(\lambda\{\bigcup_{i=1}^{\varphi}\mathcal{G}_i(k)\})^{m(k)-\varphi}e^{-\lambda\{\bigcup_{i=1}^{\varphi}\mathcal{G}_i(k)\}}}{(m(k)-\varphi)!} \end{aligned} \tag{3.50}$$

In the above, $P_{D\varphi}$ is the probability of detecting a target φ times per scan. The probability that φ measurements are target generated is then given by

$$\epsilon(m(k),\varphi) = \frac{P_{D\varphi}}{p(m(k),\varphi)} \times \frac{(\lambda\{\bigcup_{i=1}^{\varphi}\mathcal{G}_i(k)\})^{m(k)-\varphi}e^{-\lambda\{\bigcup_{i=1}^{\varphi}\mathcal{G}_i(k)\}}}{(m(k)-\varphi)!} \tag{3.51}$$

With the assumption of more than one target-originated measurements, the measurement information matrix is given by

$$J_z(k) = \sum_{\varphi=0}^{m(k)} p(m(k), \varphi) J_{z_\varphi}(k) \tag{3.52}$$

where

$$J_{z_\varphi}(k) = E\left[-\Delta_{x_{k+1}}^{x_{k+1}} \ln\, p(z_\varphi | x(k), m(k), \varphi)\right]. \tag{3.53}$$

Here, $z_\varphi = \left\{z_{\varphi,n_\varphi}\right\}_{n_\varphi=1}^{c_{\varphi m}(k)}$ and $p(z_\varphi|x(k), m(k), \varphi)$ is given by

$$\begin{aligned} p(z_\varphi|x(k), m(k), \varphi) = \frac{1-\epsilon(m(k),\varphi)}{\{\bigcup_{i=1}^{\varphi} \mathcal{G}_i(k)\}^{m(k)}} + \\ \frac{\epsilon(m(k),\varphi)}{c_{\varphi m}(k)\{\bigcup_{i=1}^{\varphi} \mathcal{G}_i(k)\}^{m(k)-\varphi}} \sum_{n_\varphi=1}^{c_{\varphi m}(k)} p(z_{\varphi,n_\varphi}|x(k)) \end{aligned} \tag{3.54}$$

where $p(z_{\varphi,n_\varphi}|x(k))$ is the pdf of the measurement set originated from a target.

3.4 Simulations

In the first part of this section, the comparison of the MD-PDAF with PDAF in terms of estimation accuracy is studied. The simulation is performed using a 2D sensor that returns multiple target-originated detection per scan. Later, a multitarget scenario is considered in this simulation that demonstrates the performance of the proposed MD-JPDA algorithm.

In the final part of simulation, the MD-JPDAF is applied to multipath tracking with OTHR and performance analysis is made with respect to estimation accuracy.

3.4.1 2D Sensor Single Target Scenario

A surveillance region covering a $1500\,\mathrm{m} \times 1500\,\mathrm{m}$ is considered. In this region, there is a target that starts from $[500\,\mathrm{m}, 800\,\mathrm{m}]$ with initial velocity $[8\,\mathrm{m/s}, 5\,\mathrm{m/s}]$. Track initialization is done using the two-point target initialization method. The scan interval (sampling period) is $1\,\mathrm{s}$ and the data set consists of 30 scans.

A multiple-detection sensor that returns more than one target-originated measurement per scan is used in this experiment. A 2D radar with low probability of detecting a target once per scan of the measurement data ($P_{D1} = 0.05$) and with high probability of detecting a target twice per scan of the measurement data ($P_{D2} = 0.90$) is considered. Hence, the total probability of detecting a target in a scan of the measurement data (i.e., P_D used for PDAF) will become $P_D = P_{D1} + P_{D2} = 0.95$. The false alarm rate is 5 false alarms per scan.

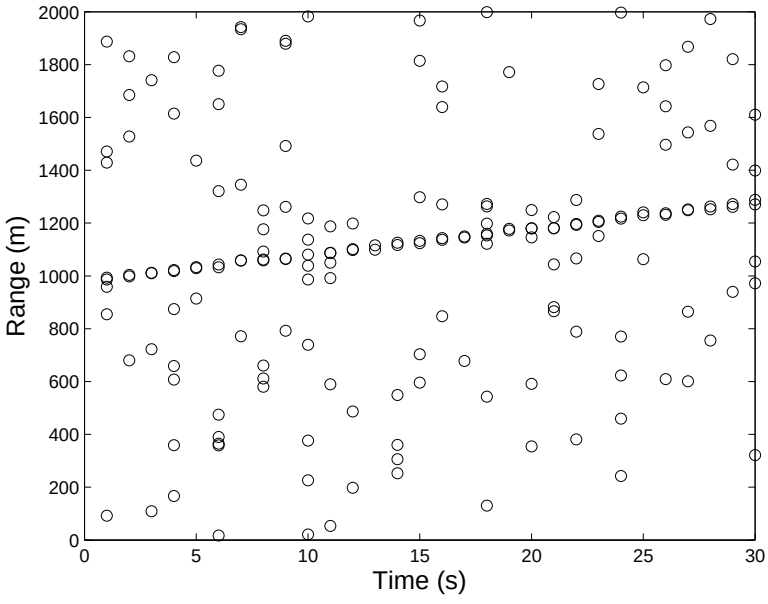

Figure 3.5: Range measurements in a single run.

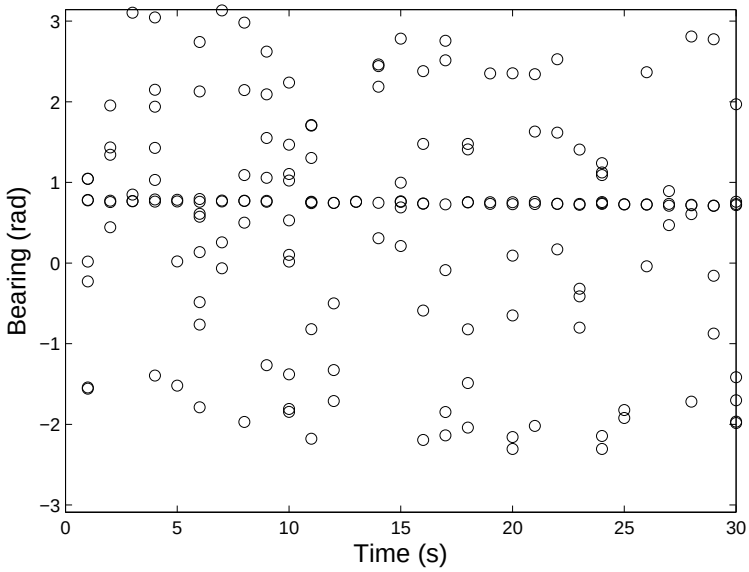

Figure 3.6: Bearing measurements in a single run.

Figure 3.5 and Figure 3.6 show the range and bearing measurements from a multiple-detection sensor. In the multiple target-originated measurements case, the probabilities of detection used with the MD-PDAF are P_{D1} and P_{D2} while $P_D = P_{D1} + P_{D2}$ is the total probability of detecting a target in PDAF.

Figure 3.7 shows the Root Mean Square Error (RMSE) for position estimation based on 500 MonteCarlo runs. The figure demonstrates the improved performance of the multiple-detection approach over the conventional probabilistic data association approach. While PDAF tends to apportion the weights among the target originated measurement, MD-PDAF assigns weights to measurement sets, rather than to a single measurement, that originated from a target. From the same figure it can be also seen that the state estimation accuracy of the MD-PDAF is close to the PCRLB that was derived for multiple detection.

Furthermore, the MD-PDAF is compared with PDAF for the case of a 2D radar

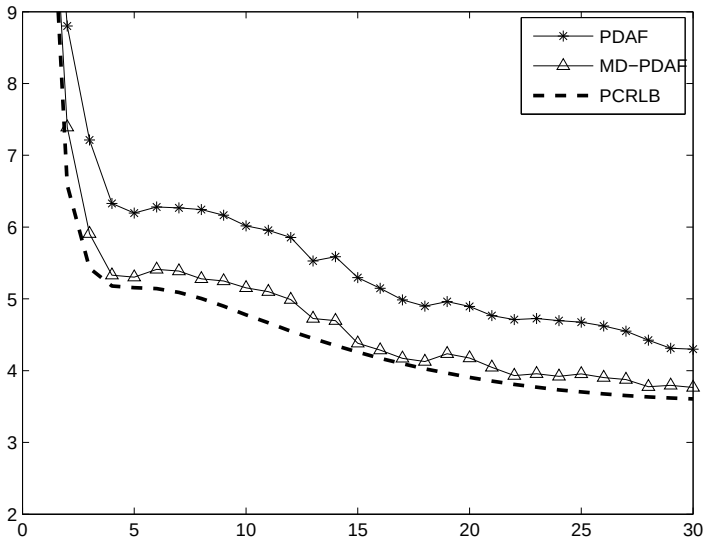

Figure 3.7: Position RMSE evaluation for MD-PDAF vs. PDAF and PCRLB ($P_{D1} = 0.05, P_{D2} = 0.90$).

with high probability of detecting a target once per scan of the measurement data ($P_{D1} = 0.90$) and with low probability of detecting a target twice per scan of the measurement data ($P_{D2} = 0.05$). As shown in Figure 3.8 the performance of MD-PDAF is similar with PDAF as MD-PDAF reduces to PDAF in a single detection scenario.

3.4.2 2D Sensor Multiple Target Scenario

A multitarget scenario with two closely spaced targets is considered to evaluate the performance of the proposed MD-JPDA algorithm. The first target (labeled as T-1) starts from $[700\,\mathrm{m}, 700\,\mathrm{m}]$ with initial velocity $[10\,\mathrm{m/s}, 3\,\mathrm{m/s}]$ and the second target (labeled as T-2) starts from $[700\,\mathrm{m}, 750\,\mathrm{m}]$ with initial velocity $[10\,\mathrm{m/s}, -3\,\mathrm{m/s}]$. The measurement validation regions of the targets overlap during the duration of $9 - 18\,\mathrm{s}$

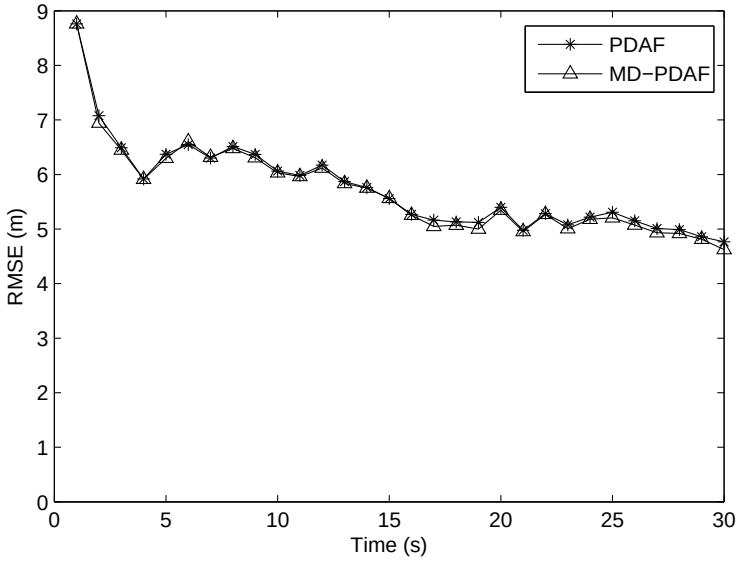

Figure 3.8: Position RMSE evaluation for MD-PDAF vs. PDAF ($P_{D1} = 0.90, P_{D2} = 0.05$).

that necessitates the evaluation of joint measurement set association events.

The targets are observed with a multiple detection sensor with similar multiple detection probabilities as the single target case above. The estimation error results, which are based on 100 MonteCarlo runs, are shown in Figure 3.9 and, as expected, it reveals the performance gain of the MD-JPDAF over the JPDAF in a multitarget scenario with multiple detection.

3.4.3 Over-the-Horizon Radar Scenario

In the OTHR scenario, transmitted signals scattered by the target arrive at the receiver via different propagation paths. Multipath propagation arises from the presence of regions with relatively high electron density in the ionosphere. As shown in Figure 3.10, a signal transmitted from the senor can be scattered by one of the two

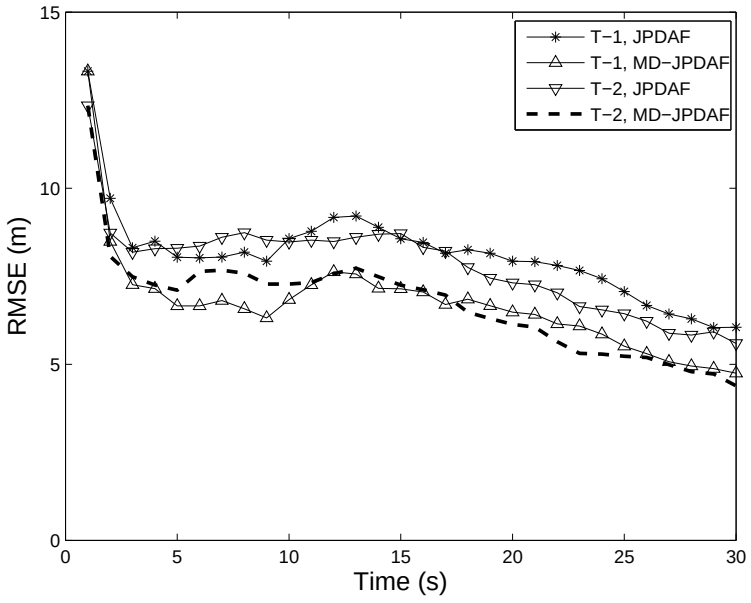

Figure 3.9: Position RMSE evaluation for MD-JPDAF vs. JPDAF (T-1 denotes the first target and T-2 denotes the second target).

ionospheric layers, scattered from the target and scattered again by one of the two ionospheric layers before it reaches the receiver. This phenomenon leads to more than one detection of the same target in a scan.

The OTHR measurement model used in this work is based on [65]. According to the model, the signal paths from the transmitter to the target and from the target to the receiver are scattering from idealized ionospheric layers with virtual heights h_E and h_F. With two ionospheric layers, denoted by E and F, there are four propagation modes:

- EE - transmit on E and receive on E,
- EF - transmit on E and receive on F,
- FE - transmit on F and receive on E,

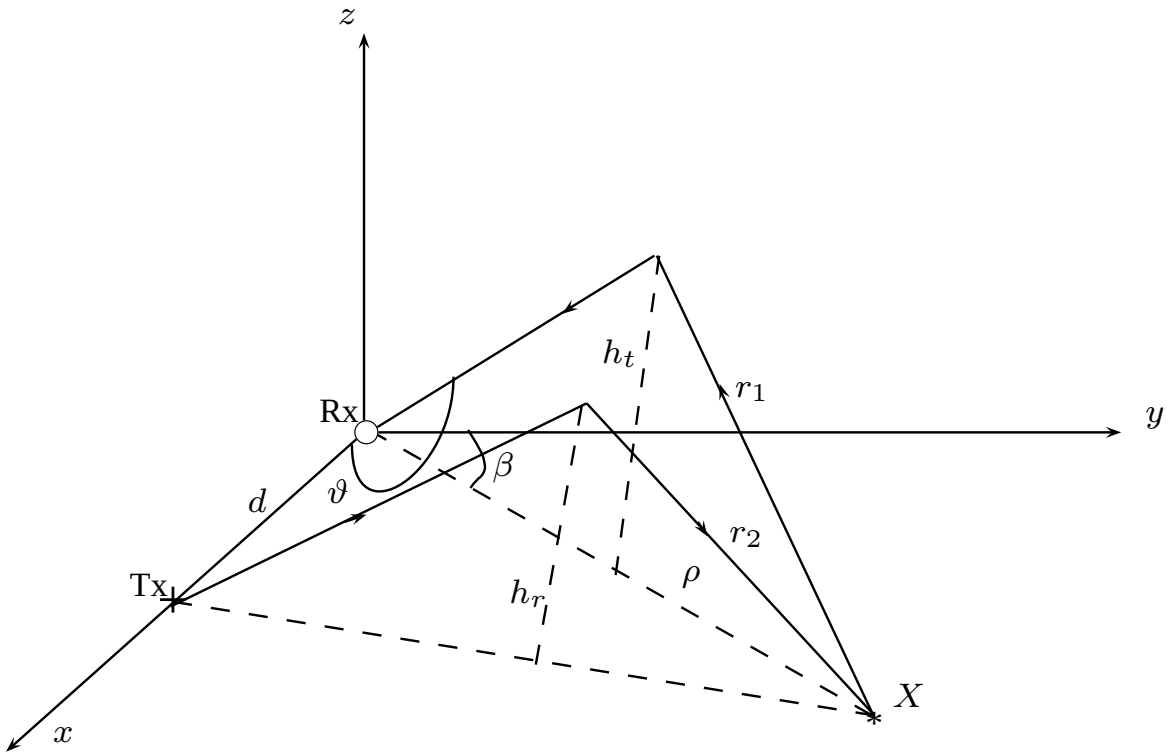

Figure 3.10: Over-the-horizon radar planar model (Tx - transmitter, Rx - receiver, X - target).

- FF - transmit on F and receive on F.

The ionospheric layer heights are assumed to be constant for the duration of the tracking. Actual models that take multiple-hop modes, ionospheric tilt, the curvature of the earth and uncertainty in the heights of ionospheric layers are not included for simplicity [37].

The measurements from the OTHR are mode-dependent azimuth, slant range and Doppler given by

$$z(k) = \begin{cases} h_{\mathrm{EE}}(x(k)) + w_{\mathrm{EE}}(k) & \text{mode EE, with } P_{D_{\mathrm{EE}}}, \\ h_{\mathrm{EF}}(x(k)) + w_{\mathrm{EF}}(k) & \text{mode EF, with } P_{D_{\mathrm{EF}}}, \\ h_{\mathrm{FE}}(x(k)) + w_{\mathrm{FE}}(k) & \text{mode FE, with } P_{D_{\mathrm{FE}}}, \\ h_{\mathrm{FF}}(x(k)) + w_{\mathrm{FF}}(k) & \text{mode FF, with } P_{D_{\mathrm{FF}}}, \\ \text{clutter} & \text{otherwise}, \end{cases} \tag{3.55}$$

where the target state variables are represented in ground coordinates as,

$$x(k) = [\rho(k), \dot{\rho}(k), \beta(k), \dot{\beta}(k)]' \tag{3.56}$$

Here, the nonlinear measurement model for the OTHR is given by

$$h(x(k)) = \begin{bmatrix} \sqrt{(\rho(k)/2)^2 + h_r^2} + \sqrt{(\rho(k)/2)^2 - d\rho(k)\sin(\beta(k))/2 + (d/2)^2 + h_t^2} \\ \frac{\rho(k)\dot{\rho}(k)}{4\sqrt{(\rho/2)^2+h_r^2}} + \frac{\rho(k)\dot{\rho}(k) - d\sin(\beta(k))\dot{\rho}(k)}{4\sqrt{(\rho/2)^2 - d\sin(\beta(k))/2 + (d/2)^2 + h_t^2}} \\ \arcsin\left(\frac{\rho(k)\sin(\beta(k))}{2\sqrt{(\rho(k)/2)^2+h_r^2}}\right) \end{bmatrix} \tag{3.57}$$

and the Jacobian $H(k)$ is derived in Appendix B.

In the simulation experiment, initially a single target that starts at $[850\,\mathrm{km}, 670\,\mathrm{km}]$

with initial velocity $[0.25\,\text{km/s}, 0.2\,\text{km/s}]$ and that follows a system transition matrix (2.3) with process noise model (2.4) is considered to compare the performance of the single target tracking filters (PDAF, MPDAF and MD-PDAF). Afterwards, a second target that starts $[855\,\text{km}, 695\,\text{km}]$ with initial velocity $[0.15\,\text{km/s}, -0.3\,\text{km/s}]$ is added in the simulation experiment in order to evaluate the performance of the MD-JPDAF.

The standard deviation of the bearing, slant range and Doppler measurement errors are $\sigma_\beta = 0.002$ rad, $\sigma_\rho = 0.1\,\text{km}$, and $\sigma_{\dot{\rho}} = 0.005\,\text{km/s}$, respectively. In contrast to the assumption made in the formulation of MPDAF [65], a signal propagation mode dependent probabilities of target detection are considered ($P_{D_{\text{EE}}} = P_{D_{\text{FF}}} = 0.7$ and $P_{D_{\text{EF}}} = P_{D_{\text{FE}}} = 0.8$). For the MPDAF the average probability of detection $P_D = 0.75$ is used. However, in the MD-PDAF, the probability of detection to a given measurement set-to-track association event is calculated as

$$P_{D_\varphi} = \prod_{i=1}^{\varphi} P_{D_i}, i \in (\text{EE}, \text{EF}, \text{FE}, \text{FF}) \tag{3.58}$$

The PDAF initializes and maintains on average three false tracks due to measurements being received via different modes from the same target while the MD-PDAF combines these measurements into a single track, thereby reducing the number of false tracks significantly.

Figure 3.11 shows the RMSE comparison between the PDAF and MPDAF (assuming $P_D = 0.75$ in both cases) and MD-PDAF. As shown in the figure, in a single target scenario the performances of MPDAF and MD-PDAF are significantly better than of the PDAF with a small performance gain of MD-PDAF over MPDAF due to the correct handling of mode dependent probabilities of detection.

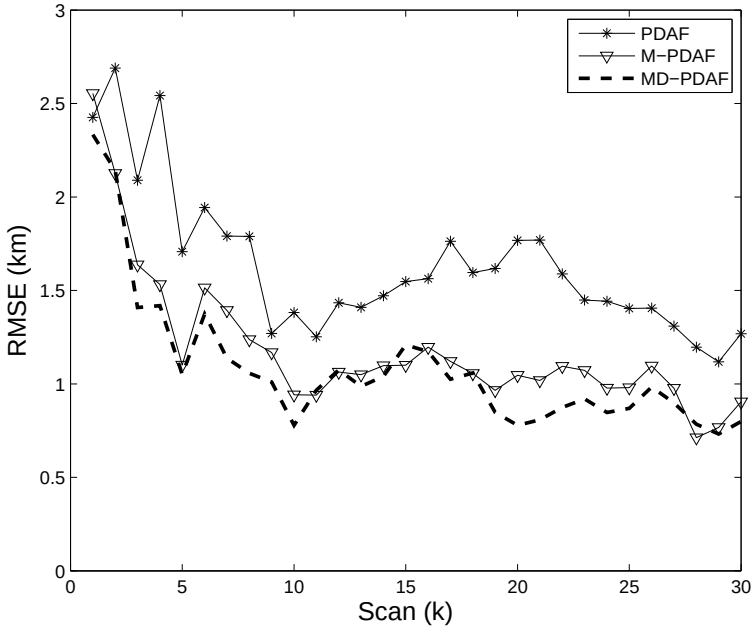

Figure 3.11: Position RMSE evaluation for PDAF, MPDAF and MD-PDAF with OTHR data.

Finally, the performance of the multitarget tracking algorithm MD-JPDAF is evaluated in a multiple targets scenario with OTHR. The estimation errors for various bearing measurement standard deviation are shown in Figure 3.12. Note that the MPDAF does not handle multiple targets.

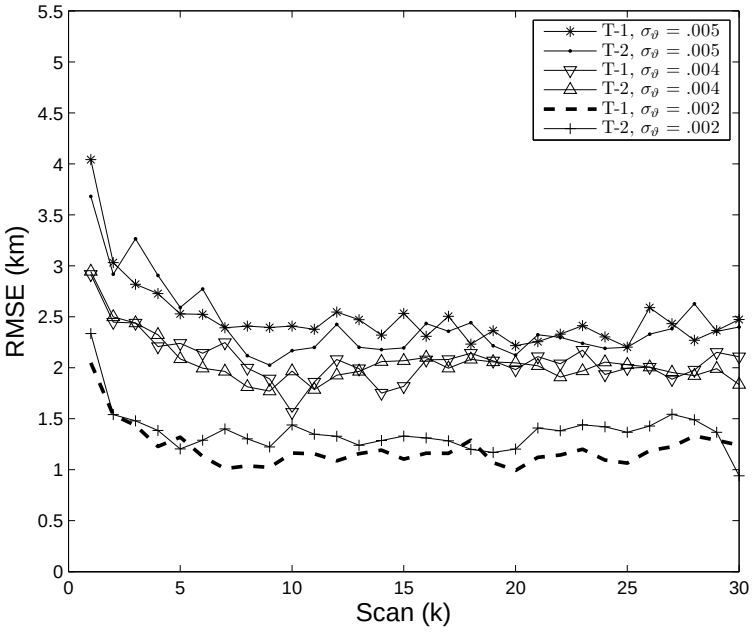

Figure 3.12: Position RMSE evaluation MD-JPDAF with OTHR data.

Chapter 4

Continuous association

Conventional target tracking algorithms rely on receiving all the measurements in a scan or frame to perform measurement-to-track association in order to satisfy the common one measurement per track assumption [14][19][76]. For example, the multitarget tracking algorithms presented in Chapter 2 such as the JPDAF [57][71], the Finite Set Statistics (FISST) based PHD filter[10][11], the MHT [19] and the MFA [53][76] require the full set of measurements in a scan in order to proceed with measurement-to-track association and/or filtering. However, most mechanically steered radar systems return measurements continuously, at the instant of each detection or in sectors, while sweeping from one region to another. Waiting for the full set of measurements in a scan (e.g., 360^o) to perform data association and filtering results in delayed track estimates. This problem becomes challenging when tracking maneuvering, high speed targets with low scan rate sensors as in the Airborne Early Warning (AEW) system [25].

In many multitarget tracking problems, the 2-D assignment algorithm for measurement-to-track association has been shown to be a practical and efficient alternative to the

optimal MHT approach without the exponentially growing enumeration [14][91][70]. In 2-D assignment the measurements in the current scan are associated with the list of initialized tracks, where the association between the measurements and the tracks is formulated as a one-to-one combinatorial optimization problem [53].

Measurements from multiple sensors can be fused together to update a global track by extending the 2-D assignment to multidimensional assignment [76][91]. In multidimensional assignment, Lagrangian relaxation-based methods are used to successively solve the association problem as a series of 2-D assignments [62][64][63][67]. Similar multidimensional formulations can also be applied to improve estimation accuracy of targets by using multiple frames over time from a single sensor. Furthermore, clustering techniques are applied to reduce the number of feasible measurement-to-track associations, thereby increasing the efficiency of the assignment algorithm [53]. However, in all variants of 2-D assignment, the optimization is done using the data from the whole frame. As a result, the measurement-to-track association and the subsequent filtering step have to wait for all measurements in a scan to be received. This results in updating all targets states at the end of the scan although the measurement from some targets may be received before the end of the scan. In addition, with ever-increasing communication bandwidth and signal processing speed, measurements can be made available more frequently than the full frame rate. For some radar systems, the scan time or the revisit interval can be long (e.g., upto 15 s in the case of AEW radar [25]) resulting in significant delays in target state update. This provides the motivation for this work to develop a continuous assignment algorithm that is capable of updating targets states while the radar is in rotation without having to wait for the full frame of data.

In mechanically steered radar systems, the complete scan can be automatically partitioned into sectors, which could be as small as a single detection, depending on the scanning rate and the sparsity of targets and the required target state update speed. The measurement-to-track association followed by filtering and target state update can also be done within the duration of a scan while sweeping from one end to the other. In multi-sector (e.g., eight 45^o sectors for full rotation) radar measurement space one possibility is to perform 2-D association at the end of each sector to update target states before the end of the scan. However, this approach does not take advantage of the measurement-to-track association cost matrix computed already in the proceeding sector, which makes the process computationally inefficient. In addition, arbitrary sector demarcation can introduce inconsistencies around sector boundaries at the end of each frame.

In this chapter, a dynamic sector based multitarget tracking algorithm with continuous 2-D assignment is proposed. This method is applicable to rotating radars that return measurements while sweeping the surveillance region instead of transmitting at the end of each frame. Based on gating, tracks are clustered and each track's state is updated based on its gate and the cluster it belongs to according to a new dynamic sector update algorithm. The proposed tracking algorithm solves the assignment problem based on an efficient incremental assignment formulation. As a result, it utilizes the already computed minimum cost matrix as part of the input to determine the whole assignment problem. Thus the previous track-to-measurement associations are combined with the newly added tracks and measurements for optimal assignment.

There are many advantages with the proposed dynamic association algorithm.

First, it will reduce the latency in track update by processing measurements as they arrive instead of waiting for the whole frame. Second, the latency, which is the gap between receiving a measurement and using it in track update, will be uniform across different targets. In frame-based algorithms targets located at the start of a scan can have longer latencies than those located at the end of a scan. Furthermore, by adaptively breaking the frame in to smaller chunks, the computation is spread over the whole scan instead of spiking at the end of the scan.

The remainder of the chapter is organized as follows. In Section 4.1 the problem statement for continuous track update is presented. Section 4.2 discusses the system model for a multi-sector measurement space based on a rotating radar model. An algorithm for dynamic sector update is also presented in this section. The extension of the 2-D assignment to dynamic 2-D assignment algorithm based on incremental Hungarian association is presented in Section 4.3. Simulation results that demonstrate the effectiveness of the proposed technique are presented in Section 4.4.

4.1 Problem Statement

A realistic multitarget tracking problem with an unknown number of targets, false alarms and miss detection is considered here. The measurements are obtained from a 2-D rotating radar (see Section 2.1.2) that continuously sweeps the surveillance region. A target moving through a state space $\mathbb{X}$ and at time step k has state $x_t(k)$ where t is the target index (see Section 2.1.1).

The full measurement set in each scan (i.e., 360^o field of view) is categorized into sectors. Hence, the measurement set in the k^{th} scan with N_s sectors encompasses sector measurement set $\mathcal{Z}_s(t_{ks}), s = 1, \cdots, N_s$, where t_{ks} is the end time of the s^{th}

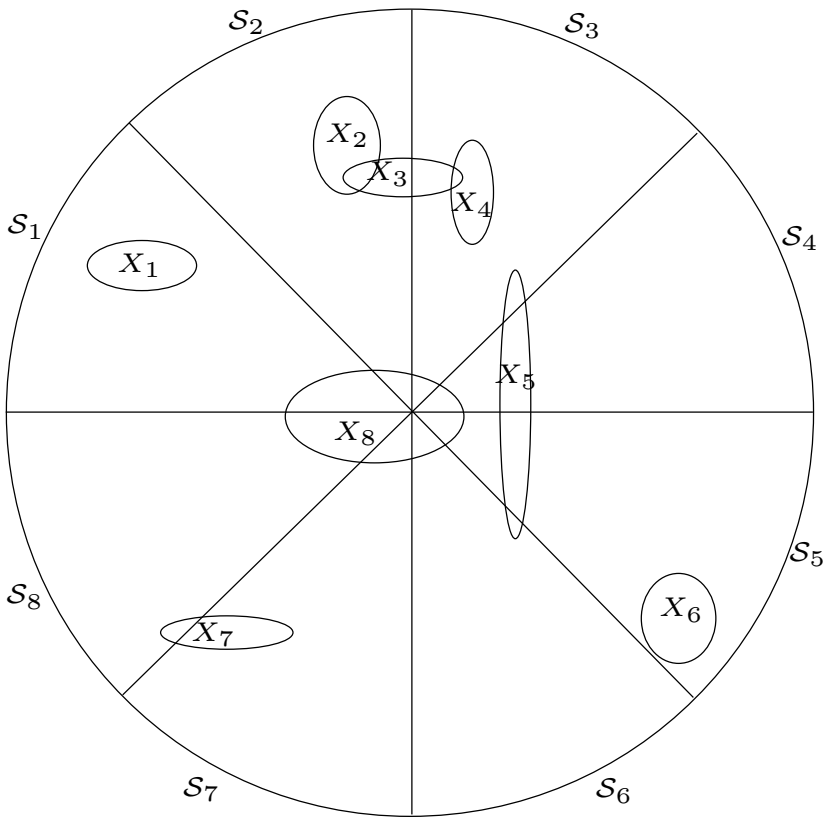

Figure 4.1: Measurement space of a rotating radar with eight 45^o sectors $(\mathcal{S}_1, \cdots, \mathcal{S}_8)$. The measurement validation region for each target $(X_1, \cdots, X_8)$ is shown by the corresponding ellipse.

sector in the k^{th} scan. The set of tracks at time step k is denoted by $X(k)$, $X(k) = \{X_1(k), \cdots, X_T(k)\}$, where T is the total number of active tracks.

In the presence of multiple targets, false alarms and missed detection a joint assignment is required since there is uncertainty as to from which target, if any, a particular measurement originated. Hence, track clusters are formed and maintained for each time step k based on the measurement validation gate of tracks. Target clusters or groups are denoted by $\mathcal{C}(k) = \{\mathcal{C}_1(k), \cdots, \mathcal{C}_g(k)\}$, where C is total number of clusters at the time step k.

A representative scenario is shown in Figure 4.1 with eight initialized tracks[1] $\{X_1(k), \cdots, X_8(k)\}$ with their respective measurement validation regions and a tracks cluster $\mathcal{C}_1(k) = \{X_2(k), X_3(k), X_4(k)\}$. As shown in the figure, a track's measurement validation region can be entirely with in a sector (e.g., $X_1(k), X_6(k)$) or span more than sector (e.g., $X_2(k), X_3(k), X_4(k), X_5(k), X_7(k)$) or span all of the sectors with in a frame (e.g., $X_8(k)$).

4.2 Dynamic Sector Update

The number of sectors can be chosen depending on the scan time of the sensor, sparsity of tracks and required track state update rate (or latency). The initial step is to construct a validation gate for each track and group tracks into clusters. The measurement validation gate $\mathcal{G}_{X_t(k)}$ for the t^{th} track is an n_z-dimensional ellipsoid that is given by (2.14).

The measurement-to-track association is performed per sector. Each sector contains the measurement set $\mathcal{Z}_s(t_{ks})$ to be associated with track list in the sector. The sector in which a track state is updated is determined based on the sector where its validation region lies and whether the track belongs to a cluster or not. Hence, the next step is to form clusters based on the measurement validation region of tracks and to classify tracks into clusters. This is performed at the beginning of each scan with the following cluster construction procedure:

1: **for all** $X_i(k) \in X(k)$ **do**
2: **for all** $\mathcal{C}_h(k) \in \mathcal{C}(k)$ **do**
3: **if** $\mathcal{G}_{X_i(k)} \bigcap \mathcal{G}_{\mathcal{C}_h(k)} \neq \varnothing$ **then**

[1]Time index is dropped in the figure for simplicity.

4: $\mathcal{C}_n(k) \leftarrow \{\mathcal{C}_h(k), X_i(k)\}$
5: **end if**
6: **end for**

7: **for all** $X_j(k) \in X(k) \bigcap X_j(k) \notin \mathcal{C}(k) \bigcap j \neq i$ **do**
8: **if** $\mathcal{G}_{X_i(k)} \bigcap \mathcal{G}_{X_j(k)} \neq \varnothing$ **then**
9: $C \leftarrow C + 1$
10: $\mathcal{C}_g(k) \leftarrow \{X_i(k), X_j(k)\}$
11: **end if**
12: **end for**
13: **end for**

where $\mathcal{G}_{X_i(k)}$ is the measurement validation gate corresponding to $X_i(k)$, and $\mathcal{G}_{\mathcal{C}_h(k)}$ is the union of measurement validation gates of tracks in the cluster, $\mathcal{C}_n(k)$. At initialization (i.e., $k = 1$), one has $\mathcal{C}(k) = \varnothing$, and target clusters are formed in the following time steps.

Then the sector number, $n_{X_i(k)}$ in which a target state is updated will be evaluated according to the following procedure:

1: **while** $\mathcal{S}_n \neq$ end **do**
2: **for all** $\mathcal{G}_{X_i(k)} \bigcap \mathcal{S}_n \neq \varnothing$ **do**
3: **if** $\mathcal{G}_{X_i(k)} \in \mathcal{C}(k)$ **then**
4: **goto** Cluster processing
5: BREAK

else
  if $\mathcal{G}_{X_i(k)} \notin \mathcal{S}_{n+1}$ **then**
    update target state
    $n_{X_i(k)} \leftarrow \mathcal{S}_n$
  end if
end if
end for
$\mathcal{S}_n \leftarrow \mathcal{S}_{n+1}$
end while

4.2.1 Cluster Processing

For tracks in clusters, the cluster processing routine below is used to determine the sector in which target state is updated:

Cluster processing:

for all $\mathcal{C}_h(k) \in \mathcal{S}_n$ **do**
  if $\mathcal{C}_h(k) \notin \mathcal{S}_{n+1}$ **then**
    for all $\mathcal{G}_{X_i(k)} \in \mathcal{C}_h(k)$ **do**
      update target state
      $n_{X_i(k)} \leftarrow \mathcal{S}_n$
    end for
  else
    perform incremental 2-D assignment

9: $\mathcal{S}_n \leftarrow \mathcal{S}_{n+1}$

10: **end if**

11: **end for**

For example, in Figure 4.1, the full frame-based association algorithm waits till $\mathcal{S}_8$ to perform data association and to update the state of all tracks in $\mathcal{S}_1$. In contrast with continuous association the assignment is divided into sectors and tracks are updated continuously as follows:

Here, $X_1(k)$ does not belong to a cluster of tracks and hence association can be made using measurement set $\mathcal{Z}_1(t_{k1})$ received in $\mathcal{S}_1$ and its state can be updated in the first sector. This will reduce the track latency by a factor of 8 compared to the frame based association. However, $X_2(k)$ belongs to a cluster with $X_3(k)$ and $X_4(k)$ and hence it has to wait for $\mathcal{S}_3$ for update with measurement set in $\mathcal{S}_2$ and $\mathcal{S}_3$, i.e., $\{\mathcal{Z}_2(t_{k2}), \mathcal{Z}_3(t_{k3})\}$.

The sectors in which the target states are updated for the scenario in Figure 4.1 are shown in Table 4.1.

In [84], a method for breaking measurements from an airborne Ground Moving Target Indicator (GMTI) sensor based on radar footprints was proposed. However, this method does not take into account the validation gates, which can significantly affect association results. This amounts to using predefined sectors for the rotating radar considered here. The disadvantages have already been discussed in the introduction section.

Table 4.1: Sector Numbers for Tracks State Update

Target id	Sector number of target state update
1	$\mathcal{S}_1$
2	$\mathcal{S}_3$
3	$\mathcal{S}_3$
4	$\mathcal{S}_3$
5	$\mathcal{S}_6$
6	$\mathcal{S}_5$
7	$\mathcal{S}_8$
8	$\mathcal{S}_8$

4.2.2 Assignment Cost

Each received measurement $z(k) \in \mathcal{Z}_s(t_{ks})$ either originated from a true target $x_t(k)$, in which case it is given by (2.1.2) or is from a clutter or false alarm, in which case it is given by (2.12). False alarms are assumed to be uniformly distributed within the senor's field of view.

A likelihood ratio, which involves the target state estimates for the candidate associations, is used to assign costs to each feasible measurement [14]. Therefore, the cost of associating the measurement j to track i is given by negative log-likelihood ratio as

$$c_{ij,s} = -\ln\frac{\Lambda_{ij}(k)}{\Lambda_{0j}(k)} \tag{4.1}$$

where $\Lambda_{ij}(k)$ is the likelihood that a measurement originated from track i and $\Lambda_{0j}(k)$

is the likelihood that the measurement is a false alarm. Hence, the cost is given as

$$c_{ij,s} = \frac{1}{2}[z_j(k) - h(x_i(k))]' S_{ij}(k)^{-1}[z_j(k) - h(x_i(k))] + \ln\left(\frac{|2\pi S_{ij}(k)|^{1/2}}{P_D \mathcal{G}_{X_i(k)}}\right) \tag{4.2}$$

where P_D is the probability of detecting a target and $S_{ij}(k)$ is the innovation covariance.

The goal is to determine the measurement-to-track association that minimizes the overall cost. For n number of targets and m number of measurements the assignment problem can be formulated as [60]

$$\begin{aligned} \min \quad & \sum_{i=1}^{n}\sum_{j=1}^{m} c_{ij,s}\phi_{ij} \\ \text{subject to} \quad & \sum_{i=1}^{n} \phi_{ij} = 1 \qquad \forall j = 1, 2, \cdots, m \\ & \sum_{j=1}^{m} \phi_{ij} = 1 \qquad \forall i = 1, 2, \cdots, n \\ & \phi \in \{0, 1\} \end{aligned} \tag{4.3}$$

where ϕ is the assignment operator, and the constraint insures one-to-one measurement-to-track association.

The dual linear problem to the above assignment problem can be formulated by assigning the dual variables $\alpha_{i,s}$ and $\beta_{j,s}$ such that

$$\sum_{i=1}^{n}\sum_{j=1}^{m} c_{ij,s} \geq \sum_{i=1}^{n} \alpha_{i,s} + \sum_{j=1}^{m} \beta_{j,s} \tag{4.4}$$

Here, $\sum_{i=1}^{n} \alpha_{i,s} + \sum_{j=1}^{m} \beta_{j,s}$ becomes a lower bound on the total cost of the minimum cost for perfect matching. As a result, the dual problem is to maximize the summation of dual variable to achieve the best lower bound, which is given as [60]

$$\begin{aligned} \max \quad & \sum_{i=1}^{n} \alpha_{i,s} + \sum_{j=1}^{m} \beta_{j,s} \\ \text{subject to } & c_{ij,s} \geq \alpha_{i,s} + \beta_{j,s} \end{aligned}$$

In order for the solutions $\alpha_{i,s}$ and $\beta_{j,s}$ to the dual problem to be optimal, the complementary slackness optimality condition should be satisfied as

$$\dot{c}_{ij,s} = c_{ij,s} - \alpha_{i,s} - \beta_{j,s} = 0 \tag{4.5}$$

For $\forall i = 1, 2, \cdots, n$ and $\forall j = 1, 2, \cdots, m$.

4.3 Continuous 2-D Assignment

The conventional frame-based 2-D assignment algorithm uses the complete set of measurements, $\mathcal{Z}(k)$, in the scan for measurement-to-track association and state estimation, which requires waiting till the end of the scan. In contrast, in sector-based 2-D assignment algorithm a partial set of measurements, $\mathcal{Z}_s(t_{ks}) \in \mathcal{Z}(k)$, i.e., measurements in a given sector, are used for the measurement-to-track association and state estimation.

One way of implementing the sector-based 2-D assignment is to perform 2-D association at the end of each sector and estimate target states. However, this approach poses a problem whenever the measurement validation region of targets or cluster

of targets lies in more than one sector, e.g., targets $X_5(k), X_7(k)$ and targets cluster $\mathcal{C}_1(k) = \{X_2(k), X_3(k), X_4(k)\}$ in Figure 4.1. Furthermore, this approach does not make use of the minimum cost matrix already computed in the previous sector while computing the association in the current sector, which leads to computational inefficiency.

The continuous association algorithm proposed in this chapter implements an incremental assignment technique while performing measurement-to-track association and state estimation simultaneously. It utilizes the minimum cost matrix already computed in the previous measurement-to-track association and the dual variables as part of the input to determine the new association problem with added set of measurements and tracks modified by the dual variables. Intermediate track results are kept and final track states are updated according to the procedure in Section 4.2.

In this section, first a discussion in the minimum cost bi-partite matching is presented and later the extension to the incremental minimum cost bi-partite matching with application to sector-based measurement-to-track association and estimation is presented.

4.3.1 Minimum Cost Bi-partite Matching

The measurement-to-track association problem can be formulated as a graph matching problem [48]. The sets of tracks and measurements to be associated become the vertices of the matching graph, G, and the measurement-to-track association costs, $c_{ij,s}$, become the edges, E, of the graph.

Here, since track-to-track or measurement-to-measurement association is not feasible, the vertices, V, can be partitioned into set of tracks, $X(k)$, and set of measurements, $\mathcal{Z}(k)$, resulting in a bi-partite matching graph, $G = \{X(k), \mathcal{Z}(k), E\}$, as shown in Figure 4.2.

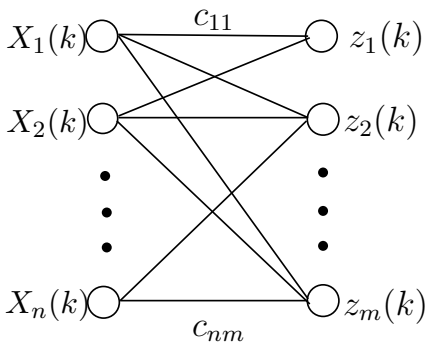

Figure 4.2: Measurement-to-track association as a bi-partite matching graph

The assignment algorithm, also called the Hungarian algorithm [48], searches iteratively for the optimal measurement-to-track association in the feasible association that minimizes the global association cost. With each iteration the dual feasible solution is maintained and the algorithm tries to find the primal feasible solution under the complementary slackness condition.

The first step in the assignment algorithm is the initialization of the dual variables α_i and β_j as:

$$\begin{aligned} \alpha_{i,s} &= 0 \\ \beta_{j,s} &= \min_i \{c_{ij,s}\} \end{aligned} \tag{4.6}$$

and initial matching $\mathcal{M}_i$, i.e., $\mathcal{M}_i = \varnothing$. An augmenting path, $\mathcal{P}$, in a bi-partite graph with matching $\mathcal{M}$ is defined as a path that starts and ends with unmatched vertices

and alternates between matched and unmatched edges. If the initial matching $\mathcal{M}$ is optimal, then there will be no augmenting path. However, the existence of augmenting path implies that the matching is not optimal and the algorithms has to search for augmenting paths.

Let

$$\theta = \frac{1}{2} \min_{i \in (X-\mathcal{P}), j \notin (\mathcal{Z}-\mathcal{P})} \{c_{ij} - \alpha_i - \beta_j\} \tag{4.7}$$

Then, the dual solution variables are updated as

$$\alpha_i = \begin{cases} \alpha_i & i \in X - \mathcal{P} \\ \alpha_i + \theta & i \in X \bigcap \mathcal{P} \end{cases} \tag{4.8}$$

and

$$\beta_j = \begin{cases} \beta_j & j \in \mathcal{Z} - \mathcal{P} \\ \beta_j - \theta & j \in \mathcal{Z} \bigcap \mathcal{P} \end{cases} \tag{4.9}$$

where $\mathcal{P}$ is the set of edges on the augmenting path and the augmentation is given as

$$\mathcal{M}_{k+1} = (\mathcal{M}_k - \mathcal{P}) \cup (\mathcal{P} - \mathcal{M}_k) \tag{4.10}$$

The algorithm can be summarized as

1: Initialize
2: LABEL
3: **while** $\alpha, \beta, \mathcal{M}$ not optimal **do**
4: **if** $\exists$ augmenting path **then**
5: AUGMENT

6: **else**

7: MODIFY

8: **end if**

9: **end while**

The algorithm terminates with the optimal matching and also with dual feasible solutions that satisfy the complementary slackness conditions.

4.3.2 Incremental 2D Assignment

The minimum cost bi-partite matching is sufficient for a frame-based 2D assignment, where association and state estimation are done at the end of the scan. However, in sector-based assignment a new set of measurements and tracks $\{X_n(k) \rightarrow X_{n+t}, z_m(k) \rightarrow z_{m+p}(k)\}$ are added to the matching graph while sweeping from one sector to another as shown in Figure 4.3. In order to handle the new set of measurements and tracks that are added to the bipartite graph while moving to the next sector an incremental assignment [88] method is applied.

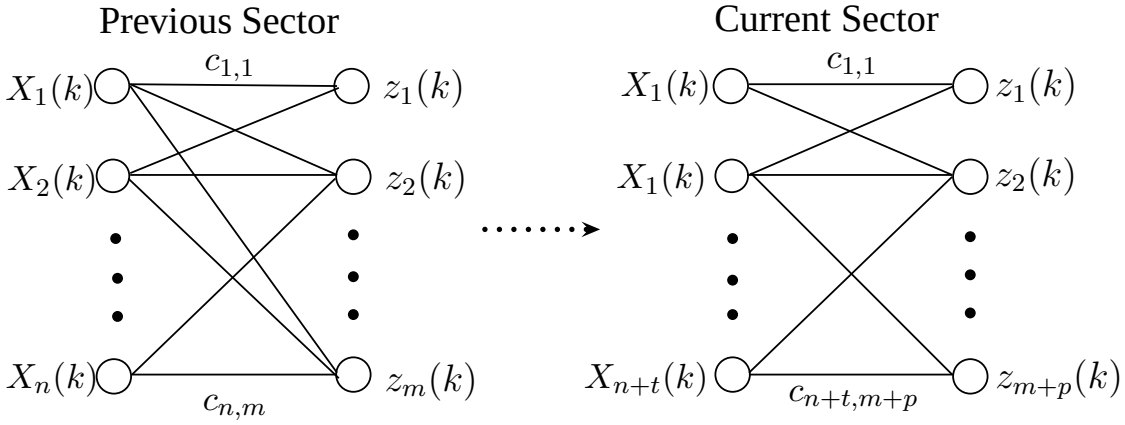

Figure 4.3: Incremental measurement-to-track assignment

The incremental algorithm assigns any feasible labels to the newly added set of measurements and by using these labels determines the minimum-weighted matching of the new bi-partite matching. As a result the minimum cost matrix already computed in the previous measurement-to-track association and the dual variables are utilized as part of the input to determine the new association problem with the added set of measurements and tracks modified by the dual variables.

The search for the new optimal measurement-to-track matching with additional set of p-vertices, i.e., p-additional set of tracks and measurements, is performed by the procedure below as:

1: BEGIN
2: $\mathcal{M}_{s+1} \leftarrow \mathcal{M}_s$
3: $\alpha_{1:n,s+1} \leftarrow \alpha_{1:n,s}$
4: $\beta_{1:n,s+1} \leftarrow \beta_{1:n,s}$
5: ASSIGN
6: **for all** $p \leftarrow 1 : P$ **do**
7: $\quad \alpha_{n+p,s+1} \leftarrow \min_{1 \le j \le n+p} \{c_{(n+p),j} - \beta_{j,s}\}$
8: $\quad \beta_{n+p,s+1} \leftarrow \min\{\min_{1 \le i \le n} \{c_{i,(n+p)} - \alpha_{i,s}\}, c_{(n+p),(n+p)}\}$
9: $\quad$ **goto** LABEL
10: **end for**

Hence, at the beginning of the scan, in the first sector, the assignment costs $c_{ij,s}$ are evaluated and the minimum cost bi-partite matching is applied to determine the optimal matching $\mathcal{M}_s$. Based on dynamic sector algorithm (see Section 4.2), if there

are tracks that can be updated, filtering will follow association and only those tracks will be updated. The optimal matching matrix with modified costs $\dot{c}_{ij,s}$ and the value of the dual variables α and β in the matching steps will be kept for the next sector. The modified cost is given as:

$$\dot{c}_{ij,s} = c_{ij,s} - \alpha_{i,s} - \beta_{j,s} \tag{4.11}$$

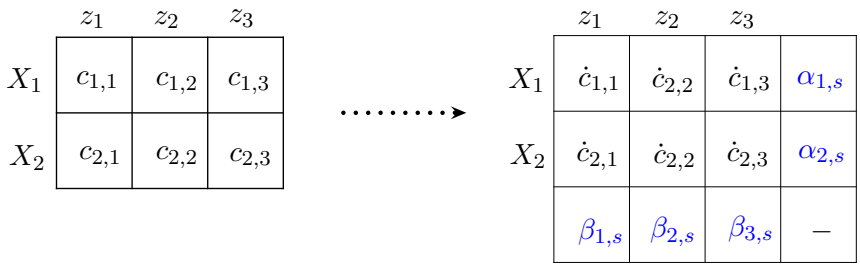

Figure 4.4: Measurement-to-track assignment in current sector.

Figure 4.4[2] shows a representative 2×3 measurement-to-track association problem within a sector. In the next sector, the optimal solution to the $n \times n$ problem in previous sector $\mathcal{M}_s$, the dual variables α_s and β_s are used in the incremental assignment algorithm to calculate the optimal matching $\mathcal{M}_{s+1}$. Similarly,

$$\ddot{c}_{ij,s+1} = \dot{c}_{ij,s+1} - \alpha_{i,s+1} - \beta_{j,s+1} \tag{4.12}$$

The incremental assignment procedure continues until the end of the sector is reached. At each step, each track will be updated with the associated measurement. Figure 4.5 shows an example 2×3 to 3×4 measurement-to-track association problem while

[2]Time index is dropped in the figure for simplicity.

transiting from one sector to another.

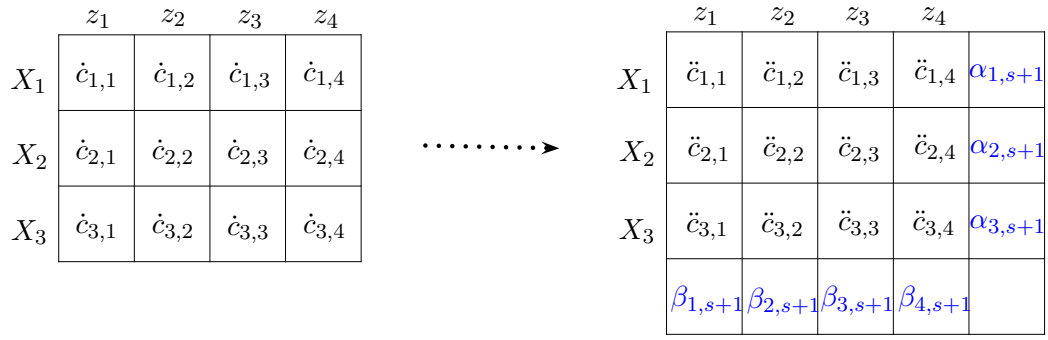

Figure 4.5: Measurement-to-track assignment in next sector.

4.4 Simulations and Results

4.4.1 Simulation Setup

In the simulation experiment, a surveillance area of 3000 m ×3000 m is considered. Six targets, spanning multiple sectors, are located in the sensor's field of view. The target initial position, velocity and sector number are summarized in Table 4.2.

Table 4.2: Initial States of Simulated targets

Target No.	Initial x (m)	Initial $\dot{x}$ (m/s)	Initial y (m)	Initial $\dot{y}$ (m/s)	Sector no.
Target 1	2200	-12	1520	17	1
Target 2	1750	-15	2300	-17	3
Target 3	1500	0	2100	10	4
Target 4	1300	15	2400	-17	4
Target 5	600	18	1600	17	6
Target 6	1700	-18	1000	10	10

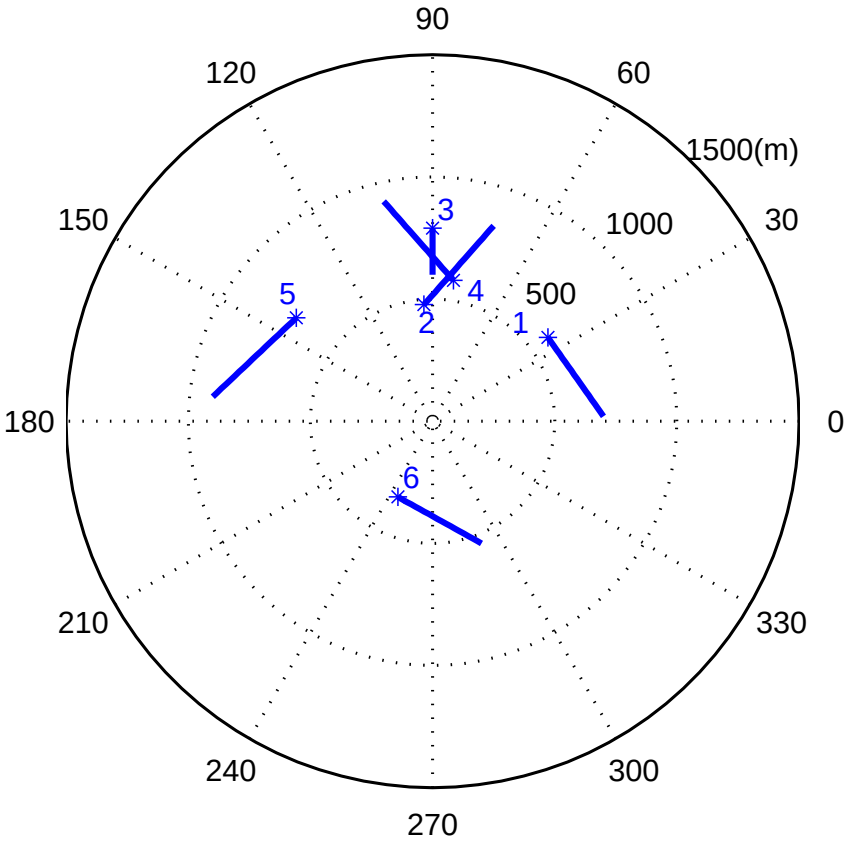

Figure 4.6: Target trajectories ('·' - start point of target and '*' - end point of target).

The targets follow a Nearly Constant Velocity (NCV) motion model [93]. It is also possible to apply the algorithm with maneuvering targets. However, in this work the focus is to demonstrate the track update efficiency of the proposed sector-based association compared to the standard frame-based association. The target trajectories for a duration of 20 scans are shown in Figure 4.6.

It can be noted in Figure 4.6 that some of the targets cross consecutive sectors in

their lifetime (targets 1,2,4, 5 and 6), some move in the clockwise direction (targets 4, 5 and 6), some move in the counter-clockwise direction (targets 1 and 2) and that others move in the radial direction (target 3). In addition, a set of targets is clustered in multiple sectors with overlapping measurement validation region (targets 2, 3 and 4).

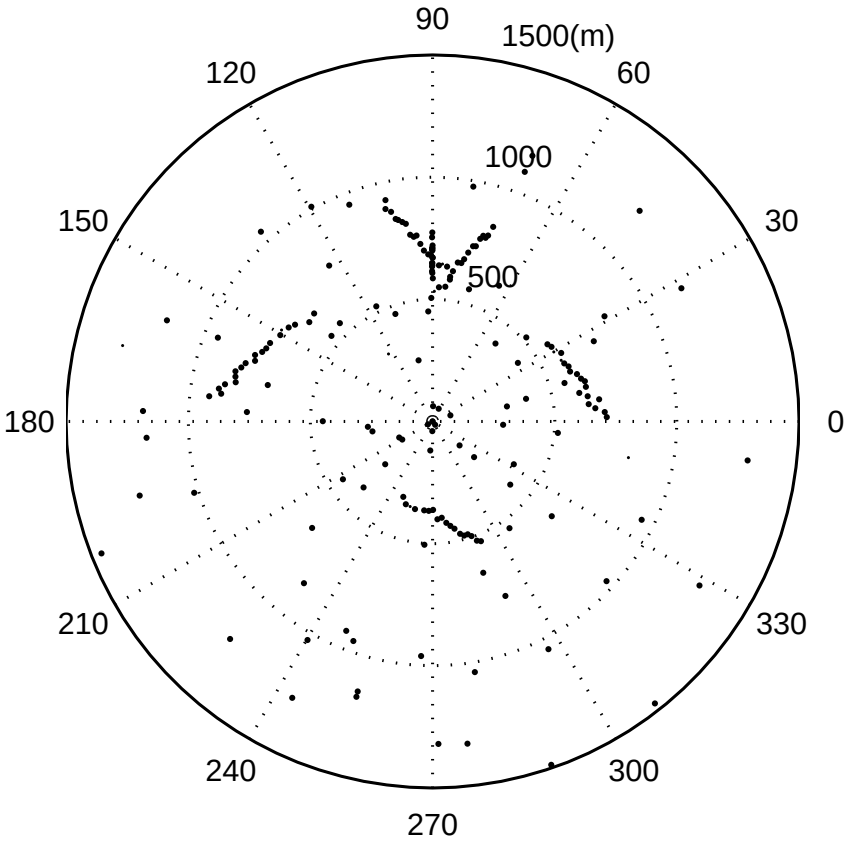

Figure 4.7: Range and bearing measurements of a rotating radar.

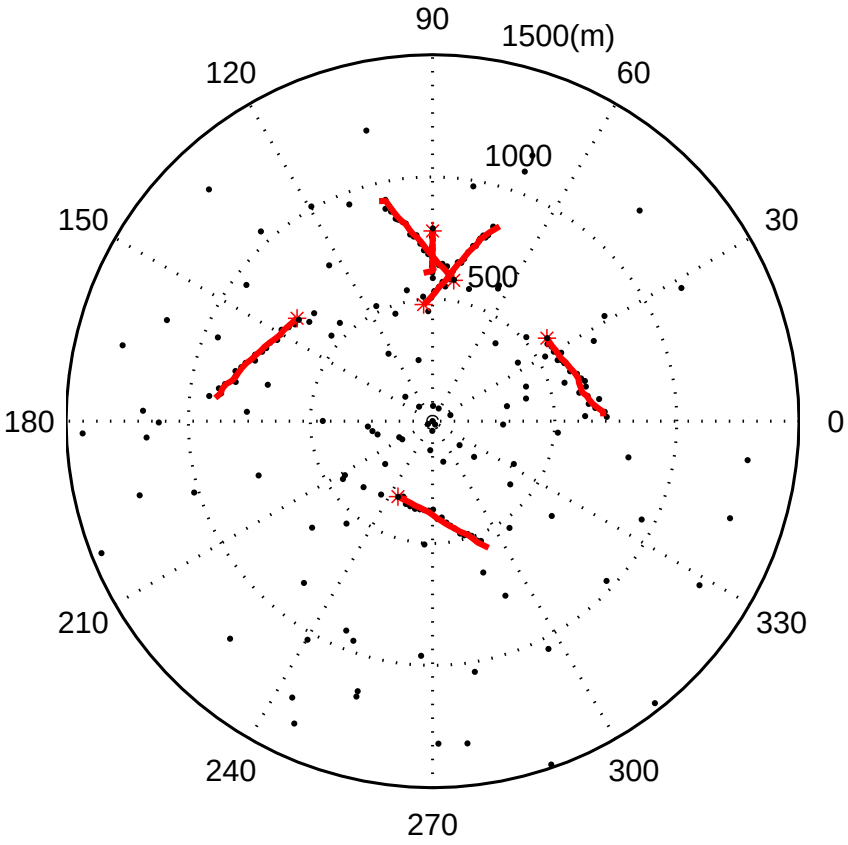

Figure 4.8: Tracks with incremental 2-D association ('·' - start point of track and '*' - end point of track).

A stationary 2-D radar located at [1500 m, 1500 m] is used for observing the targets. The period of a complete scan is one second where the radar starts at zero and scans in the clockwise direction. Experiments are also conducted with a sampling interval of 12 s, which is representative of an AEW system [25]. False alarms are uniformly distributed with $P_{FA} = 10^{-3}/\,\mathrm{m}^2$ and probability of detection is 0.95. The range and azimuth measurement standard deviations are $\sigma_r = 15\,\mathrm{m}$ and $\sigma_\theta = 0.01\,\mathrm{rad}$,

respectively. Thus a measurement vector contains range and bearing measurements with measurement interval, $t \in [0\ 1]$. The radar measurements for a single Monte Carlo experiment are shown in Figure 4.7.

Target tracking is handled with both the standard frame-based and the proposed sector-based approaches with 2-D assignment for measurement-to-track association and the Extended Kalman Filter (EKF) for filtering. Tracking results with the proposed sector-based association are shown in Figure 4.8. With the sector based dynamic association approach the full scan is divided into twelve sectors so that each sector lasts for $\frac{1}{12}$ s. The Root Mean Squared Error (RMSE) values of targets state estimation are the same for both algorithms while the performance advantage of the dynamic association the frame-based approach is in terms of the magnitude and uniformity of track latency.

In this experiment the track latency is defined as the difference between the time stamp of the received measurement and that of the track updated based on the same measurement. Note that signal processing and detection also cause latency, which will be applicable to both methods. Thus, the latency due to common processing steps is ignored.

4.4.2 Simulation Results

Two key points can be observed here. Targets located in the region that correspond to the start of a scan have larger track latency with the frame-based association than those located in the regions that correspond to the end of a scan. Furthermore, targets located near the senor and moving primarily in a tangential direction experience more variation in the track latency than those located farther from the sensor and moving

primarily in a radial direction with respect to the sensor.

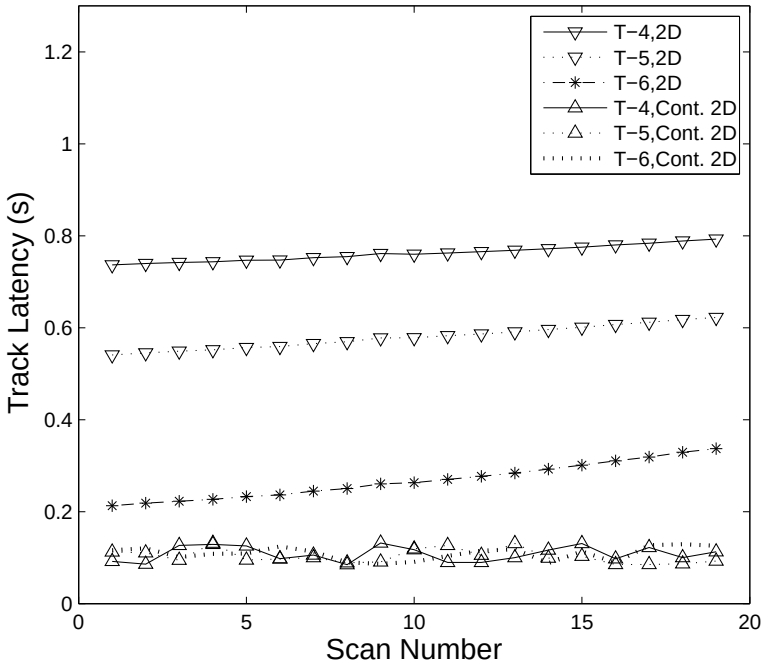

Figure 4.9: Tracks with increasing latency.

The comparison between the frame-based and dynamic association techniques with respect to track latency based on 100 MoteCarlo runs is shown in Figures 4.9–4.10. In Figure 4.9 the track latency for the targets that move in counterclockwise direction is shown. It can be noted that the track latency with frame based approach increases over time for clockwise moving targets. Targets that move mainly in a radial direction have a relatively constant track latency compared to those moving tangentially as shown in Figure 4.10.

In Figure 4.11 the track latency for the targets that move in a clockwise direction is shown. Note that the latency with frame-based approach increases as the clockwise

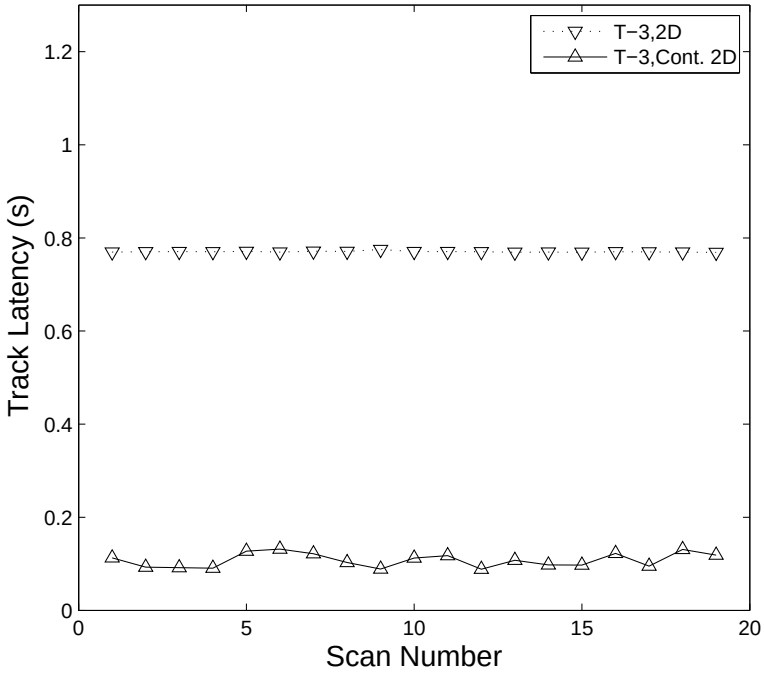

Figure 4.10: Track with constant latency.

target evolves over time. In all cases, the track latency with dynamic 2-D association approach is smaller and more uniform compared to frame based 2-D association approach as summarized in Figure 4.12. Furthermore, Figure 4.13 demonstrates a significant improvement in the average track latency when the scan period is increased to 12 s. Airborne surveillance system like the AEW operate with low revisit rates, in which case the proposed algorithm significantly reduces the latency.

The computational requirement for the standard frame-based 2D assignment vs. continuous 2D assignment is shown in Figure 4.14. As it can be seen from the figure, the computation for continuous 2D assignment is spread over the whole scan instead of a big spike at the end of the scan as in the case of the frame-based 2D assignment. This is a critical advantages of the proposed method because computer overload or

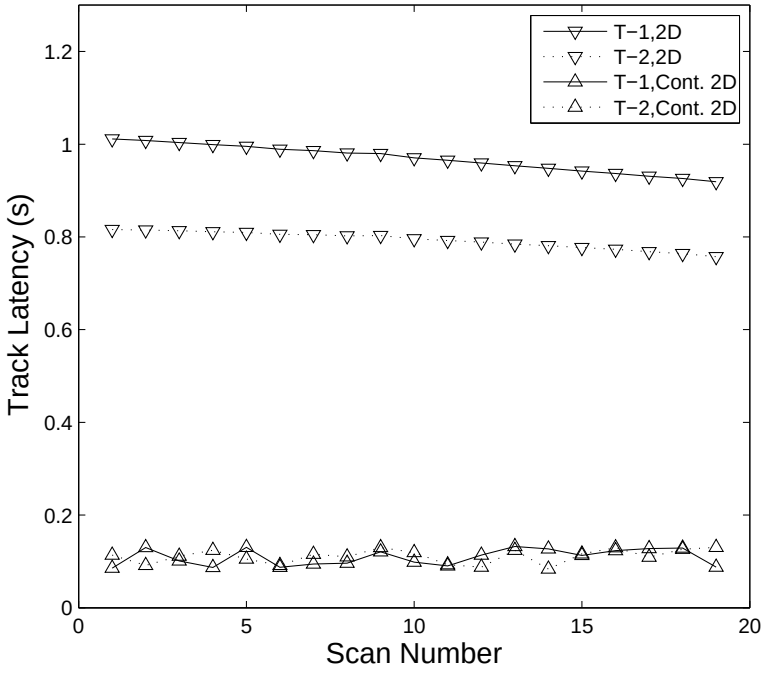

Figure 4.11: Tracks with decreasing latency.

spike is highly undesirable in real-time systems. Finally, the RMSE metrics of the algorithms are shown in Figure 4.15, which demonstrate that there is no loss in estimation accuracy as a result of breaking down the association and estimation from frames into sectors.

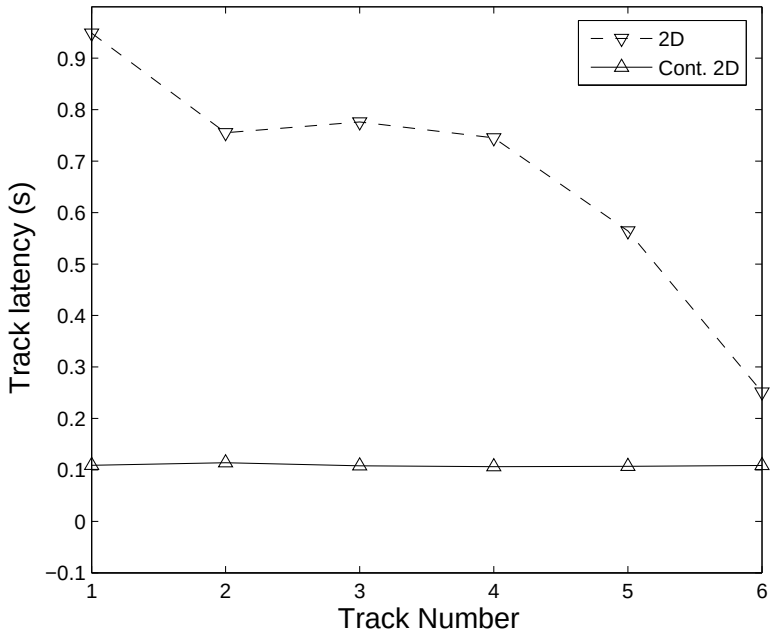

Figure 4.12: Average track latency

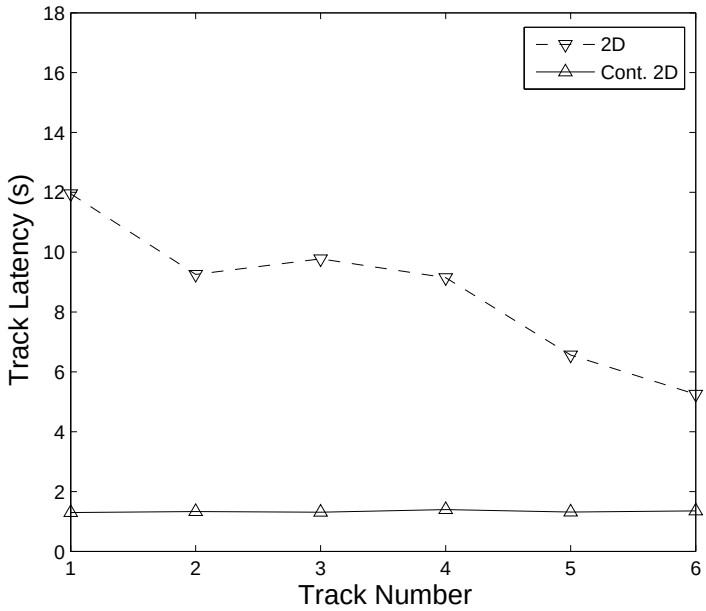

Figure 4.13: Average track latency with scan time 12 s

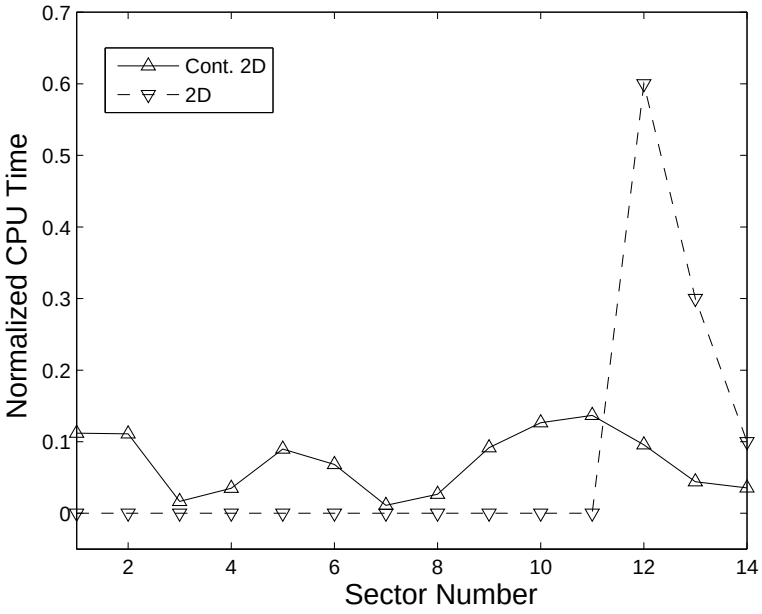

Figure 4.14: Computation time

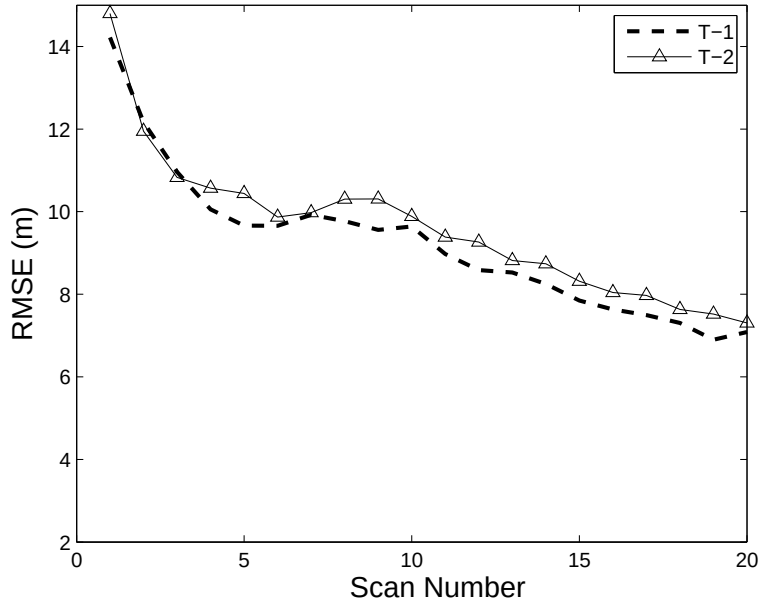

Figure 4.15: RMSE of position estimates

Chapter 5

Multi source fusion

In maritime surveillance, a wide range of sensors such as radars, sonar, imaging sensors can be deployed simultaneously to monitor a specific region. Furthermore, with the Automatic Identification System (AIS) [83][87], Global Position System (GPS) enabled onboard transponders mounted on vessel itself broadcast the vessels location together with other vessel specific information that can be picked by other vessels in the vicinity or the fusion center.

Multiple sensors network can be broadly categorized as homogenous (e.g., multistatic radar system) in which case the observation from all sensors mapped to the same measurement space [42], or heterogenous (e.g., AIS/radar surveillance system) where the observations are mapped in to different kinematic measurement space and non-kinematic observation such as target ID and type [79][86]. Each sensor could process the observation and report its track estimates or forward the observations to centralized fusion center. With a centralized fusion architecture and heterogenous sensor network, diversified information from multiple sources can be effectively fused to yield a single estimate [18]. In general the fused estimates from multiple

sources have improved overall tracking performance with respect to estimation accuracy, number of false tracks and miss detection over the estimates from a single source [36].

One way of multiple sensor information fusion is a track-to-track fusion [12][13] [14][42]. In track-to-track fusion the fusion is done at track level such that tracks are initiated and maintained from each senor and later combined. In a multitarget scenario the track-to-track fusion is done in two steps. The first step is to determine if the tracks are from the same target and the next step is to combine the associated tracks together. In [12][13] track-to-track fusion based on Baysian Minimum Mean Square Error (MMSE) is presented for homogenous sensor network. The optimal track-to-track fusion is proposed in [42] that effectively computes the cross-covariance between tracks of different sensors considering the common process noise. The performance limits of track-to-track fusion versus centralized estimation is further investigated in [35] and track-to-track fusion with heterogenous sensors is presented in [79][86]. An alternative approach to a distributed tracking with Probability Hypothesis Density (PHD) Filter is also proposed in [7] that uses Huffman coding technique to effectively encode and transmit a measurement set with false alarms.

Although track-to-track fusion is a computationally efficient approach, estimation error resulted from each track and from the fusion process get accumulated and as a result the overall estimation error becomes large. In addition, there will be a processing delay to estimate tracks from each source before fusing and reporting the final estimate. Also, the performance of fusion from sensors can be degraded due to disassociation as investigated in [24]. Another alternative to a multisensor information fusion problem is a measurement level fusion [33] where measurements from

different sources are forwarded to centralized fusion center and processed jointly in the measurement-to-track association algorithm to initialize and maintain tracks. In [8][9] the joint processing of measurements from multiple propagation modes and homogenous sensor network is handled as a multiple detection problem. The measurement level fusion offers improved tracking performance with the requirements of more computational resources as well as sufficient bandwidth between the synchronized senors and fusion center.

Information fusion with heterogenous sensor network could be the case of vessels tracking in maritime environment. In maritime environment radars are primarily used as for the surveillance near the ports. Radars provide the range, bearing measurements of the vessels in the vicinity. Also, vessels identify themselves intermittently by broadcasting their location information using the Automatic Identification System (AIS) [87]. The AIS messages broadcasted in maritime scenario include position estimates with GPS level accuracy, rate of turn, course and speed. In addition, extra information such as destination, estimated time of arrival, vessel name and type can be included in the broadcasted AIS messages.

The initial purpose of exchanging AIS information between nearby vessels was to avoid a collision and also to gather additional information for navigation and route planning. The AIS information is available from the transponder that use a GPS system integrated with a standard Very High Frequency (VHF) transceiver mounted on the vessel. The broadcasted AIS messages can be picked by other vessels in the vicinity, vessel traffic services (VTS) or satellite overhead [83]. However, the use of self-organizing time division multiple access (SO-TDMA) for bandwidth sharing make the AIS prone to message interference, conflicting AIS IDs and missing AIS IDs. In

addition, the transmission rate for the AIS depends on the relative postion of the vessel from the coast line and the type of vessels. The vessel's transponder could be intentionally or non-intentionally turned off as well.

The aforementioned issues with the AIS framework make it intermittent as the data availability depends on the type and behavior of the vessel. On the other hand, radars report measurements at a constant revisit interval although they are prone to large measurement error and false alarms compared to AIS messages. In the literature, previous works mainly focus on track level fusion of radar and AIS measurements [22][27][51]. Track level fusion between the AIS data and Over-the-Horizon (OTH) radar has been presented in [27]. In this track level fusion, separate tracks are generated for the AIS and OTH radar and letter fused. Also, the performance of fusion from sensors can be degraded due to disassociation resulted in the use of multiple sensors with different measurement errors is investigated in [24] based on simulations.

In this research, a measurement-level fusion of AIS messages and radar measurements is proposed based on the Joint Probabilistic Data Association (JPDA) framework. Tracks are initialized based on radar measurements and are assigned to the list of AIS IDs based on the initial distributions. As a result once the target is associated with the AIS ID its states can be updated with radar observations even if the ship is not transmitting its AIS data. For targets that are widely separated there will be no ambiguity for the AIS ID-to-track association. However, as the vessels get close there will be ambiguity for AIS ID-to-track assignment. A probabilistic AIS IDs-to-tracks assignment technique is proposed to resolve the assignment ambiguity. As a result, each track keeps a list of AIS IDs with probabilities that will be updated by Bayesian

inference made on AIS messages, radar measurements and other tracks.

The effectiveness of the proposed measurement level fusion algorithm is compared with track-to-track fusion, which uses a Bayesian MMSE approach to fuse radar only and AIS only track estimates. Furthermore, the optimality of the proposed method is demonstrated by comparing with the Posterior Cramér-Rao Lower Bound (PCRLB) derived for AIS/Radar network under various AIS revisit intervals and radar measurement errors. Computational load analysis is also conducted that evaluates the relative computational requirements of the measurement-level fusion algorithm.

The rest of the chapter is organized as follows. In Section 5.1 mathematical modeling for target dynamics, the radar measurements and AIS messages is presented. In Section 5.2 the AIS only tracking based on ID matching and Kalman filtering, radar only tracking based on joint probabilistic data association are presented. The track-to-track fusion and the measurement-level fusion are presented in Section 5.3. The PCRLB that is derived for AIS/Radar network is also discussed in this section. Simulation results based on closely spaced multiple targets is presented in Section 5.4 that demonstrate the improved performance of the proposed measurement-level fusion algorithm.

5.1 System Model

In maritime environment vessels trajectory can be modeled as a linear constant velocity with some level of process noise (see Section 2.1.1). Based on vessels type and behavior, other nonlinear motion models such as coordinated turn and acceleration models [93] can be incorporated as well.

5.1.1 Target Dynamics

Targets (vessels) follow motion model given as

$$x_t(k) = F_t x_t(k-1) + v_t(k) \tag{5.1}$$

where F_t it the state transition matrix and $v_t(k)$ is the process noise level, which is assumed to be a white Gaussian noise.

Here, the level of process noise can be chosen based on the type and size of vessel. For example, bulk carrier moves almost in a straight path and can be modeled with a very small process noise level compared to small boats.

5.1.2 Radar Measurements

The radar measurement model is given by (see Section 2.1.2)

$$z_r(k) = h(x_t(k)) + w(k) \tag{5.2}$$

where $z_r(k) \in \mathbb{R}^{n_z}$ represents the target-originated measurement above the detection threshold, n_z is the dimension of the measurement space, $h(\cdot)$ is the nonlinear measurement function of the target state and $w(k)$ is the measurements noise.

5.1.3 AIS measurements

AIS messages are broadcast at longer intervals than the radar revisit intervals. Hence, n_k time step is used in the AIS observation model where n is a factor that denotes the relative sampling interval of the AIS messages compared to that of the radar

measurements. For example, $n = 1$ implies the radar and AIS massages have same revisit interval. In practical scenarios, the AIS messages arrive at a slower rate than the radar detection, i.e., $(n_k > 1)$.

The AIS messages from vessels include position, horizontal speed, course and consistent target ID given by

$$z_a(k) = \begin{cases} g(x_t(k)) + w(k) & k = n_k \\ \\ 0 & n_k < k < n_{k+1} \end{cases} \tag{5.3}$$

where

$$g(x_t(k)) = \begin{bmatrix} x(k) \\ y(k) \end{bmatrix} \tag{5.4}$$

with a covariance R_a given by

$$R_a = \begin{bmatrix} \sigma_x^2 & 0 \\ 0 & \sigma_y^2 \end{bmatrix} \tag{5.5}$$

where σ_x and σ_y are the standard deviations in the Cartesian $X - Y$ coordinates. Furthermore, each AIS message has AIS ID tag $\xi_t(k)$.

The speed information in the AIS messages is filtered from the position coordinates, hence, only the position information from the AIS massages is considered for estimation.

5.2 AIS/Radar Tracking

The set of measurements that consists of both radar and AIS measurements at time k is denoted by

$$Z(k) = \begin{cases} Z_r(k) & n_k < k < n_{k+1} \\ \\ \{Z_r(k), Z_a(k)\} & k = n_k \end{cases} \tag{5.6}$$

where $Z_r(k)$ and $Z_a(k)$ denote measurements at time step k from the radar and AIS, respectively, such that

$$Z_r(k) = \left\{z_r^i(k)\right\}_{i=1}^{m_k^r} \tag{5.7}$$

$$Z_a(k) = \left\{z_a^i(k)\right\}_{j=1}^{m_k^a} \tag{5.8}$$

where m_k^r and m_k^a are the total number of radar and AIS measurements, respectively.

5.2.1 Radar-Only Tracking

Radar observation include target-originated measurements mixed with false alarms without ID information. Multitarget algorithms such as the MHT [19] or the PHD filter [56] could be used with the radar data set. However, these algorithms are computationally intensive (especially when the false alarm rate is very high due to ocean waves and sea clutter) and hence in this work the JPDA [28][57] framework is chosen. The measurement-level fusion algorithm, which is proposed in Section 5.3, is also developed based on the JPDA framework.

Tracks are initialized with a two-point track initialization procedure. In the probabilistic data association framework, the final estimate is a weighted sum of estimates under all measurement-to-track association events. Using the total probability theorem over the current measurement association events, the state at time k can be written as

$$\hat{x}^r(k|k) = \sum_{i=1}^{m_k^r} E[x_k|\theta_i(k), Z_r^k] P\{\theta_i(k)|Z_r^k\} \tag{5.9}$$

$$= \sum_{i=1}^{m_k^r} \hat{x}^i(k|k)\beta_i(k) \tag{5.10}$$

where $m(k)$ is the number of measurements, $\hat{x}^i(k|k)$ is the updated state conditioned on the event that the i-th candidate association is correct and

$$\beta_i(k) \triangleq P\{\theta_i(k)|Z_r^k\} \tag{5.11}$$

The above formulation considers all candidate measurements within a given scan. However in practice, the total number of candidate measurements can be reduced by applying gating techniques presented in Section 2.3.

Furthermore, in a multitarget scenario overlapping gates imply closely-spaced target and thus joint association events have to be considered. The next step is to combine the innovation from each candidate measurement to yield the final state and covariance update as

$$\hat{x}^r(k|k) = \hat{x}(k|k-1) + W(k)\nu(k) \tag{5.12}$$

where the combined innovation is

$$\nu(k) = \sum_{i=1}^{m_k^r} \beta_i(k)\nu_i(k) \tag{5.13}$$

The covariance associated with the updated state is

$$P^r(k|k) = P^c(k|k) + \tilde{P}(k) \tag{5.14}$$

where the covariance of the state updated with the correct measurement is

$$P^c(k|k) = P(k|k-1) - (1-\beta_0)W(k)S(k)W(k)' \tag{5.15}$$

and the spread of the innovations term is

$$\tilde{P}(k) \triangleq W(k)[\sum_{i=1}^{m_k^r} \beta_{i,k}\nu_i(k)\nu_i(k)' - \nu(k)\nu(k)']W(k) \tag{5.16}$$

5.2.2 AIS-Only Tracking

The AIS messages include position estimates in Cartesian coordinates. Hence, based on the ID match between a track and an AIS message a Kalman filter is used for estimation due to the linear observation model of AIS messages.

- Case 1:

- during the time steps with AIS messages ($k = n_k$)

$$\hat{x}^a(k|k) = \hat{x}(k|k-1) \tag{5.17}$$

$$+W(k)(z_a(k) - g(\hat{x}(k|k-1))) \tag{5.18}$$

$$P^a(k|k) = P(k|k-1) - W(k)S(k)W(k)' \tag{5.19}$$

where

$$W(k) = P(k|k-1)G(k)S(k)^{-1} \tag{5.20}$$

$$S(k) = G(k)P(k|k-1)G(k)' + R_a(k) \tag{5.21}$$

Here, $R_a(k)$ is the AIS measurement covariance and $G(k)$ is the linear observation model of AIS given by.

$$G(k) = \begin{bmatrix} 1 & 0 & 0 & 0 \\ 0 & 0 & 1 & 0 \end{bmatrix} \tag{5.22}$$

- Case 2:

  - during the time steps without AIS messages ($n_k < k < n_{k+1}$)

$$\hat{x}^a(k|k) = \hat{x}(k|k-1) \tag{5.23}$$

$$P^a(k|k) = P(k|k-1) \tag{5.24}$$

Note that AIS-only tracking performs poorly whenever there is an AIS ID swap among tracks as a result of incorrect AIS ID-to-track associations. In addition, missing

AIS IDs will result in prediction only estimates.

5.3 Fused AIS-Radar Tracking

In this section the track-to-track fusion of AIS and radar estimates, the measurement-level fusion algorithm developed based on JPDA framework and the PCRLB derived for the combined AIS/radar observations are presented.

5.3.1 Track-to-Track Fusion

In the track-to-track fusion approach [13][42] independent estimates from the radar measurements $\{\hat{x}^r(k|k), P^r(k|k)\}$ and AIS data $\{\hat{x}^a(k|k), P^a(k|k)\}$ are initially tested if two tracks are from the same target based on hypothesis generated by the difference between the two estimates. The difference is given by

$$\hat{\Delta}^{ra}(k) = \hat{x}^r(k|k) - \hat{x}^a(k|k) \tag{5.25}$$

and the hypothesis that the estimates are from the same target is accepted when

$$\begin{aligned} D &= \hat{\Delta}^{ra}(k)'[P^r(k|k) + P^a(k|k)]^{-1}\hat{\Delta}^{ra}(k) \\ &\leq D_\alpha \end{aligned} \tag{5.26}$$

where D_α is the threshold distance.

The associated tracks are then combined according to the Baysian Minimum Mean

Squared Error (MMSE) criterion [14] to yield the fused estimate as

$$\begin{aligned}\hat{x}^c(k|k) = \hat{x}^r(k|k) + (P^r(k|k) - P^{ra}(k|k)) \\ \times (P^r(k|k) + P^a(k|k) - P^{ra}(k|k) - P^{ar}(k|k))^{-1} \\ \times(\hat{x}^a(k|k) - \hat{x}^r(k|k))\end{aligned} \tag{5.27}$$

and the covariance as

$$\begin{aligned}P^c(k|k) = P^r(k|k) - (P^r(k|k) - P^{ra}(k|k)) \\ \times(P^r(k|k) + P^a(k|k) - P^{ra}(k|k) - P^{ar}(k|k))^{-1} \\ \times(P^r(k|k) - P^{ar}(k|k))\end{aligned} \tag{5.28}$$

where $\hat{x}^c(k|k)$ is the combined estimate, $P^c(k|k)$ is the corresponding combined covariance and $P^{ra}(k|k))$ is the cross-covariance between $\hat{x}^r(k|k)$ and $\hat{x}^a(k|k)$.

5.3.2 Measurement-Level Fusion

With the measurement-level fusion approach, at each time step the radar measurements and AIS data (if available) are directly used for a single track estimate.

Initialization

Tracks are initialized using the two-point approach [14] using radar measurements. Let $X(k)$ denote the set of tracks at time step k. That is,

$$X(k) = \{X_1(k), \cdots, X_T(k)\} \tag{5.29}$$

with AIS IDs and their probabilities for each track $X_t(k)$ being denoted by

$$\xi_t(k) = [\xi_t^1(k), \cdots, \xi_t^T(k)] \tag{5.30}$$

and

$$p(\xi_t(k)) = [p(\xi_t^1(k)), \cdots, p(\xi_t^T(k))] \tag{5.31}$$

respectively.

Prior to receiving AIS measurements, track IDs are assumed to have equal probability. That is,

$$p(\xi_t^i(k)) = 1/N_T(k) \tag{5.32}$$

where $N_t(k)$ is the total number of initialized tracks at time step k.

The measurement-level fusion procedure for a given scan is shown is Figure 5.1. As shown in Figure 5.1, when AIS is available, a track's AIS ID probabilities are evaluated based on AIS messages. When AIS is not available, a track's AIS ID probabilities are evaluated based on Baysian inference made on radar measurements, and other tracks with validation gates overlapping with a given track. In the first case, tracks are updated with stacked AIS/radar data set according to the assigned AIS ID probabilities, and in the latter case, tracks are updated with radar measurements. The evaluation of a track's AIS ID probabilities and update procedure are discussed in the following sections.

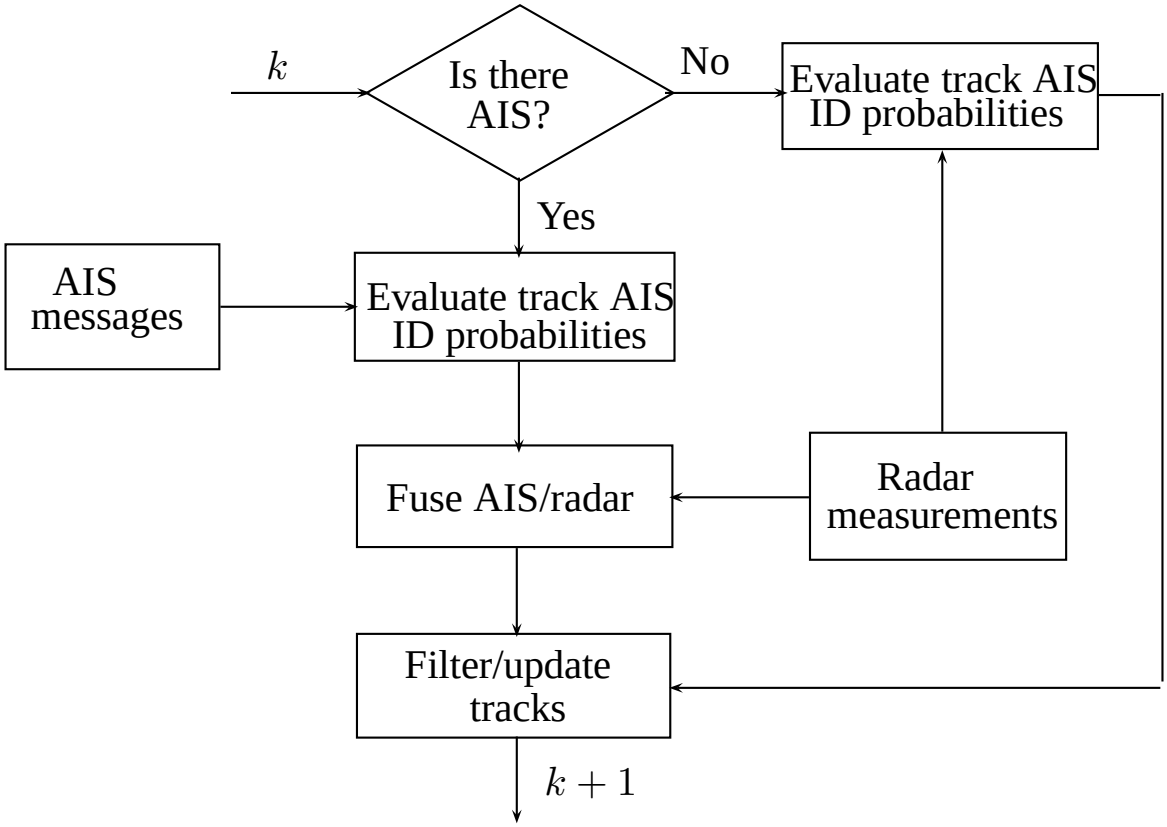

Figure 5.1: Measurement-level AIS/radar fusion.

AIS ID probability update based on AIS messages

The AIS ID probability for a given track based on the set of AIS measurement is given by

$$p(\xi_t^i(k)|X_t(k), Z_a^k) = \frac{p(Z_a^k|\xi_t^i(k), X_t(k))p(\xi_t^i(x), X_t(k))}{p(Z_a^k, X_t(k))} \tag{5.33}$$

Applying conditional probability to the above gives

$$p(\xi_t^i(k)|X_t(k), Z_a^k) = \frac{p(Z_a^k|\xi_t^i(k), X_t(k))p(\xi_t^i(x)|X_t(k))}{p(Z_a^k|X_t(k))} \tag{5.34}$$

The measurement set $Z_a^k = \left\{Z_a(k), Z_a^{k-1}\right\}$ includes current AIS measurements, $Z^a(k)$, and all the measurements up to time step k, which can be summarized by Z^{k-1}. Then

$$\begin{aligned} p(\xi_t^i(k)|X_t(k), Z_a(k), Z_a^{k-1}) = &\frac{p(Z_a(k)|\xi_t^i(k), X_t(k), Z_a^{k-1})p(Z_a^{k-1}|X_t(k), \xi_t^i(k))}{p(Z_a(k)|X_t(k), Z_a^{k-1})} \\ &\times \frac{p(\xi_t^i(k)|X_t(k))}{p(Z_a^{k-1}|X_t(k)} \end{aligned} \tag{5.35}$$

The conditional probabilities of AIS measurements are only dependent on the targets states. Thus,

$$p(Z_a^{k-1}|X_t(k), \xi_t(k)) \propto p(Z_a^{k-1}|X_t(k)) \tag{5.36}$$

Therefore, (5.35) reduces to

$$p(\xi_t^i(k)|X_t(k), Z_a(k), Z_a^{k-1}) \tag{5.37}$$

$$= \frac{p(Z_a(k)|\xi_t^i(k), X_t(k), Z_a^{k-1})p(\xi_t^i(k)|X_t(k))}{p(Z_a(k)|X_t(k), Z_a^{k-1})} \tag{5.38}$$

Since an AIS position measurement and the corresponding ID are independent [82],

one has

$$p(Z_a(k)|\xi_t^i(k), X_t(k), Z_a^{k-1}) \propto p(Z_a(k)|\xi_t^i(k), Z_a^{k-1}) \times p(Z_a(k)|X_t(k), Z_a^{k-1})$$

where the first part, $p(Z_a(k)|\xi_t^i(k), Z_a^{k-1})$, is the ID information available from AIS data and the second part, $p(Z_a(k)|X_t(k), Z_a^{k-1})$, is the kinematic information. The prior information is

$$p(Z_a(k)|\xi_t^i(k), X_t(k), Z_a^{k-1}) = \begin{cases} 1 & \text{if} \quad \xi_t^i(k) \in Z_a(k) \\ 0 & \text{otherwise} \end{cases} \tag{5.39}$$

Furthermore, the denominator term in (5.38), $p(Z_a(k)|X_t(k), Z_a^{k-1})$, denotes the association probabilities based on position measurements from the AIS data given by $p(Z_a(k)|X_t(k), Z_a^{k-1}) = \sum_{i=1}^{m_k^a} p(z_a^i(k)|X_t(k), Z_a^{k-1})$, where

$$p(z_a^i(k)|X_t(k), Z_a^{k-1}) = \mathcal{N}[z_a^i(k); \hat{z}_a(k|k-1), S^a(k)] \tag{5.40}$$

AIS ID probability update based on radar measurements

Unlike AIS data, radar measurements do not include ID information. Hence, probabilistic inference is made on the radar measurements and other tracks in order to update a given AIS ID-to-track assignment probability.

Thus, the AIS ID probability for a given track based on the set of radar measurements in the validation gate is given by

$$\begin{aligned} &p(\xi_t^i(k), X_t(k)|X_1(k), \cdots, X_{n_T}(k), Z_r^k) \\ &\quad = \frac{p(Z_r^k, X_t(k)|\xi_t^i(k), X_1(k), \cdots, X_{n_T}(k))}{p(Z_r^k, X_1(k), \cdots, X_{n_T}(k))} \\ &\qquad \times p(\xi_t^i(x), X_1(k), \cdots, X_{n_T}(k)) \end{aligned} \tag{5.41}$$

where $\{X_1(k), \cdots, X_{n_T}(k)\}$ is the list of tracks with validation gates overlapping with those of track $X_t(k)$.

Applying the total probability theorem and assuming that different targets generate radar measurements independently,

$$\begin{aligned} p(\xi_t^i(k), X_t(k)|X_1(k), \cdots, X_{n_T}(k), Z_r^k) = &\frac{p(Z_r^k|X_t(k))}{\sum_{i=1, i\neq t}^{n_T} p(Z_r^k|X_i(k))} \\ &\times \sum_{i=1, i\neq t}^{n_T} p(\xi_t^i(x)|X_i(k)) \end{aligned} \tag{5.42}$$

Denote $Z_r^k = \left\{Z_r(k), Z_r^{k-1}\right\}$ such that $Z_r(k)$ contains current radar measurements and Z_r^{k-1} summarizes all the measurements up to time step k. Then,

$$\begin{aligned} p(\xi_t^i(k), X_t(k)|X_1(k), \cdots, X_{n_T}(k), Z_r(k), Z_r^{k-1}) = &\frac{p(Z_r(k), X_t(k)|Z_r^{k-1})}{\sum_{i=1, i\neq t}^{n_T} p(Z_r(k)|X_i(k), Z_r^{k-1})} \\ &\times \sum_{i=1, i\neq t}^{n_T} p(\xi_t^i(x)|X_i(k)) \end{aligned} \tag{5.43}$$

where the radar measurement likelihood is given by

$p(Z_r(k)|X_t(k), Z_r^{k-1}) = \sum_{i=1}^{m_k^r} p(z_r^i(k)|X_t(k), Z_r^{k-1})$, where

$$p(z_r^i(k)|X_t(k), Z_r^{k-1}) = \mathcal{N}[z_r^i(k); \hat{z}_r(k|k-1), S^r(k)] \tag{5.44}$$

The updated AIS ID probabilities for a track based on radar measurements are maintained for the correct AIS ID-to-track assignment. Finally the tracks are updated with the combined innovation from the radar measurements and AIS messages as

$$\hat{x}^{mf}(k|k) = \hat{x}(k|k-1) + W^{mf}(k)\nu^{mf}(k) \tag{5.45}$$

where $W^{mf}(k)$ is given by

$$W^{mf}(k) = \begin{cases} P(k|k-1)[H(k) \oslash G(k)]S^{mf}(k)^{-1} \\ \qquad\qquad k = n_k \\ P(k|k-1)[H(k)]S^{mf}(k)^{-1} \\ \qquad\qquad n_k < k < n_{k+1} \end{cases} \tag{5.46}$$

and

$$S^{mf}(k) = \begin{cases} [H(k) \oslash G(k)]P(k|k-1)[H(k) \oslash G(k)]' \\ +R_r(k) \otimes R_a(k) \\ \qquad\qquad\qquad\qquad k = n_k \\ H(k)P(k|k-1)H(k)' + R_r(k) \\ \qquad\qquad\qquad\qquad n_k < k < n_{k+1} \end{cases} \tag{5.47}$$

Here, $A \oslash B \triangleq [A\ B]'$ and $A \otimes B \triangleq [A\ 0; 0\ B]$.

5.3.3 PCRLB for AIS/Radar Network

A theoretical lower bound, which can be used as a benchmark for the performance evaluation of the proposed measurement level fusion algorithm, can be provided by the Posterior Cramér-Rao Lower Bound (PCRLB) [59]. However, previous works on multisensor PCRLB focus on the derivation of the lower bound for homogeneous sensors with measurement origin uncertainty and sensor management based on the computed PCRLB results [68]. Furthermore, it is usually assumed that all sensors report measurements at each time step with some less-than unity detection probability and non-zero false alarms.

In this section, the extension of the PCRLB to heterogeneous sensors with variable scan rate is discussed. Note that the background on PCRLB is presented in Section 3.3.1 and the measurement contribution factor is presented below.

Measurement contribution of AIS/radar

For m_k^r number of radar measurements and m_k^a number of AIS messages that are received at time k, the independent AIS and radar observation process implies

$$p(Z(k)|X(k), m_k^r, m_k^a) = \begin{cases} p(Z_r(k)|X(k), m_k^r) \times p(Z_a(k)|X(k), m_k^a) \\ \qquad\qquad k = n_k \\ \\ p(Z_r(k)|X(k), m_k^r) \\ \qquad\qquad n_k < k < n_{k+1} \end{cases} \tag{5.48}$$

and taking the logarithm of both sides of (5.48) gives

$$\log p(Z(k)|X(k), m_k^r, m_k^a) = \begin{cases} \log p(Z_r(k)|X(k), m_k^r) + \log p(Z_a(k)|X(k), m_k^a) \\ \qquad\qquad\qquad\qquad k = n_k \\ \log p(Z_r(k)|X(k), m_k^r) \qquad\qquad n_k < k < n_{k+1} \end{cases} \tag{5.49}$$

Hence, the multiple heterogenous sensors generalization becomes

$$J_z(k+1) = \sum_{h_k} p(h_k) J_{z_h} \tag{5.50}$$

where h_k is the number of heterogenous sensors reporting measurements at time step k. Furthermore, for the radar measurements, under the assumption that false alarms are uniformly distributed in the measurement space and the number of false alarms is Poisson distributed, the measurement contribution is given by

$$J_z(k) = \begin{cases} \prod_{m_k^a}(1 - P_m^a) J_{z_a}(k) \\ \left[(1 - P_D^r)\mu_{FA}(m(k)) + P_D^r \mu_{FA}(m(k) - 1)\right] J_{z_r}(k) \\ \qquad\qquad k = n_k \\ \left[(1 - P_D^r)\mu_{FA}(m(k)) + P_D^r \mu_{FA}(m(k) - 1)\right] J_{z_r}(k) \\ \qquad\qquad n_k < k < n_{k+1} \end{cases} \tag{5.51}$$

where

$$J_{z_r}(k) = E\left[-\Delta_{x_{k+1}}^{x_{k+1}} \log p(Z_r(k)|X(k), m_k^r)\right] \tag{5.52}$$

$$J_{z_a}(k) = E\left[-\Delta_{x_{k+1}}^{x_{k+1}} \log p(Z_a(k)|X(k), m_k^a)\right] \tag{5.53}$$

Table 5.1: Initial Conditions

Initial	Target-1	Target-2
x	700	800
$\dot{x}$	10	10
y	700	780
$\dot{y}$	3	-3
σ_p	0.1	1

5.4 Simulations and Results

In this section, the tracking performance of the proposed measurement-level fusion algorithm is compared with radar-only tracking, AIS-only tracking, track-to-track fusion and the PCRLB. Experimental results are presented based on 100 Monte Carlo simulations.

5.4.1 Simulation Setup

In the simulation studies, a two dimensional tracking example is considered. A surveillance region of 1 km $\times$ 1 km that consists of two closely spaced targets is considered. The initial conditions for the target states are summarized in Table 5.1.

The measurements from to the radar that is located at origin $(0, 0)$ has a sampling period of 1 s. Additional parameters for the radar are: probability of detection, $P_D = 0.9$; standard deviation of range measurements, $\sigma_r = 10\,\text{m}$; standard deviation of bearing measurements, $\sigma_\theta = 0.1\,\text{rad}$; false alarm rate, $\lambda = 5 \times 10^{-3}\,\text{m}^{-1}\,\text{rad}^{-1}$.

In addition, the AIS messages broadcast from the targets have the following parameters: standard deviation of the x-coordinate measurements, $\sigma_x = 3\,\text{m}$; standard deviation of y-coordinate measurements, $\sigma_y = 3\,\text{m}$; probability of AIS message with missing ID, $P_m = 0.2$; and probability of ID swap, $P_s = 0.1$. Various AIS revisit intervals $n \in (3, 12)$ are considered evaluating the performance of the proposed target tracking approaches.

5.4.2 Simulation Results

The simulation results presented in this section are based on 100 Monte Carlo Runs. Figure 5.2 shows the position Root Mean Squared Error (RMSE) comparison of various techniques for the first target. In the Figure 'Radar-Only' refers to tracks from only the radar measurements with JPDA; 'AIS-Only' refers to tracks with only AIS messages based on the ID match and Kalman Filter; 'T2T' refers to the fused tracks of 'Radar Only' and 'AIS-Only' outputs; 'Proposed-Fusion' refers to the proposed measurement level fusion method and finally the 'PCRLB' refers to the theoretical PCRLB.

As demonstrated in the figure, measurement-level fusion gives better performance than track-to-track fusion, radar-only and AIS-only methods. Furthermore, the performance of the measurement-level fusion is closer to the theoretical limit, i.e., PCRLB, than other methods. Similarly, Figure 5.3 shows the position RMSE comparison of various techniques for the second target. The second target exhibits large process noise, which resulted in large prediction errors. This effect can be seen with AIS data only tracking.

In the figure, it is also demonstrated that for AIS-only tracking the estimation has

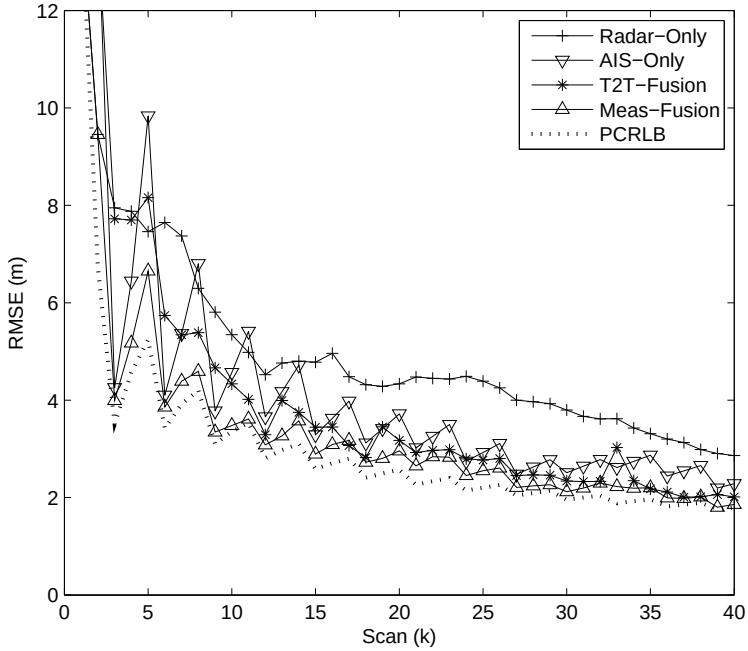

Figure 5.2: RMSE for Target 1.

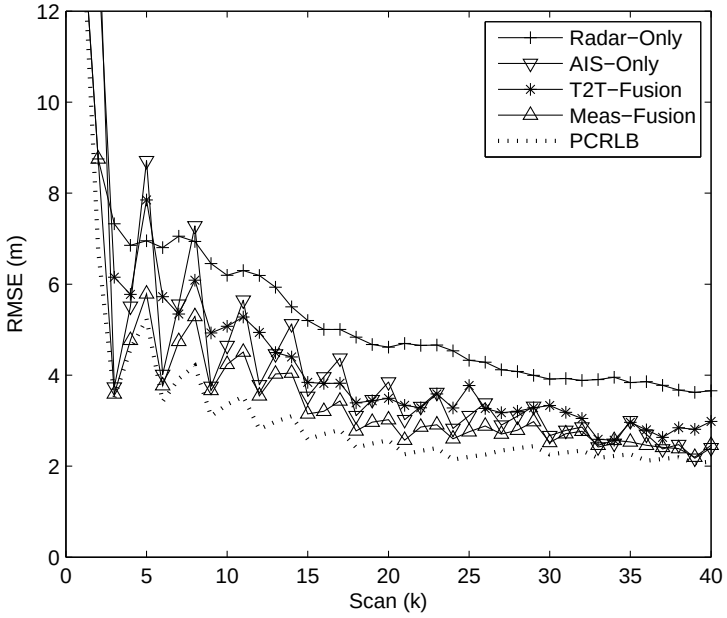

Figure 5.3: RMSE for Target 2.

to relay on prediction during the interval ($n_k < k < n_{k+1}$) when the AIS messages are not available. Although radar-only estimates do not rely on prediction since measurement arrive during each scan, the accuracy is limited due to large measurement errors associated with range and bearing measurements. Note that the AIS-only and track-to-track fusion methods yield degraded results due to missing AIS ID information and ID swaps between the targets. This is handled more accurately by the proposed measurements level fusion algorithm with ID probabilities shown in Figure 5.4.

In Figure 5.5 the time-averaged position RMSE for Target 1 is shown for different AIS message revisit intervals. From the figure it can be seen that as the AIS revisit interval becomes large, the performances of the track-to-track fusion as well as the measurement level fusion methods get closer to that of radar-only tracking. Similarly, the time-averaged position RMSE for Target 2 is shown in Figure 5.6

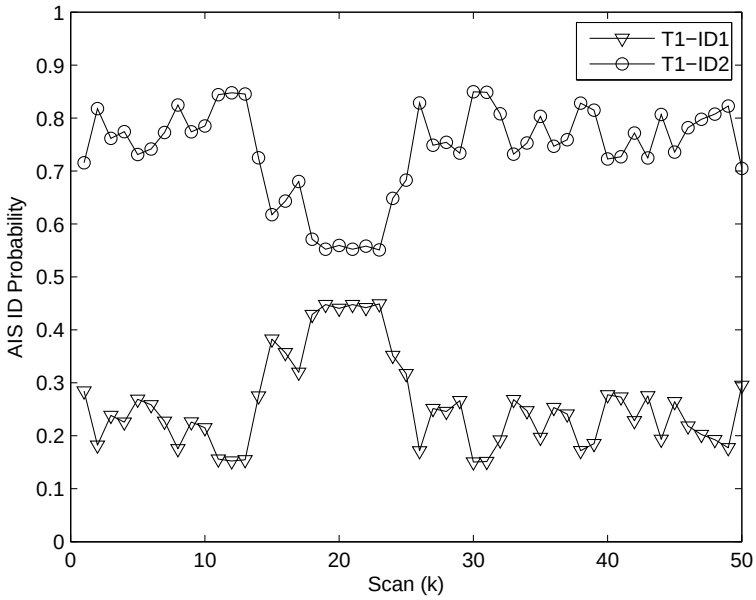

Figure 5.4: AIS ID probabilities.

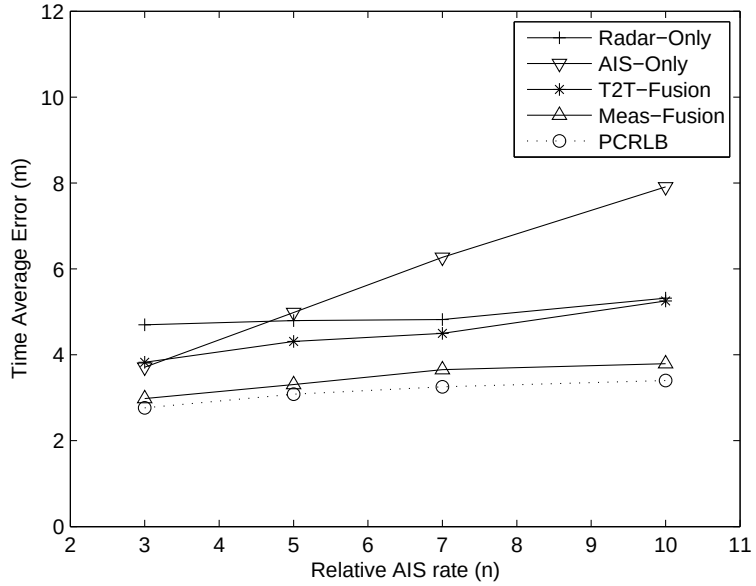

Figure 5.5: Time-averaged position RMSE of target 1 for various AIS revisit rates (σ_r =5 m, $\sigma_\theta = 0.1$ rad).

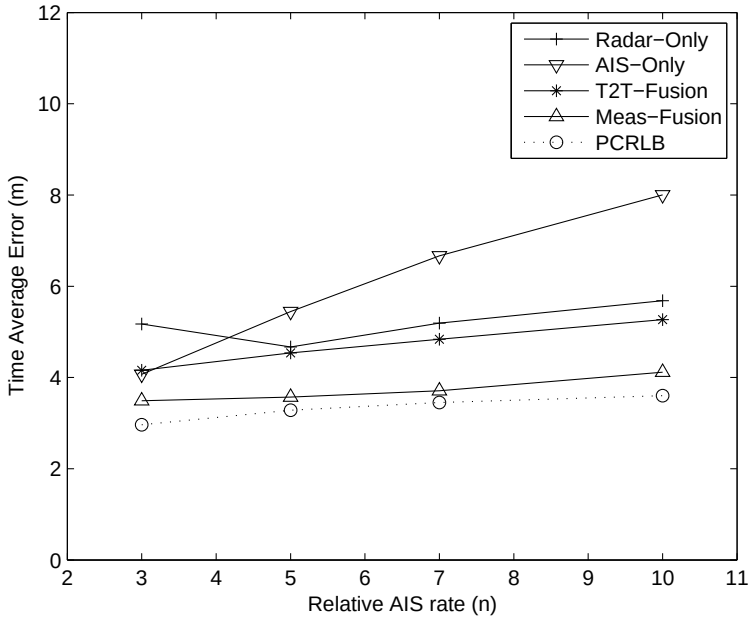

Figure 5.6: Time-averaged position RMSE of target 2 for various AIS revisit rates (σ_r =5 m, $\sigma_\theta = 0.1$ rad).

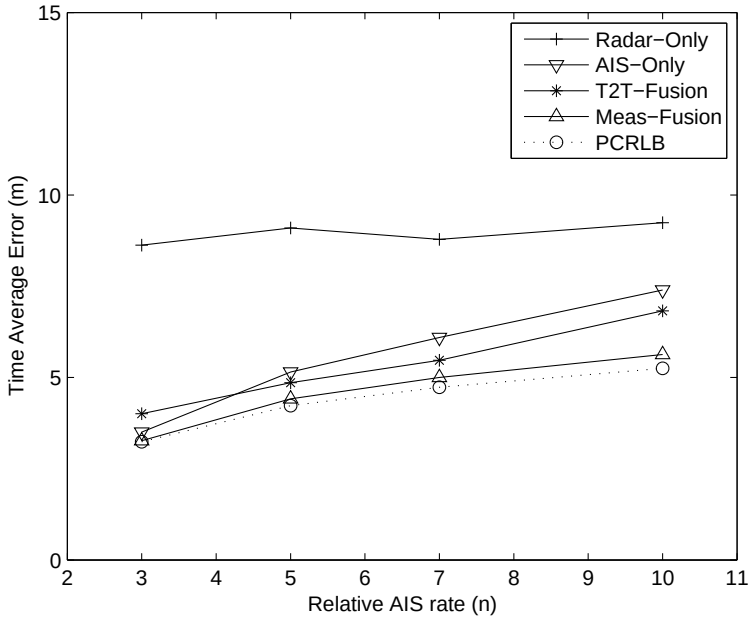

Figure 5.7: Time-averaged position RMSE of target 1 for various AIS revisit rates (σ_r =10 m, $\sigma_\theta = 0.5$ rad).

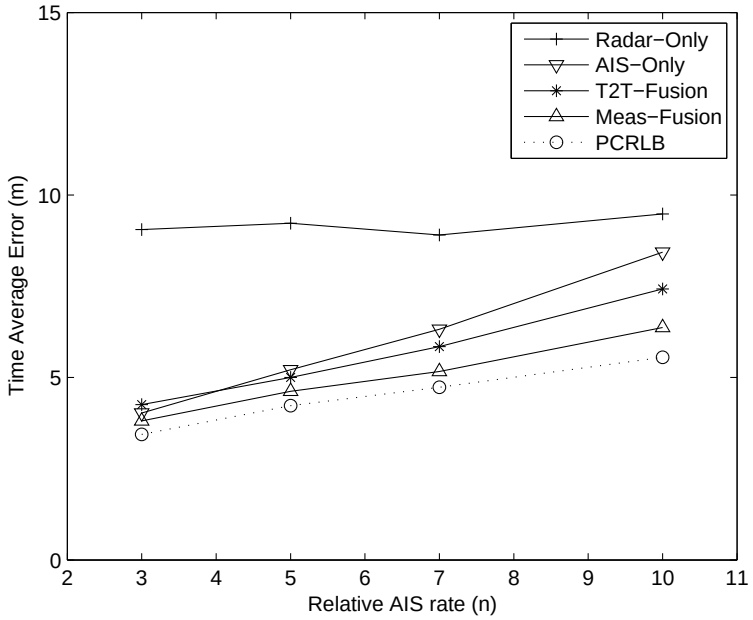

Figure 5.8: Time-averaged position RMSE of target 2 for various AIS revisit rates (σ_r =10 m, $\sigma_\theta = 0.5$ rad).

Table 5.2: Computational Load Comparison

Algorithm	Normalized Computation Time		
	$n = 3$	$n = 5$	$n = 10$
Radar-Only	0.2111	0.2135	0.2148
AIS-Only	0.1097	0.1206	0.1074
T2T-Fusion	0.3985	0.3968	0.4056
Proposed-Fusion	0.2807	0.2692	0.2722

In Figures 5.7 and 5.8 similar results are shown with larger radar measurement covariances (σ_r =10 m, $\sigma_\theta = 0.5$ rad).

Table 5.2 summarizes the relative computational loads of AIS-only, radar-only, and track-to-track fused and measurement wise fused AIS/radar estimates. As demonstrated in the table, the computational requirement of measurement-level fusion is slightly higher than that of the radar-only method and significantly lower than that of track-to-track fusion.

Chapter 6

Conclusions

This thesis studied the limitations of data association techniques used in multitarget tracking algorithms and proposed effective solutions.

In this thesis, a new Multiple-Detection Joint Probabilistic Data Association Filter (MD-JPDAF) was proposed for tracking multiple targets when multiple detection from a target per scan arises. When multiple detection from a target fall within the association gate, the standard JPDAF returns degraded state estimates due to violation of the one-measurement-per-scan assumption. In the proposed MD-JPDAF, combinatorial association events were formed to handle the possibility of multiple measurements from a target in a scan. Modified association probabilities were calculated with the explicit assumption of multiple detection. In order to provide a benchmark for performance comparison, the PCRLB was derived for this multiple-detection scenario for a single target tracking problem. Monte Carlo simulations were performed with a 2D sensor and an OTHR to test the performance of the proposed filter. Experimental results demonstrated the effectiveness of the proposed algorithm.

This thesis also proposed a continuous measurement-to-track association algorithm for continuously scanning radars. The proposed algorithms allows targets state update within the duration of a scan thereby increasing the track update speed. A complete scan was automatically divided into sectors, which could be as small as a single detection, depending on the scanning rate, sparsity of targets and the required target state update speed. Measurement-to-track association, filtering and target state update were performed simultaneously while sweeping from one end to another without waiting for the end of a scan. The proposed continuous 2-D assignment algorithm implements an incremental assignment technique in order to match new set of measurements and tracks with the existing ones. Experimental results based on rotating radars showed the track latency with continuous 2-D assignment technique is far less and more uniform than that of the frame based 2-D assignment without sacrificing accuracy.

A measurement-level fusion algorithms for combining radar measurements with AIS messages was also proposed in this thesis. In the proposed fusion algorithm, the ambiguity in the AIS ID messages that result due to targets being close to one another was resolved by multiple AIS IDs that are assigned to a track. The assigned AIS ID-to-track assignment probabilities were updated by both AIS and radar measurements based on kinematic and non-kinematic Bayesian inference. The performance of the proposed measurement level fusion technique was demonstrated with simulated data and compared with those of track-to-track fusion, and the theoretical Posterior Cramér-Rao Lower Bound.

Appendix A

MDPDA

A.0.1 Probabilistic Inference

In the MD-PDAF, multiple-detection association probabilities are evaluated by probabilistic inference, which is made on

- the number of measurements in the validation region, $m(k)$,
- the number of target-originated measurements, φ,
- the location of measurements.

This is expressed as

$$\begin{aligned} \beta_{\varphi,n_\varphi}(k) &= p(\theta_{\varphi,n_\varphi}(k)|Z^k, m(k), \varphi, Z^{k-1}) \\ &= \frac{1}{c} p(Z^k|\theta_{\varphi,n_\varphi}(k), m(k), \varphi, Z^{k-1}) \times p(\theta_{\varphi,n_\varphi}(k)|m(k), \varphi, Z^{k-1}) \quad \text{(A.1)} \end{aligned}$$

The first and second terms in (A.1) refer to measurement location and source inference, respectively.

Measurement Location Inference

the joint pdf of the correct measurement based on location inference is

$$p(Z^k|\theta_{\varphi,n_\varphi}(k), m(k), \varphi, Z^{k-1}) = \begin{cases} \frac{1}{P_G} \times \{\bigcup_{i=1}^{\varphi} \mathcal{G}_i(k)\}^{-m(k)+\varphi} \mathcal{N}(\nu_{\varphi,n_\varphi}(k); 0, S_{\varphi,n_\varphi}(k)) & \\ \qquad\qquad\qquad\qquad\qquad\qquad n_\varphi = 1, ..., c_{\varphi m}(k) & \\ \{\bigcup_{i=1}^{\varphi} \mathcal{G}_i(k)\}^{-m(k)} \qquad\qquad\qquad n_\varphi = 0 & \end{cases} \tag{A.2}$$

Measurement Source Inference

this evaluates the event $\theta_{\varphi,n_\varphi}$ conditioned on the total number of validated measurements $\mathcal{M} = m(k)$ and number of target-originated measurements, φ. Here $\mathcal{M}$ denotes the random variable and $m(k)$ its realization [14]. Then,

$$\begin{aligned} p(\theta_{\varphi,n_\varphi}(k)|m(k), \varphi, Z^{k-1}) &= p(\theta_{\varphi,n_\varphi}|\mathcal{M} = m(k), \varphi) \\ &= p(\theta_{\varphi,n_\varphi}|\Psi = m(k) - \varphi, \mathcal{M} = m(k)) \\ &\quad \times p(\Psi = m(k) - \varphi|\mathcal{M} = m(k)) \\ &\quad + p(\theta_{\varphi,n_\varphi}|\Psi = m(k), \mathcal{M} = m(k)) \\ &\quad \times p(\Psi = m(k)|\mathcal{M} = m(k)) \end{aligned} \tag{A.3}$$

where Ψ is the number of false measurements. For φ target-originated measurements, Ψ must be either $m(k) - \varphi$ or $m(k)$. Thus,

$$p(\theta_{\varphi,n_\varphi}(k)|m(k),\varphi,Z^{k-1}) = \begin{cases} \frac{1}{m(k)} \times p(\Psi = m(k) - \varphi|\mathcal{M} = m(k)) \\ \qquad\qquad\qquad\qquad n_\varphi = 1, ..., c_{\varphi m}(k) \\ p(\Psi = m(k)|\mathcal{M} = m(k)) \\ \qquad\qquad\qquad\qquad n_\varphi = 0 \end{cases} \tag{A.4}$$

where

$$\begin{aligned} p(\Psi = m(k) - \varphi|\mathcal{M} = m(k)) &= \frac{p(\mathcal{M} = m(k)|\Psi = m(k) - \varphi)p(\Psi = m(k) - \varphi)}{p(\mathcal{M} = m(k))} \\ &= \frac{P_{D\varphi}P_G\mu(m(k) - \varphi)}{p(\mathcal{M} = m(k))} \end{aligned} \tag{A.5}$$

and

$$\begin{aligned} p(\Psi = m(k)|\mathcal{M} = m(k)) &= \frac{p(\mathcal{M} = m(k)|\Psi = m(k))p(\Psi = m(k))}{p(\mathcal{M} = m(k))} \\ &= \frac{(1 - P_DP_G)\mu(m(k))}{p(\mathcal{M} = m(k))} \end{aligned} \tag{A.6}$$

$P_{D\varphi}$ is the probability of detecting a target φ times per scan. The total probability of detection P_D will become the superposition of detection probabilities of $P_{D\varphi}$. Also, $P_{D\varphi}P_G$ is the probability that the target has been detected and φ measurements originated from it are inside the gate and $(1 - P_DP_G)$ is the probability that the measurements in the gate are false alarms. Thus,

$$p(\mathcal{M} = m(k)) = \sum_{\varphi=1}^{m(k)} P_{D\varphi}P_G\mu(m(k) - \varphi) + (1 - P_DP_G)\mu(m(k)) \tag{A.7}$$

Substituting (A.7) in (A.5) and (A.6), the result in (A.4), we get

$$p(\theta_{\varphi,n_\varphi}(k)|m(k),\varphi,Z^{k-1}) = \begin{cases} \frac{1}{m(k)} \frac{P_{D\varphi}P_G\mu(m(k)-\varphi)}{\sum_{\varphi=1}^{m(k)} P_{D\varphi}P_G\mu(m(k)-\varphi)+(1-P_DP_G)\mu(m(k))} \\ \qquad\qquad n_\varphi = 1,...,c_{\varphi m}(k) \\ \frac{(1-P_DP_G)\mu(m(k))}{\sum_{\varphi=1}^{m(k)} P_{D\varphi}P_G\mu(m(k)-\varphi)+(1-P_DP_G)\mu(m(k))} \\ \qquad\qquad n_\varphi = 0 \end{cases} \tag{A.8}$$

A.0.2 Special Case

With only one target-originated measurement ($P_{D1},\cdots,P_{D\varphi}=P_D$)

$$p(\theta_{\varphi,n_\varphi}(k)|m(k),\varphi,Z^{k-1}) = \begin{cases} \frac{1}{m(k)} \frac{P_DP_G\mu(m(k)-1)}{P_DP_G\mu(m(k)-1)+(1-P_DP_G)\mu(m(k))} \\ \qquad\qquad n_\varphi = 1,...,c_{\varphi m}(k) \\ \frac{(1-P_DP_G)\mu(m(k))}{P_DP_G\mu(m(k)-1)+(1-P_DP_G)\mu(m(k))} \\ \qquad\qquad n_\varphi = 0 \end{cases} \tag{A.9}$$

Then the MD-PDAF reduces to the standard PDAF.

Appendix B

OTHR

B.0.3 OTHR Model

The range measurement is given by

$$r_g(k) = r_1(k) + r_2(k) \tag{B.10}$$

where

$$r_1(k) = \sqrt{(\rho(k)/2)^2 + h_r^2} \tag{B.11}$$

$$r_2(k) = \sqrt{(\rho(k)/2)^2 - d\sin(\beta(k))/2 + (d/2)^2 + h_t^2} \tag{B.12}$$

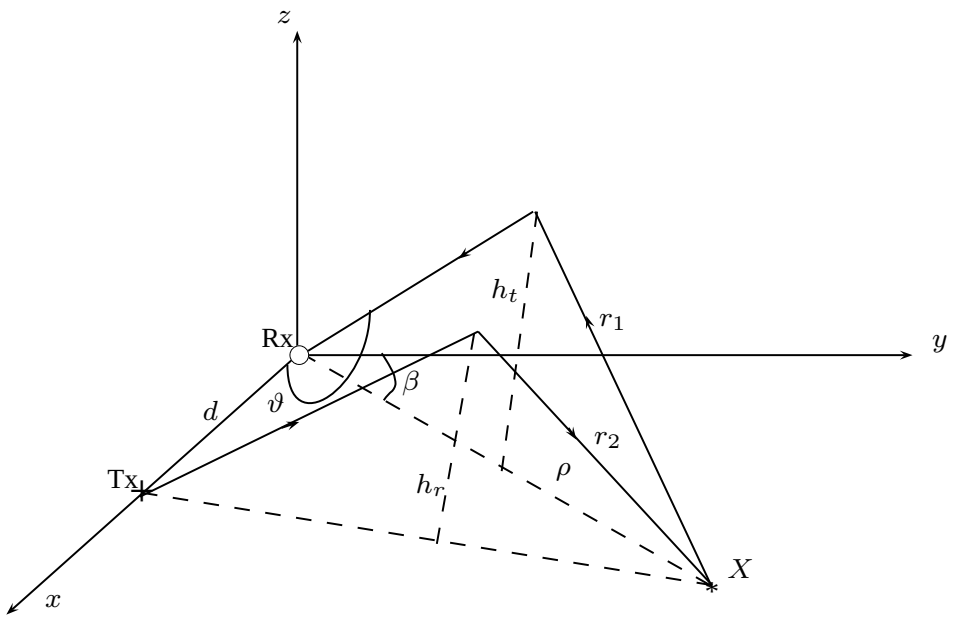

Figure B.1: Over-the-horizon radar planar model (Tx - transmitter, Rx - receiver, X - target).

the range-rate is given by

$$\dot{r_g}(k) = \frac{dr_g(k)}{dt} \tag{B.13}$$

$$= \frac{dr_1(k)}{dt} + \frac{dr_2(k)}{dt} \tag{B.14}$$

$$= \frac{\rho(k)\dot{\rho}(k)}{4\sqrt{(\rho/2)^2 + h_r^2}} + \frac{\rho(k)\dot{\rho}(k) - d\sin(\beta(k))\dot{\rho}(k)}{4\sqrt{(\rho/2)^2 - d\sin(\beta(k))/2 + (d/2)^2 + h_t^2}} \tag{B.15}$$

and the Azimuth is given by

$$\vartheta(k) = \arcsin\left(\frac{\rho(k)\sin(\beta(k))}{2\sqrt{(\rho(k)/2)^2 + h_r^2}}\right) \tag{B.16}$$

Hence, the nonlinear measurement model for the OTHR is given by

$$h(x(k)) = \begin{bmatrix} \sqrt{(\rho(k)/2)^2 + h_r^2} + \sqrt{(\rho(k)/2)^2 - d\rho(k)\sin(\beta(k))/2 + (d/2)^2 + h_t^2} \\ \frac{\rho(k)\dot{\rho}(k)}{4\sqrt{(\rho/2)^2+h_r^2}} + \frac{\rho(k)\dot{\rho}(k) - d\sin(\beta(k))\dot{\rho}(k)}{4\sqrt{(\rho/2)^2 - d\sin(\beta(k))/2 + (d/2)^2 + h_t^2}} \\ \arcsin\left(\frac{\rho(k)\sin(\beta(k))}{2\sqrt{(\rho(k)/2)^2+h_r^2}}\right) \end{bmatrix} \tag{B.17}$$

The Jacobian matrix for linear estimate is given by

$$H(k) = \begin{bmatrix} \frac{\partial r_g(k)}{\partial \rho(k)} & \frac{\partial r_g(k)}{\partial \dot{\rho}(k)} & \frac{\partial r_g(k)}{\partial \beta(k)} & \frac{\partial r_g(k)}{\partial \dot{\beta}(k)} \\ \frac{\partial \dot{r_g}(k)}{\partial \rho(k)} & \frac{\partial \dot{r_g}(k)}{\partial \dot{\rho}(k)} & \frac{\partial \dot{r_g}(k)}{\partial \beta(k)} & \frac{\partial \dot{r_g}(k)}{\partial \dot{\beta}(k)} \\ \frac{\partial \vartheta(k)}{\partial \rho(k)} & \frac{\partial \vartheta(k)}{\partial \dot{\rho}(k)} & \frac{\partial \vartheta(k)}{\partial \beta(k)} & \frac{\partial \vartheta(k)}{\partial \dot{\beta}(k)} \end{bmatrix} \tag{B.18}$$

where

$$\begin{aligned} J_{11} &= \frac{\partial r_g(k)}{\partial \rho(k)} \\ &= \frac{1}{4}\left(\frac{\rho(k)}{r_1(k)} + \frac{\eta(k)}{r_2(k)}\right) && \text{(B.19)} \\ J_{13} &= \frac{\partial r_g(k)}{\partial \beta(k)} \\ &= -\frac{d\rho(k)\cos(\beta(k))}{4r_2(k)} && \text{(B.20)} \\ J_{21} &= \frac{\partial \dot{r_g}(k)}{\partial \rho(k)} \\ &= \frac{\dot{\rho}(k)}{4}\left(\frac{1}{r_1(k)} + \frac{1}{r_2(k)} - \frac{\rho^2(k)}{4r_1^3(k)} - \frac{\eta(k)}{4r_2^3(k)}\right) && \text{(B.21)} \\ J_{22} &= \frac{\partial \dot{r_g}(k)}{\partial \dot{\rho}(k)} \\ &= \frac{1}{4}\left(\frac{\rho(k)}{r_1(k)} + \frac{\eta(k)}{r_2(k)}\right) && \text{(B.22)} \end{aligned}$$

$$
\begin{aligned}
J_{23} &= \frac{\partial \dot{r_g}(k)}{\partial \beta(k)} \\
&= -\frac{d\dot{\rho}(k)\cos(\beta(k))}{4r_2(k)}\left(1-\frac{\rho(k)\eta(k)}{4r_2^2(k)}\right) \qquad \text{(B.23)} \\
J_{31} &= \frac{\partial \vartheta(k)}{\partial \rho(k)} \\
&= \frac{\sin(\beta(k))}{2r_1(k)\cos(\vartheta(k))}\left(1-\frac{\rho^2(k)}{4r_1^2(k)}\right) \qquad \text{(B.24)} \\
J_{33} &= \frac{\partial \vartheta(k)}{\partial \beta(k)} \\
&= \frac{\rho(k)\cos(\beta(k))}{2r_1(k)\cos(\vartheta(k))} \qquad \text{(B.25)}
\end{aligned}
$$

and the rest of terms are zero. Here, $\eta(k)$ is defined as

$$\eta(k) \triangleq \rho(k) - d\sin(\beta(k)) \qquad \text{(B.26)}$$

Bibliography

[1] Anderson, R. H. and Krolik, J. L. (1998). Over-the-Horizon Radar Target Localization using a Hidden Markov Model Estimated from Ionosonde Data. *Radio Science*, **33**(4), 1199–1213.

[2] Aoki, E. H. and Kienitz, K. H. (2009). Suboptimal JPDA for Tracking in the Presence of Clutter and Missed Detections. *12th International Conference on Information Fusion*, pages 818–825.

[3] B. Habtemariam, R. Tharmarasa, E. M. and Kirubarajan, T. (2012a). Measurement level AIS/Radar Fusion for Multitarget Tracking. *SPIE Conference on Signal and Data Processing of Small Targets*, pages 1–8.

[4] B. Habtemariam, R. Tharmarasa, M. M. and Kirubarajan, T. (2012b). Performance Comparison of a Multiple-Detection Probabilistic Data Association Filter with PCRLB. *International Conference on Control, Automation and Information Sciences*, pages 18–23.

[5] B. Habtemariam, R. Tharmarasa, M. P. and Kirubarajan, T. (2011a). Dynamic Sector Processing Using 2D Assignment for Rotating Radars. *SPIE Conference on Signal and Data Processing of Small Targets*, pages 1–8.

[6] B. Habtemariam, R. Tharmarasa, N. N. M. M. and Kirubarajan, T. (2011b). Improved Multiframe Association for Tracking Maneuvering Targets. *SPIE Conference on Signal and Data Processing of Small Targets*, pages 1–8.

[7] B. Habtemariam, A. Aravinthan, R. T. K. P. T. L. and Kirubarajan, T. (2012c). Distributed Tracking with a PHD Filter using Efficient Measurement Encoding. *Journal of Advances in Information Fusion*, **7**(2), 114–130.

[8] B. Habtemariam, R. Tharmarasa, T. K. D. G. and Wakayama, C. (2011). Multiple Detection Probabilistic Data Association Filter for Multistatic Target Tracking. *14th International Conference on Information Fusion*, pages 1–8.

[9] B. Habtemariam, R. Tharmarasa, T. T. M. M. and Kirubarajan, T. (2013). A Multiple-Detection Joint Probabilistic Data Association Filter. *IEEE Journal of Selected Topics in Signal Processing*, **7**(3), 461–471.

[10] B.-N. Vo, S. S. and Doucet, A. (2005). Sequential Monte Carlo Methods for Multitarget Filtering with Random Finite Sets. *IEEE Transactions on Aerospace and Electronic Systems*, **41**(4), 1224–1245.

[11] B.-T. Vo, B.-N. V. and Cantoni, A. (2008). Bayesian Filtering with Random Finite Set Observations. *IEEE Transactions on Signal Processing*, **56**(4), 1313–1326.

[12] Bar-Shalom, Y. (1981). On the Track-to-Ttrack Correlation Problem. *IEEE Transactions on Automatic Control*, **26**(2), 571–572.

[13] Bar-Shalom, Y. and Campo, L. (1986). The Effect of the Common Process Noise

on the Two-Sensor Fused Track Covariance. *IEEE Transactions on Aerospace and Electronic Systems*, **22**(6), 803–805.

[14] Bar-Shalom, Y. and Li, X. R. (1995). *Multitarget-Multisensor Tracking: Principles and Techniques*. YBS Publishing.

[15] Bar-Shalom, Y. and Tse, E. (1975). Tracking in a Cluttered Environment with Probabilistic Data Association. *Automatica*, **11**, 451–460.

[16] Bertsekas, D. P. (1981). A New Algorithm for the Assignment Problem. *Mathematical Programming*, **21**(1), 152–171.

[17] Bertsekas, D. P. (1988). The Auction Algorithm: A Distributed Relaxation Method for the Assignment Problem. *Annals of Operations Research*, **14**(1), 105–123.

[18] Blackman, S. S. (1986). *Multiple-Target Tracking with Radar Applications*. The Archtech House Radar Library.

[19] Blackman, S. S. (2004). Multiple Hypothesis Tracking for Multiple Target Tracking. *IEEE Aerospace and Electronic Systems Megazine*, **19**(1), 5–18.

[20] Blom, H. A. P. and Bloem, E. A. (2002). Interacting Multiple Model Joint Probabilistic Data Association, Avoiding Track Coalescence. *41st IEEE Conf. Decision and Control*, **3**, 3408–3415.

[21] Burkard, R. E. (2002). Selected Topics on Assignment Problems. *Discrete Applied Mathematics*, **123**(1), 257–302.

[22] C. Carthel, S. C. and Grignan, P. (2007). Multisensor Tracking and Fusion for Maritime Surveillance. *10th International Conference on Information Fusion*, pages 1–6.

[23] Chang, K. C. and Bar-Shlom, Y. (1984). Joint Probabilistic Data Association for Multitarget Tacking with Possibly Unresolved Measurements and Maneuvers. *IEEE Transactions on Automatic Control*, **29**(7), 585–594.

[24] Charles, R. and Silbert, M. (2011). The Effect of Relative Update Rates on Tracking Performance. *SPIE Defense, Security, and Sensing. International Society for Optics and Photonics*, **39**(2), 386–400.

[25] Clarke, J. (1985). Airborne Early Warning Radar. *Proceedings of the IEEE*, **73**(2), 312–324.

[26] D. Bourgeois, C. M. and M.Flcheux (2004). MCMC Data Association Algorithm applied to the French Over-The-Horizon Radar Nostradamus. *7th International Conference on Information Fusion*, pages 1–6.

[27] D. Danu, A. Sinha, T. K. M. F. and Brookes, D. (2007). Fusion of Over-the-Horizon Radar and Automatic Identification Systems for Overall Maritime Picture. *10th International Conference on Information Fusion*, pages 1–8.

[28] D. Musicki, R. E. and Stankovic, S. (1994). Integrated Probabilistic Data Association. *IEEE Transactions on Automatic Control*, **39**(6), 1237–1241.

[29] E. Fortunato, W. Kreamer, S. M. C. Y. C. and Castanon, G. (2007). Generalized Murty's Algorithm with Application to Multiple Hypothesis Ttracking. *10th International Conference on Information Fusion*, pages 1–8.

[30] E. Mazor, A. Averbuch, Y. B.-S. and Dayan, J. (1998). Interacting Multiple Model Methods in Target Tracking: A Survey. *IEEE Transactions on Aerospace and Electronic Systems*, **34**(1), 103–123.

[31] F. C. Robey, D. R. Fuhrmann, E. J. K. and Nitzberg, R. (1992). A CFAR Adaptive Matched Filter Detector. *IEEE Transactions on Aerospace and Electronic Systems*, **28**(1), 208–216.

[32] G. Wang, X.-G. Xia, B. R. V. C. Y. Z. and Amin, M. (2003). Manoeuvring Target Detection in Over-the-Horizon Radar using Adaptive Clutter Rejection and Adaptive Chirplet Transform. *IEEE Transactions on Signal Processing*, **150**(4).

[33] Gan, Q. and Harris, C. J. (2001). Comparison of Two Measurement Fusion Methods for Kalman-filter-based Multisensor Data Fusion. *IEEE Transactions on Aerospace and Electronic Systems*, **37**(1), 273–279.

[34] Georges, T. M. and Harlan, J. A. (1994). New Horizons for Over-the-Horizon Radar? *IEEE Antennas and Propagation Magazine*, **36**(4), 14–24.

[35] H. Chen, T. and Bar-Shalom, Y. (2003). Performance Limits of Track-to-Track Fusion versus Centralized Estimation: Theory and Application. *IEEE Transactions on Aerospace and Electronic Systems*, **39**(2), 386–400.

[36] Hall, D. D. L. and McMullen, S. A. H. (2004). Mathematical Techniques in Multisensor Data Fusion. *Artech House*.

[37] Headrick, J. M. (1990). Looking over the Horizon [HF radar]. *IEEE Spectrum*, **27**(7), 36–39.

[38] Hong, L. (2002). Distributed Interacting Multipattern Data Association for Multiplatform Target Tracking. *Signal Processing*, **82**, 1007–1021.

[39] Hong, L. and Cui, N. (2001). An Interacting Multipattern Probabilistic Data Association (IMP-PDA) Algorithm for Target Tracking. *IEEE Transactions on Automatic Control*, **46**(8), 1223–1236.

[40] Jonker, R. and Volgenant, A. (1987). A Shortest Augmenting Path Algorithm for Dense and Sparse Linear Assignment Problems. *Journal of Computing*, **38**(4), 325–340.

[41] Julier, S. J. and Uhlmann, J. K. (2004). Unscented Filtering and Nonlinear Estimation. *Proceedings of the IEEE*, **92**(3), 401–422.

[42] K. C. Chang, R. K. S. and Bar-Shlom, Y. (1997). On Optimal Track-to-Track Fusion. *IEEE Transactions on Aerospace and Electronic Systems*, **33**(4), 1271–1276.

[43] Kalata, P. R. (1992). $\alpha - \beta$ Target Tracking Systems: A Survey. *IEEE American Control Conference*, pages 832–836.

[44] Kirubarajan, T. and Bar-Shalom, Y. (2004). Probabilistic Data Association Techniques for Target Tracking in Clutter. *Proceedings of the IEEE*, **92**(3), 536–557.

[45] Koch, W. and Keuk, G. V. (1997). Multiple Hypothesis Track Maintenance with Possibly Unresolved Measurements. *IEEE Aerospace and Electronic Systems Magazine*, **33**(3), 883–892.

[46] Kosuge, Y. and Matsuzaki, T. (2003). The Optimum Gate Shape and Threshold for Target Tracking. *SICE 2003 Annual Conference*, **2**, 2152–2157.

[47] Krolik, J. L. and Anderson, R. H. (1997). Maximum Likelihood Coordinate Registration for Over-the-Horizon Radar. *IEEE Transactions on Signal Processing*, **45**(4), 945–959.

[48] Kuhn, H. (2005). The Hungarian Method for the Assignment Problem. *Naval Research Logistics*, **2**(1), 7–21.

[49] Kurien, T. (1990). Issues in the Design of Practical Multitarget Tracking Algorithms. *Multitarget-Multisensor Tracking: Advanced Applications*.

[50] M. G. Rutten, S. Maskell, M. B. and Gordon, N. J. (2004). Multipath track association for over-the-horizon radar using Lagrangian relaxation. *Proceedings of SPIE*.

[51] M. Guerriero, P. Willett, S. C. and Carthel, C. (2008). Radar/AIS Data Fusion and SAR Tasking for Maritime Surveillance. *11th International Conference on Information Fusion*, pages 1–5.

[52] M. L. Hernandez, A. D. Marrs, N. J. G. S. R. M. and Reed, C. M. (2002). Cramer-Rao Bounds for Non-linear Filtering with Measurement Origin Uncertainty. *5th International Conference on Information Fusion*, pages 18–25.

[53] M. R. Chummun, T. Kirubarajan, K. R. P. and Bar-Shlom, Y. (2001). Fast Data Association using Multidimensional Assignment with Clustering. *IEEE Aerospace and Electronic Systems Magazine*, **37**(3), 898–913.

[54] M. S. Arulampalam, S. Maskell, N. G. and Clapp, T. (2002). A Tutorial on Particle Filters for Online Nonlinear/Non-Gaussian Bayesian Tracking. *IEEE Transactions on Signal Processing*, **50**(2), 174–188.

[55] M. Y. Kao, T. W. Lam, W. K. S. and Ting, H. F. (2001). A Decomposition Theorem for Maximum Weight Bipartite Matchings. *SIAM Journal on Computing*, **31**(1), 18–26.

[56] Mahler, R. (2003). Multitarget Bayes Fileting via First-order Multitarget Moments. *IEEE Transactions on Aerospace and Electronic Systems*, **39**(4), 1152–1178.

[57] Musicki, D. and Evans, R. (2004). Joint Integrated Probabilistic Data Association: JIPDA. *IEEE Transactions on Aerospace and Electronic Systems*, **40**, 1093–1099.

[58] Musicki, D. and Morelande, M. (2004). Gate Volume Estimation for Target Tracking. *7th International Conference on Information Fusion*, pages 1–8.

[59] P. Tichavsky, C. H. M. and Nehorani, A. (1998). Posterior Cramér-Rao Bounds for Discrete-time Nonlinear Filtering. *IEEE Transactions on Signal Processing*, **46**, 1386–1396.

[60] Papadimitriou, C. H. and Steiglitz, K. (1998). *Combinatorial Optimization: Algorithms and Complexity*. Dover Publications, Mineola, New York.

[61] Percival, D. J. and White, K. A. (1997). Multipath Track Fusion for Over-the-Horizon Radar. *Optical Science, Engineering and Instrumentation'97, International Society for Optics and Photonics*, pages 363–374.

[62] Poore, A. B. (1994). Multidimentional Assignment Formulation of Data Association Problems Arising from Multitarget Tracking and Multisensor Data Fusion. *Computational Optimization and Applications*, **3**, 27–57.

[63] Poore, A. B. and III, A. J. R. (1997). A New Lagrangian Relaxation Based Algorithm for a Class of Multidimensional Assignment Problems. *Computational Optimization and Applications*, **8**(3), 129–150.

[64] Poore, A. B. and Rijavec, N. (1993). A Lagrangian Relaxation Algorithm for Multidimensional Assignment Problems Arising from Multitarget Tracking. *SIAM Journal on Optimization*, **3**(3), 544–563.

[65] Pulford, G. W. (1998). A Multipath Data Association Tracker for Over-the-Horizon Radar. *IEEE Transactions on Aerospace and Electronic Systems*, **34**(4), 1165–1183.

[66] Pulford, G. W. and Evans, R. J. (1996). Probabilistic Data Association for Systems with Multiple Simultaneous Measurements. *Automatica*, **32**(9), 1311–1316.

[67] R. L. Popp, T. K. and Pattipati, K. (2000). Survey of Assignment Techniques for Multitarget Tracking. *Chapter 2 in Multitarget/Multisensor Tracking: Applications and Advances III, (Y. Bar-Shalom and W.D. Blair, eds.)*.

[68] R. Tharmarasa, T. Kirubarajan, M. L. H. and Sinha, A. (2007). PCRLB-based Multisensor Array Management for Multitarget Tracking. *IEEE Transactions on Aerospace and Electronic Systems*, **43**, 539–551.

[69] Reid, D. (1979). An Algorithm for Tracking Multiple Targets. *IEEE Transactions on Automatic Control*, **24**(6), 843–854.

[70] Ristic, B. (1999). A Comparison of MHT and 2-D Assignment Algorithm for Tracking with an Airborne Pulse Doppler Radar. *5th International Symposium on Signal Processing and Its Applications*, **1**, 341–344.

[71] Roecker, J. A. (1984). A Class of Near Optimal JPDA Algorithms. *IEEE Transactions on Aerospace and Electronic Systems*, **30**(2), 504–510.

[72] Rohling, H. (1983). Radar CFAR Thresholding in Clutter and Multiple Target Situations. *IEEE Transactions on Aerospace and Electronic Systems*, **19**(4), 608–621.

[73] Rong, L. X. and Vesselin, P. J. (2003). Survey of Maneuvering Target Tracking. Part I. Dynamic Models. *IEEE Transactions on Aerospace and Electronic Systems*, **39**(4), 1333–1364.

[74] Rong, L. X. and Vesselin, P. J. (2010). Survey of Maneuvering Target Tracking. Part II: Motion Models of Ballistic and Space Targets. *IEEE Transactions on Aerospace and Electronic Systems*, **46**(1), 96–119.

[75] S. B. Colegrove, S. J. D. and Cheung, B. (2003). PDAF versus PMHT Performance on OTHR Data. *International IEEE Radar Conference*, pages 560–565.

[76] S. Deb, M. Yeddanapudi, K. P. and Bar-Shalom, Y. (1997). A Generalized S-D Assignment Algorithm for Multisensor-Multitarget State Estimation. *IEEE Aerospace and Electronic Systems Magazine*, **33**(2), 523–538.

[77] S. Jeong, J. T. (2005). Multisensor Tracking of a Maneuvering Target in Clutter using IMMPDA Filtering with Simultaneous Measurement Update. *IEEE Transactions on Aerospace and Electronic Systems*, **41**(3), 1122–1131.

[78] S. S. Blackman, R. J. Dempster, M. T. B. and Popoli, R. F. (1999). IMM/MHT Solution to Radar Benchmark Tracking Problem. *IEEE Transactions on Aerospace and Electronic Systems*, **35**(2), 730–738.

[79] Saha, R. K. (1996). Track-to-track Fusion with Dissimilar Sensors. *IEEE Transactions on Aerospace and Electronic Systems*, **32**(3), 1021–1029.

[80] Sankowski, P. (2009). Maximum Weight Bipartite Matching in Matrix Multiplication Time. *Theoretical Computer Science*, **410**(44), 4480–4488.

[81] Sarunic, P. and Rutten, M. (2000). Over-the-Horizon Radar Multipath Track Fusion Incorporating Track History. *Proceedings of the International Conference on Information Fusion*, pages 13–19.

[82] Sinha, A. and Peters, D. J. (2009). Flexible ID Association-based Tracking Algorithm. *12th International Conference on Information Fusion*, pages 2161–2168.

[83] T. Eriksen, G. Hoye, B. N. and Meland, B. J. (2006). Maritime Traffic Monitoring using a Space-Based AIS Receiver. *Acta Astronautica*, **58**(10), 537–549.

[84] T. Kirubarajan, Y. Bar-Shalom, K. R. P. and Kadar, I. (2000). Ground Target Tracking with Topography-Based Variable Structure IMM Estimator. *IEEE Transactions on Aerospace and Electronic Systems*, **36**(1), 26–46.

[85] T. Sathyan, C. Tat-Jun, S. A. and Suter, D. (2013). A Multiple Hypothesis Tracker for Multitarget Tracking With Multiple Simultaneous Measurements. *IEEE Journal of Selected Topics in Signal Processing*, **7**(3), 448–460.

[86] T. Yuan, Y. B.-S. and Tian, X. (2011). Heterogeneous Track-to-Track Fusion. *14th International Conference on Information Fusion*, pages 1–8.

[87] Tetreault, B. J. (2005). Use of the Automatic Identification System for Maritime Domain Awareness. *Proceedings of MTS/IEEE*, **2**, 1590–1594.

[88] Toroslu, I. H. and Ucoluk, G. (2007). Incremental Assignment Problem. *Information Sciences*, **177**(6), 1523–1529.

[89] Vo, B.-N. and Ma, W.-K. (2006). The Gaussian Mixture Probability Hypothesis Density Filter. *IEEE Transactions on Signal Processing*, **54**(11), 4091–4104.

[90] Wan, E. A. and Merwe, R. V. D. (2000). The Unscented Kalman Filter for Nonlinear Estimation. *The IEEE Symposium on Adaptive Systems for Signal Processing, Communications, and Control*, pages 153–158.

[91] Y. Bar-Shalom, T. K. and Gokberk, C. (2005). Tracking with Classification-Aided Multiframe Data Association. *IEEE Aerospace and Electronic Systems Megazine*, **41**(3), 868–878.

[92] Y. Bar-Shalom, T. K. and Lin, X. (2005). Probabilistic Data Association Techniques for Target Tracking with Applications to Sonar , Radar and EO Sensors. *IEEE Aerospace and Electronic Systems Megazine*, **20**(8), 37–56.

[93] Y. Bar-Shalom, X. L. and Kirubarajan, T. (2001). *Estimation with Applications to Tracking and Navigation.* John Wiley & Sons Inc., New York, NY, USA.

[94] Y. Boers, H. Driessen, J. T. M. T. R. K. and Gustafsson, F. (2006). Track-Before-Detect Algorithm for Tracking Extended Targets. *IEE Proceedings-Radar, Sonar and Navigation*, **153**(4), 345–351.

[95] Y. Boers, F. Ehlers, W. K. T. L. L. D. S. and Streit, R. L. (2008). Track Before Detect Algorithms. *EURASIP Journal on Advances in Signal Processing*, **1**, 1–3.